

DREDGED MATERIAL RESEARCH PROGRAM



CONTRACT REPORT D-76-5

DEVELOPMENT OF MODELS FOR PREDICTION OF SHORT-TERM FATE OF DREDGED MATERIAL DISCHARGED IN THE ESTUARINE ENVIRONMENT

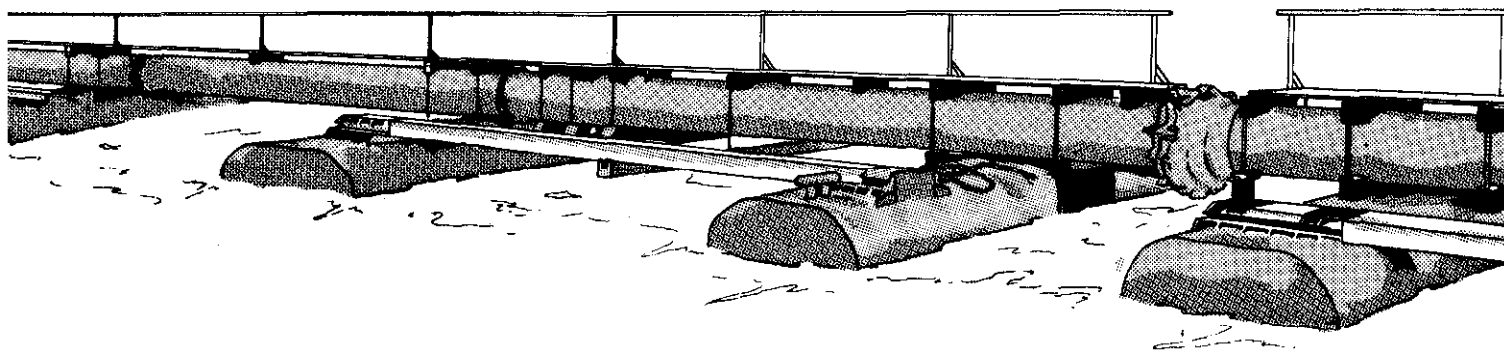
by

Maynard G. Brandsma, David J. Divoky
Tetra Tech, Incorporated
603 North Rosemead Boulevard
Pasadena, California 91107

May 1976

Final Report

Approved For Public Release; Distribution Unlimited



Prepared for Environmental Effects Laboratory
U. S. Army Engineer Waterways Experiment Station
P. O. Box 631, Vicksburg, Miss. 39180

Under Contract No. DACW39-74-C-0075
Work Unit IB02

Destroy this report when no longer needed. Do not return
it to the originator.



DEPARTMENT OF THE ARMY
WATERWAYS EXPERIMENT STATION, CORPS OF ENGINEERS
P. O. BOX 631
VICKSBURG, MISSISSIPPI 39180

IN REPLY REFER TO: WESYV

30 June 1976

SUBJECT: Transmittal of Contract Report D-76-5

TO: All Report Recipients

1. The contract report transmitted herewith represents the results of an investigation to develop a model for predicting the short-term fate of dredged material discharged in the estuarine environment. This study is one of the major efforts to be accomplished under Task 1B (Movements of Dredged Material) of the Corps of Engineers' Dredged Material Research Program (DMRP). Task 1B is part of the Environmental Impacts and Criteria Development Project of the DMRP, which is a broad, multi-faceted investigation that includes the environmental impacts and other aspects of open-water disposal of dredged material.
2. Regardless of the location or character of a disposal site, an integral part of the problem of assessing the environmental impact of open-water disposal operations is the ability to determine the spatial and temporal distribution of the dredged material following its discharge into the water. The description of the fate of material discharged into an estuary requires a model of considerable generality and complexity. The estuarine environment may include time-dependent currents that vary significantly in three dimensions, density stratification, and depths variable in both time and space. The material itself may be a composite ranging from slow-settling extremely fine particles to fast-falling coarse particles and may include a solute fraction. All of these and many other factors contribute to the complexity of water quality impacts associated with the open-water discharge of dredged material. Modeling the physical fate of dredged material will be a significant aid in the prediction of these impacts.
3. This report describes two numerical models developed during the study: one for instantaneous dumped discharge and one for fixed or moving jet discharge. The two models were developed from the Koh-Chang model that was originally designed for the barged ocean disposal of wastes. In each model, the appropriate short-term portion of the Koh-Chang model was modified and coupled to an extensive modification of a model for long-term diffusion of chemical wastes in an estuary. The models are capable of tracking up to 12 types of solid fractions and a fluid fraction through short-term dynamic phenomena and through long-term passive diffusion. The models do this for complex estuarine situations.

WESYV

30 June 1976

SUBJECT: Transmittal of Contract Report D-76-5

4. Important in the development of these models for full field utility is a comprehensive verification program. This field verification should take place in conjunction with actual discharges of dredged material and should include characteristics of the discharge, the ultimate deposition of the material discharged, and the ambient conditions during and following the discharge. Steps have already been taken under the DMRP to plan and implement field verification that will determine the confidence limits within which the model may be applied.

5. It is anticipated that, after field verification, this model will be useful in the impact evaluation of major aquatic discharges encompassing several hundred thousand cubic metres of material. The model may also find use for those smaller operations where there is significant controversy about the physical fate of this material. The model would not be used on an "everyday" basis for smaller projects where impacts are considered minimal or are fairly localized and well documented. This is in fact due to the dependency on good quality data for ambient (disposal site) water current velocities and directions. While the model will accept fairly simplified input, those users striving for the most accurate results will need to spend considerable time in determining the ambient current velocities. In fact, for highly stratified estuaries of complex geometry, almost the entire effort of a modeling program may be devoted to the determination of the hydrodynamic characteristics of the discharge site.



G. H. HILT
Colonel, Corps of Engineers
Director

REPORT DOCUMENTATION PAGE		READ INSTRUCTIONS BEFORE COMPLETING FORM
1. REPORT NUMBER Contract Report D-76-5	2. GOVT ACCESSION NO.	3. RECIPIENT'S CATALOG NUMBER
4. TITLE (and Subtitle) DEVELOPMENT OF MODELS FOR PREDICTION OF SHORT-TERM FATE OF DREDGED MATERIAL DISCHARGED IN THE ESTUARINE ENVIRONMENT	5. TYPE OF REPORT & PERIOD COVERED Final report	
	6. PERFORMING ORG. REPORT NUMBER TC-406	
7. AUTHOR(s) Maynard G. Brandsma David J. Divoky	8. CONTRACT OR GRANT NUMBER(s) DACW39-74-C-0075	
9. PERFORMING ORGANIZATION NAME AND ADDRESS Tetra Tech, Incorporated 630 North Rosemead Boulevard Pasadena, California 91107	10. PROGRAM ELEMENT, PROJECT, TASK AREA & WORK UNIT NUMBERS Work Unit 1B02	
11. CONTROLLING OFFICE NAME AND ADDRESS Office, Chief of Engineers, U. S. Army Washington, D. C. 20314	12. REPORT DATE May 1976	
	13. NUMBER OF PAGES 290	
14. MONITORING AGENCY NAME & ADDRESS (if different from Controlling Office) U. S. Army Engineer Waterways Experiment Station, Environmental Effects Laboratory P. O. Box 631, Vicksburg, Mississippi 39180	15. SECURITY CLASS. (of this report) Unclassified	
	15a. DECLASSIFICATION/DOWNGRADING SCHEDULE	
16. DISTRIBUTION STATEMENT (of this Report) Approved for public release; distribution unlimited		
17. DISTRIBUTION STATEMENT (of the abstract entered in Block 20, if different from Report)		
18. SUPPLEMENTARY NOTES		
19. KEY WORDS (Continue on reverse side if necessary and identify by block number) Dredged material disposal Estuarine environment Mathematical models		
20. ABSTRACT (Continue on reverse side if necessary and identify by block number) The Dredged Material Research Project (DMRP) has as one of its objectives to provide more definitive information on the environmental aspects of dredging and dredged material disposal operations. This study was conducted to fill the need of that program for the capability of predicting the short-term fate of dredged material discharged in the estuarine environment. Two numerical models were developed: one for the instantaneous dumped discharge and one for fixed or moving jet discharge. The models account for land boundaries, depth (Continued)		

20. ABSTRACT. Continued.

variations in the estuary, ambient current variations in three dimensions and in time, and variations of ambient density profiles in time. The models are capable of tracking up to twelve classes of solid particles plus the fluid fraction of a discharge through convective descent, dynamic collapse, and passive diffusion phases. The models were developed by coupling the appropriate short-term dynamic portions of the Koh-Chang oceanic disposal model with an extensive modification of a model, originally developed by Fischer, for predicting the fate of chemical wastes in an estuary. Although the models themselves are extremely complex, the input data requirements for most cases are quite simple and should allow the first-time user to run a simple case in a few hours. The models have undergone limited testing and the results produced are physically reasonable. A program of model exercise and testing is strongly recommended, however. When the models are used in cases involving complex ambient velocities, the models will be extremely dependent on good-quality velocity data.

THE CONTENTS OF THIS REPORT ARE NOT TO
BE USED FOR ADVERTISING, PUBLICATION,
OR PROMOTIONAL PURPOSES. CITATION OF
TRADE NAMES DOES NOT CONSTITUTE AN
OFFICIAL ENDORSEMENT OR APPROVAL OF
THE USE OF SUCH COMMERCIAL PRODUCTS.

PREFACE

The work described in this report was performed under Contract DACW39-74-C-0075, titled, "Development of a Model for Prediction of Short-Term Fate of Dredged Material Discharged in the Estuarine Environment," dated March 1974 to June 1975, between the U. S. Army Engineer Waterways Experiment Station (WES), Vicksburg, Mississippi, and Tetra Tech, Inc., Pasadena, California. The research was sponsored by the Environmental Effects Laboratory (EEL), WES, under the Dredged Material Research Program (DMRP) Work Unit 1B02.

The report describes two numerical models developed during the study: one for instantaneous dumped discharge and one for fixed or moving jet discharge.

The study was performed and the report written by Mr. Maynard Brandsma with the assistance and supervision of Mr. David Divoky. Other individuals contributed significantly to the study: Dr. Li-San Hwang provided overall direction and assistance in project planning; Dr. Hugo Fischer provided advice and helpful participation in the initial planning; and Dr. Robert Koh served as project consultant throughout the study. His contributions were both major and pervasive extending from concepts to execution, and are most gratefully acknowledged.

The contract was monitored by Dr. Robert M. Engler, Project Manager of the Environmental Impacts and Criteria Project, DMRP, under the general supervision of Dr. John Harrison, Chief, EEL. Other WES personnel, Dr. Billy H. Johnson and Mr. Barry W. Holliday, maintained close contact with the development of the models and provided much useful advice, data, and guidance.

Contracting officer was COL G. H. Hilt, Director, WES. Technical Director was Mr. F. R. Brown.

TABLE OF CONTENTS

	<u>Page</u>
1. INTRODUCTION	1
2. MODELING OF DREDGED MATERIAL DISCHARGED INTO THE ESTUARINE ENVIRONMENT	5
2.1 Characteristics of Dredged Material Discharges	5
2.2 Estuarine Ambient Conditions	7
2.2.1 Classification of Estuaries	7
2.2.2 Types of Estuarine Circulation	10
2.2.2.1 Strongly Stratified or Salt-Wedge Estuaries	10
2.2.2.2 Two-Layer Flow with Entrainment (Fjord Flow)	11
2.2.2.3 Two-Layer Flow with Vertical Mixing (Partially Mixed Estuary)	11
2.2.2.4 Vertically Mixed Estuaries	14
2.2.3 Approximation of Mixing in an Estuary	16
2.2.3.1 Diffusion Coefficients for Lateral Mixing	17
2.2.3.2 Diffusion Coefficients for Vertical Mixing	20
2.3 Requirements for Model	23
3. DEVELOPMENT OF MATHEMATICAL MODELS FOR DYNAMIC COMPUTATIONS	25
3.1 Introduction	25
3.2 Instantaneous Dumped Discharge	25
3.2.1 Convective Descent	26
3.2.2 Dynamic Collapse in Water Column	35
3.2.3 Dynamic Collapse on Bottom	46

TABLE OF CONTENTS
(Continued)

	<u>Page</u>
3.3 Jet Discharge	52
3.3.1 Convective Descent	53
3.3.2 Dynamic Collapse in Water Column	61
3.3.3 Dynamic Collapse on the Bottom	69
4. DEVELOPMENT OF MODEL FOR PASSIVE DIFFUSION	77
5. DESCRIPTION OF COMPUTER REALIZATIONS OF MODELS	88
5.1 Computer Code for Instantaneous Dump	88
5.2 Computer Code for Jet Discharge	101
6. EXAMPLE SOLUTIONS	112
7. SUMMARY AND RECOMMENDATIONS	126
LITERATURE CITED	128
BIBLIOGRAPHY	133
APPENDIX A - USER'S MANUAL Model for Instantaneous Dump Program DMF	
APPENDIX B - Listing of FORTRAN Program for Modeling Instantaneous Dumped Discharge of Dredged Material	
APPENDIX C - USER'S MANUAL Model for Jet Discharge Program DMFJ	
APPENDIX D - Listing of FORTRAN Program for Modeling Fixed or Moving Jet Discharge of Dredged Material	
APPENDIX E - Notation	

LIST OF FIGURES

<u>Figure</u>	<u>Title</u>	<u>Page</u>
2.1	Cross Section of a Salt-Wedge Estuary	12
2.2	Two-Layer Flow with Entrainment	13
2.3	Two-Layer Flow with Vertical Mixing	15
2.4	Horizontal Diffusion Coefficient as a Function of Horizontal Scale	18
3.1	Idealized Instantaneous Dump of Dredged Material Described by the Mathematical Model Developed for Descent and Collapse in the Water Column	27
3.2	Illustration of Idealized Bottom Encounter After Instantaneous Dump	28
3.3	Diagram of Descending Hemispherical Cloud	29
3.4	Aspects of Cloud Collapse	37
3.5	Slice of Collapsing Cloud	41
3.6	Idealized Jet Discharge from Moving Vessel which is Described by the Mathematical Model Developed in Section 3.2	54
3.7	Definition Sketch for a Round Jet	55
3.8	Geometry of the Collapsing Jet Plume	62
4.1	Aspects of Passive Diffusion	80
5.1	Diagram of Long-Term Passive Diffusion Grid	89
5.2	Illustration of the Various Velocity Profiles Available for Use in the Model	91
5.3	Block Diagram of Dump Discharge Model	95

LIST OF FIGURES
(continued)

<u>Figure</u>	<u>Title</u>	<u>Page</u>
5.4	Block Diagram of Jet Discharge Model	103
6.1	Listing of a Simple Program to Prepare Velocity Tape	113
6.2	Listing of Input Data for Instantaneous Dump Case	114
6.3	Input Documentation of Dump Model	115
6.4	Plot of Short-Term Behavior of the Cloud	117
6.5	Typical Printout of Solids Distribution on the Bottom	118
6.6	Printout Showing Location of the Fluid Cloud	119
6.7	Fluid Cloud Shortly After Reversal of the Ambient Velocity Field. Printout of Dilution Time at Conclusion of Calculation is also Shown	120
6.8	Portion of the Input Documentation for Jet Discharge Model	121
6.9	Results of Dynamic Computations for Jet Dis- charge from Moving Barge	122
6.10	Solids Distribution and Dilution Times for Jet Discharge.	123
6.11	Final Distributions of Solids for Fixed Pipeline Discharge.	125

LIST OF TABLES

<u>Table</u>	<u>Title</u>	<u>Page</u>
2.1	Typical Characteristics of Dredge Discharges	6
2.2	Typical Characteristics of Dredged Material at Discharge	8
2.3	Great Lakes Dredged Material Characteristics.	9
2.4	Summary of Formulas on Correlation of Vertical Diffusion Coefficient K_y with Richardson Number	22

CONVERSION FACTORS, U. S. CUSTOMARY TO
METRIC (SI) UNITS OF MEASUREMENT

U. S. customary units of measurement used in this report can be converted to metric (SI) units as follows:

<u>Multiply</u>	<u>By</u>	<u>To Obtain</u>
feet	0.3048	meters
square feet	0.09290304	square meters
cubic yards	0.7645549	cubic meters
feet per second	0.3048	meters per second
feet per hour	0.3048	meters per hour
knots (international)	0.5144444	meters per second
square feet per second	0.09290304	square meters per second
cubic feet per second	0.02831685	cubic meters per second

1. INTRODUCTION

This report presents the results of an effort to develop a numerical model of the short-term fate of dredged material discharged into an estuary. The project was sponsored by the U. S. Army Corps of Engineers as part of Task 1B (Fate of Dredged Materials) of the Dredged Material Research Program (DMRP). That large interdisciplinary program is concerned with all aspects of the dredging and disposal problem, the present topic being but a very small part. Nevertheless, it is an essential part for it addresses the fundamental question of where the material goes when discharged into the aquatic environment. Only when that question is answered can one proceed to evaluate, for example, the environmental impact of the discharge, the relative merits of alternate sites, and so forth.

The description of fate of material discharged into an estuary requires a model of considerable generality and complexity. The estuarine environment may include time-dependent currents varying significantly in three dimensions, density stratification, and depths variable in both time and space. The material itself may be a composite ranging from slow-settling extreme fines to fast-falling coarse particles and including a solute fraction. The mode of discharge might be a simple bottom dump from a barge or an extended jet discharge from a fixed or moving source. In either the dump or jet discharge case, one may be concerned with a wide range of discharge quantity, barge course and speed, discharge point depth, initial velocity of the discharge, and so on.

In contrast to the complexity of the processes being modeled, the model itself must be as simple to use as possible.

No matter how accurate, a program either too costly or too unwieldy would not be satisfactory. What is needed instead is a working tool suitable for practical application to a variety of conditions. It should not demand too much from the user in the way of input requirements, but on the other hand, it should be capable of taking as much information as he can supply in the fortunate event that a detailed description of the discharge and receiving environment is available. In large measure, such considerations have guided the form and content of the present work.

The model developed here was not begun from scratch. Instead, the study had the great advantage of building upon a model for ocean dumping developed at Tetra Tech by Koh and Chang (1973). The Koh-Chang model was identified by the Corps in their survey of available models (Johnson, 1974) as the most suitable basis for development of the more general estuarine model. In brief, the Koh-Chang model considers the ambient fluid to have a steady current structure uniform in the horizontal but varying in direction and speed with depth. Furthermore, the fluid is assumed to be density stratified with an arbitrary gradient uniform in the horizontal. The discharged material is taken to consist of a composite of discrete particle types, described by fall velocity and density, and a fluid fraction.

The behavior of material after release is considered to divide into three phases: convective descent, during which the material tends to fall as a cloud under the influence of gravity; dynamic collapse, occurring when the descending cloud either impacts the bottom or arrives at the level of neutral buoyancy at which descent is retarded and horizontal spreading dominates; and long-term passive dispersion, commencing when the cloud trans-

port and spreading is determined more by ambient currents and turbulence than by any dynamic character of its own.

For the present development it has been possible to retain much of the structure of the first two phases of the Koh-Chang model. The major modifications are those needed to permit unsteady currents and current variations in the horizontal in addition to the vertical. However, the third phase has required a new treatment. An approach developed by Fischer (1972), which is well suited to the present need, was adopted. Fischer's model--developed for the two-dimensional vertically integrated case--treats the convection and dispersion of a suspended material in an extremely efficient manner. Material concentrations are defined on a rectangular mesh system and are computed at successive time intervals, which can be quite large. For the present application, it was necessary to incorporate vertical resolution of material concentrations, settling behavior, density gradients, and so forth. Nevertheless, the method remains very economical and well suited for coupling with the earlier phases treated by the modified Koh-Chang model.

Despite the relative complexity of the overall model, it is not difficult to run. Input is relatively simple, the major labor being that required to set up the long-term depth grid and velocity tape. Once these are established for a given site, any number of simulations may be performed with very simple input modifications.

Two models are described in this report, one for a simple dump and another for a fixed or moving jet discharge. The model features are described in Chapters 3 (dynamic phases) and 4 (passive phase); while Chapter 5 describes the numerical codes.

Chapter 6 presents sample cases. A summary and recommendations appear in Chapter 7. Detailed user's manuals and program listings are contained in the Appendices.

2. MODELING OF DREDGED MATERIAL DISCHARGED INTO THE ESTUARINE ENVIRONMENT

2.1 Characteristics of Dredged Material Discharges

The parameters characterizing dredged material discharges fall into two categories: those describing the method of discharge and those describing the physical properties of the material discharged.

According to Boyd et al. (1972), hydraulic pipeline dredges account for some 69 percent of annual dredged material volume, with hopper dredges accounting for 24 percent, and all other types accounting for 7 percent.

Pipeline discharges may be characterized by flow rate of the dredged material slurry, depth of the discharge nozzle, the discharge angle below the horizontal, and the direction and speed (if any) of the discharging vessel. Hopper dredge discharges may in some cases be characterized in the same manner as pipeline discharges (i. e. , a high flow rate for a short time). Hopper dredge discharges may also be assumed to be instantaneous discharges characterized by volume of discharge and initial velocity of slurry cloud centroid. Table 2.1 shows the range of typical values for these parameters.

The physical properties of dredged material enter into consideration in this report only to the extent that they influence the short-term fate of the material. Most dredged material is a mixture of various soils with fluid. A high proportion of the total volume is usually fluid. Other materials that may be included are rock, pieces of glass, metal, wood, and other debris. There is at present no standard method for classification of dredged material. This

TABLE 2.1

TYPICAL CHARACTERISTICS OF DREDGE DISCHARGES *

Site	Vessel or Dredge Type	Average Volume (yd ³)**	Average Duration (sec)	Number of Discharge Openings	Area of One Discharge Opening (ft ²)	Depth of Discharge Openings	Vessel Speed (ft/sec)
Eatons Neck, NY	Scow	500-3000	180-600	6-8	100	12-15	1.7-3.4
New Haven, CN	Scow	1000-3000	300-600	6-8	100	12-15	1.7-3.4
Galveston, TX	Hopper	1200-1500	60-2400	6	56	21-23	6.8-10.2
Columbia River, WA	Hopper	2900	750	12	21	20-22	0
Ashtabula, OH	Hopper	1700	60-180	8	13.7	14	0

* This information was compiled from personal communications with B. W. Holliday, Environmental Effects Laboratory (EEL), and B. H. Johnson, Hydraulics Laboratory (HL), of the Waterways Experiment Station, Vicksburg, Mississippi.

** A table of factors for converting U. S. customary units of measurement to metric (SI) units is presented on page xiii.

material can be roughly divided into three different types: coarse-grained, fine-grained, and organic material. The latter two types normally cause the water-quality problems associated with dredging.

Physical properties that must be considered in calculations of dredged material fate include: the bulk density of the dredged material slurry, the particle-size distribution, the particle densities, and the voids ratios. Table 2.2 summarizes these characteristics for a variety of dredged material disposal sites. Table 2.3 gives more detailed information for several sites in the Great Lakes.

2.2 Estuarine Ambient Conditions

2.2.1 Classification of Estuaries

Pritchard (1967) defines an estuary as a semi-enclosed coastal body of water that has a free connection with the open sea and within which seawater is measurably diluted with fresh water derived from land drainage. The term "semi-enclosed" in the definition indicates the strong influence of the lateral boundaries upon circulation patterns within the estuary. "Free connection" means that the estuary receives tidal energy and sea salts from the ocean. Estuaries in which freshwater drainage and precipitation exceed evaporation so that the salinity is less than that in the ocean have been termed positive estuaries. Negative estuaries are those in which evaporation exceeds freshwater inflow, leading to hypersaline conditions. Most estuaries are positive.

Various investigators classify estuary types in different ways: by the geomorphology, by the dominant physical processes in movement and mixing within the estuary, and by the salinity

TABLE 2.2

TYPICAL CHARACTERISTICS OF DREDGED MATERIAL AT
DISCHARGE *

Site	Average Bulk Density (gm/cc)	Average Solids Concentration (Volume Ratio)	Average Solids Density (gm/cc)	Particle Size Description
Eatons Neck, NY	1.3	.19	2.6	Mostly fine-grained material, mud, sand, silt
New Haven, CN	1.3	.19	2.6	Mud and organic silt
Galveston, TX	N/A	N/A	2.67	Silty sand, sandy silt and sandy clay
Columbia River, WA	N/A	N/A	2.72	2% medium sand 98% fine sand
Ashtabula, OH	N/A	N/A	2.48	Sand, silt and clay

* This information was compiled from personal communications with B. W. Holliday, Environmental Effects Laboratory (EEL), and B. H. Johnson, Hydraulics Laboratory (HL), of the Waterways Experiment Station, Vicksburg, Mississippi.

TABLE 2.3

GREAT LAKES DREDGED MATERIAL CHARACTERISTICS *

Location	Percent Solids	Average Density (gm/ml)	Settling Velocity (ft/hr <u>a/</u>)	Average Percentage by Weight			
				Gravel (d>2 mm)	Sand (63 μ <d<2mm)	Silt (4 μ <d<63 μ)	Clay (d<4 μ)
Buffalo, NY	37.0	1.27	0.068	0.1	18.4	70.6	10.7
Calumet, MI	40.7	1.33	0.144	0.2	20.8	48.5	31.1
Cleveland, OH	44.9	1.36	0.201	1.9	9.1	72.3	16.0
Green Bay, WI	43.0	1.37	0.103	10.6	29.1	26.2	34.1
Indiana, IL	35.2	1.23	0.150	1.9	29.2	53.1	13.8
Rouge River, MI	43.7	1.28	0.290	1.9	40.9	35.9	20.7
Sodus Bay, NY	53.1	1.51	0.506	0.0	50.8	41.2	8.1
Toledo, OH	39.0	1.30	0.023	0.8	10.9	47.2	41.1

a/ Based on 30 minute settling

Average Bulk Density = 1.33 m/LL
Average Solid Concentration = 40%
Average Settling velocity = 0.5×10^{-4} ft/sec

* From Clark et al (1971)

structure. Geomorphological classifications divide estuaries into four types: (1) drowned river valleys, (2) fjord-type estuaries, (3) bar-built estuaries, and (4) estuaries produced by tectonic processes. Classifications by physical processes divide estuaries into groups where the movement and mixing is dominated by winds or tides or river flow. Cameron and Pritchard (1963) have classified estuaries according to their salinity distributions and stratification characteristics. The four main types are: highly stratified or salt-wedge estuaries, fjords, partially mixed estuaries, and homogeneous estuaries. This last group is further divided into laterally and sectionally homogeneous types.

There is some correlation among the results of classification by geomorphology, physical processes, and salinity structure.

2.2.2 Types of Estuarine Circulation

In the present work, the most important estuarine characteristic is the pattern of water circulation. This is generally a function of the estuary type as characterized by its geomorphology and by the relative strengths of river flow, tides, and winds. Following is a discussion similar to those by Bowden (1967) and Dyer (1973) on the circulation characteristics typical of estuaries.

2.2.2.1 Strongly Stratified or Salt-Wedge Estuaries

In an estuary where the freshwater inflow is the dominant process, the fresh water lies over a layer of saline water that extends as a wedge into the river. If there were no friction, the interface would be horizontal and extend upriver to the point where

the bed is at sea level. Since there is a small amount of friction, the interface slopes slightly downward in the upstream direction. The steep density gradient at the interface greatly inhibits vertical mixing. Figure 2.1 shows a section along a salt-wedge estuary with typical salinity and velocity profiles.

3.2.2.2 Two-Layer Flow with Entrainment (Fjord Flow)

This type of flow occurs when the velocity of the seaward moving layer of fresh water is great enough to cause breaking internal waves at the interface. This breaking causes entrainment of salt water into the upper freshwater layer, which results in a slow movement of salt water upward into the freshwater layer. In the ideal case, there is no corresponding movement of fresh water down into the saltwater layer. The salinity and volume of the water in the upper layer are increased by entrainment. The increased volume usually results in an increased flow velocity rather than an increase in the depth of the layer. The salinity of the lower layer is unchanged and there is a slow upstream movement to compensate for the entrained fluid. In the usual nonideal case, there is a certain amount of vertical mixing that results in low salinity water from the upper layer moving down into the lower layer. In this case the interface is replaced by a steep density gradient. This is the type of flow commonly occurring in fjords. Figure 2.2 shows the structure of two-layer flow with entrainment.

2.2.2.3 Two-Layer Flow with Vertical Mixing (Partially Mixed Estuary)

In a comparatively shallow estuary, tidal currents become increasingly important, causing vertical mixing through the entire water column. There is no sharp halocline, but the salinity

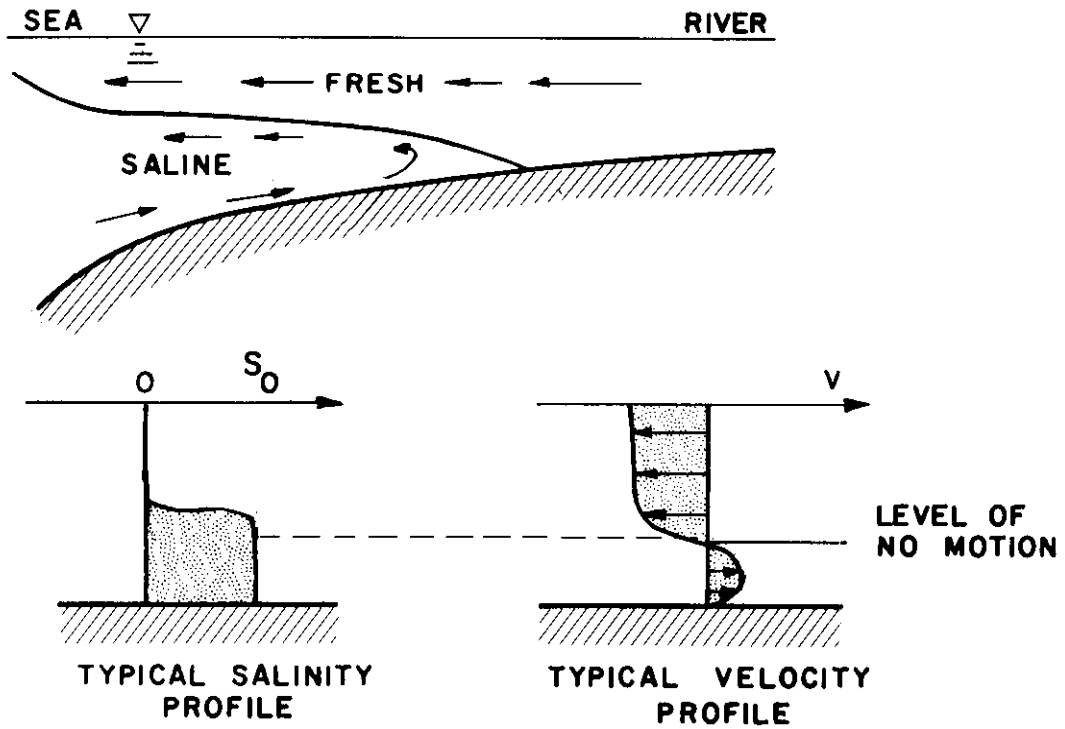


Figure 2.1 Cross Section of a Salt-Water Estuary with Typical Salinity and Velocity Profiles (after Bowden, 1967)

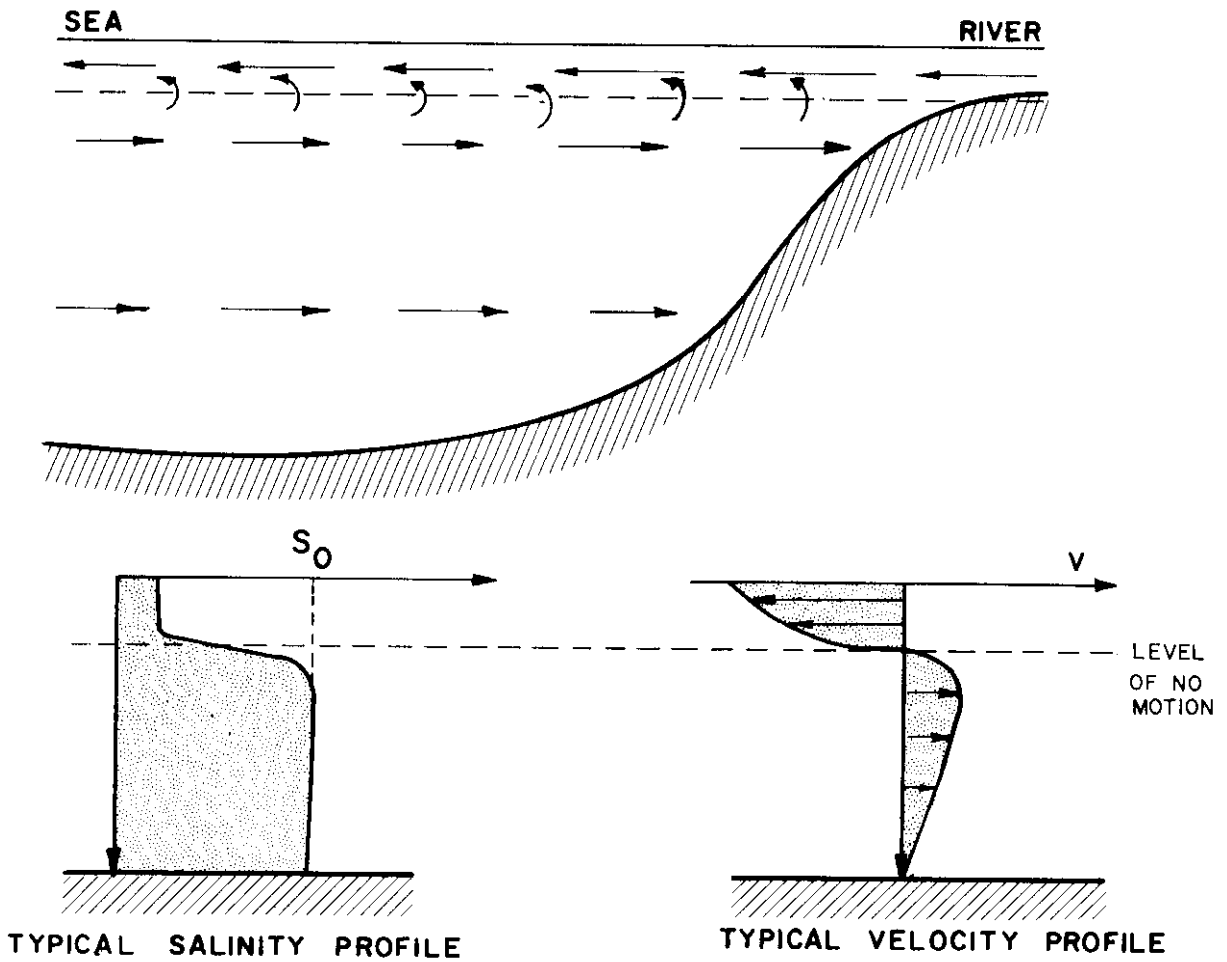


Figure 2.2 Two-Layer Flow with Entrainment Showing Typical Salinity and Velocity Profiles (after Bowden, 1967)

increases steadily with depth. The maximum salinity gradient occurs near the level of no motion. The amount of mixing depends upon the ratio of tidal current amplitude to river flow. Since this ratio may vary widely, there is a similar variation in the degree of stratification to be expected. The variation in salinity from surface to bottom may range between 10‰ and 1‰. The total flow volume in this type of estuary may be many times the river flow. Figure 2.3 illustrates the characteristics of a partially mixed estuary.

2.2.2.4 Vertically Mixed Estuaries

Very strong tidal currents can provide sufficient vertical mixing to destroy any salinity gradient. Though there is essentially no variation in salinity from surface to bottom, there is some horizontal variation in salinity from the head to the mouth of the estuary. Estuaries of this type are subdivided into laterally homogeneous estuaries and estuaries with lateral variation.

Lateral variations in salinity may occur in estuaries with a sufficiently large width-to-depth ratio. This variation is caused by the Coriolis force, and the salinity decreases to the right of an observer looking downstream (in the northern hemisphere). There is a net seaward flow of lower salinity water on the right-hand side (looking downstream) and a compensating landward flow of higher salinity water on the left-hand side.

If the width-to-depth ratio is small, there is frequently little variation in salinity across the channel.

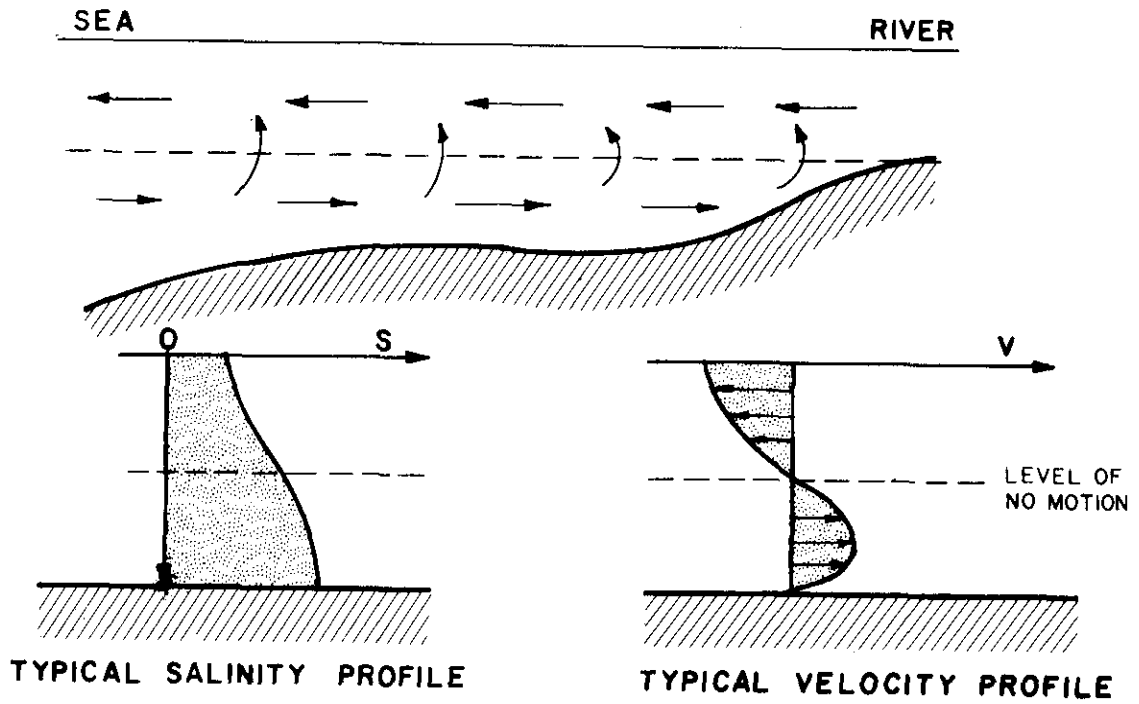


Figure 2.3 Two-Layer Flow with Vertical Mixing, Showing Typical Salinity and Velocity Profiles (after Bowden, 1967)

Because of the extremely complicated nature of the circulation in estuaries, techniques for modeling these water bodies invariably involve some averaging process. These simplified models contain two types of terms describing the transport of suspended or dissolved material through the estuary. Convective terms describe the gross movement of material, while the dispersive terms lump together all the effects of averaging. The dispersive terms contain a coefficient known variously in the literature as a coefficient of turbulent or eddy dispersion, diffusion, or mixing. This variation in terminology has caused a certain amount of confusion; following is a brief digression to discuss the meanings of these terms.

Spreading of a tracer patch associated with molecular action and with turbulence is properly called diffusion; while spreading associated with velocity variations across the patch is termed dispersion. More rigorously, Holley (1969) has proposed the following definitions. Diffusion is spreading in a given direction at a point in the flow due to the difference between true convection in that direction and the time average of the convection in that direction. Dispersion is the spreading in a given direction due to the difference between true convection in that direction and the spatial average in that direction. The magnitudes of these two effects may be seen to depend upon the temporal and spatial scales used in the averaging process. In comparison, the magnitude of molecular diffusion is very small and henceforth will be neglected.

The perceptive reader will realize that dispersion or diffusion are more characteristic of the modeling technique than they are inherent properties of the estuary being modeled. In other words,

if each point in a tracer patch could be convected with the velocity at that point alone and if this could be done very many times with very small time steps, then the spreading of the patch would be completely described by convective terms, and there would be no need for dispersion or diffusion terms or the associated coefficient. Since this kind of detail is not feasible at present, it is necessary to resort to diffusion or dispersion coefficients.

For convenience in the rest of this report, the term diffusion will be used to include the effects of both diffusion and dispersion.

2.2.3.1 Diffusion Coefficients for Lateral Mixing

Experimental studies have shown that diffusion coefficients are not constant entities but rather depend upon the relative length scales of the cloud of diffusing material and the turbulent eddies and also on the gross current pattern. To amplify a little: a cloud of diffusing material sees an eddy very much larger than itself as a current convecting it along but not causing it to disperse; but when the cloud grows to a size comparable to the eddy, then the cloud sees the eddy as shearing currents acting to disperse it.

Most studies of horizontal diffusion have concentrated on the ocean. These have consisted of the release of dye or some other tracer to form a cloud that was observed (at the surface) as it grew with time. Horizontal diffusion coefficients were then derived based upon some diffusion model and ignoring current shear and vertical currents. The values obtained in these studies are plotted in Figure 2.4, which shows an increase in the diffusion coefficient with the size of the diffusing patch. Although the data are fairly scattered, the general

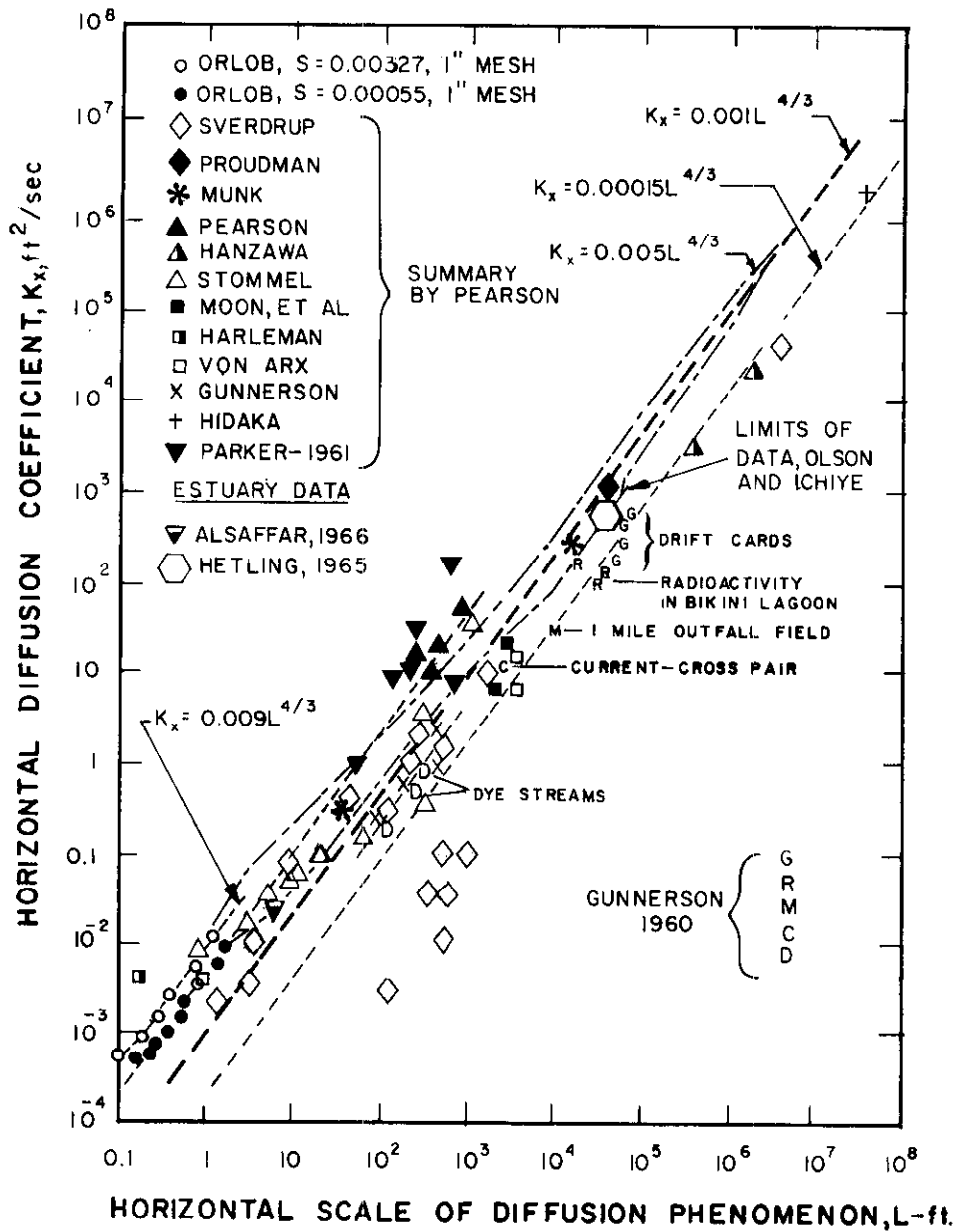


Figure 2.4 Horizontal Diffusion Coefficient as a Function of Horizontal Scale (adapted from Orlob, 1959). The results of investigators working in estuaries have been added.

trend follows a four-thirds power law:

$$K_x = A_L L^{4/3} \quad (2.1)$$

where K_x is the horizontal diffusion coefficient and A_L is a constant called the dissipation parameter ($\text{ft}^{2/3}/\text{sec}$ in fps system and $\text{cm}^{2/3}/\text{sec}$ in cgs system). The value of A_L varied from 0.005 to $0.00015 \text{ ft}^{2/3}/\text{sec}$. Diffusion coefficients obtained in the ocean are not strictly applicable to the flow situations found in estuaries; however, they are useful in illustrating trends and magnitudes.

There have been few investigations of diffusion coefficients in tidal estuaries. Alsaffar (1966) performed a limited number of experiments in the tidal estuary of the San Joaquin River in California. His data were obtained by photographing floating particles. They were obtained within a relatively small region of the estuary. Analysis by Richardson's neighbor distribution hypothesis showed the data could be represented by a four-thirds law. His results are plotted in Figure 2.4. Hetling et al.(1965) estimated diffusion coefficients for the Potomac River Estuary by three different methods: by a four-thirds law, by a random process analogy, and by a turbulent pipe flow analogy. The four-thirds law and the random process analogy formulas gave diffusion coefficients in the proper order of magnitude for the brackish portion of the Potomac Estuary. The four-thirds law results were verified by chlorinity data. These results are also plotted in Figure 2.4.

It can be seen that the estuary data lies right in the ocean data. This permits more confidence in applying a four-thirds law to the estimation of horizontal diffusion coefficients in estuaries.

2. 2. 3. 2 Diffusion Coefficients for Vertical Mixing

The presence of density stratification in an estuary tends to suppress vertical mixing. The vertical diffusivity is expected to be a monotonically decreasing function of density stratification. Velocity shear tends to be a destabilizing influence with consequent increase in vertical mixing. Vertical diffusivity, then, can be expected to be a monotonically increasing function of velocity shear. Experiments have shown that vertical diffusivity is a monotonically nonincreasing function of the gradient Richardson number defined as:

$$R_i = \frac{\frac{g}{\rho} \cdot \frac{d\rho}{dy}}{\left(\frac{du}{dy}\right)^2} \quad (2.2)$$

This agrees with the intuitive notions stated above.

Kent and Pritchard (1959) give the dependence of K_y on R_i as

$$K_y = K_{y_0} (1 + \beta R_i)^{-2} \quad (2.3)$$

where $K_{y_0} = K_y$ for $R_i = 0$; and β is a constant which they determined to be 0.276 from their James River data. They gave K_{y_0} for a vertically well-mixed estuary with no wind as

$$K_{y_0} = 8.6 \times 10^{-3} \frac{Uz^2 (h-z)^2}{h^3} \quad (2.4)$$

where U is the mean horizontal velocity; z is the depth of the point of interest; and h is the bottom depth. The maximum value, occurring at mid-depth, was found to be $5.4 \times 10^{-4} Uh$. For a depth of 50 feet and mean velocity of 2 feet/sec, the value 0.05 is suggested for K_{y_0} . For cases where there is no velocity gradient, Pritchard (1960) defined a Richardson number to apply to the whole depth; it is

$$R_i = \frac{\frac{g}{\rho} \cdot \frac{\partial \rho}{\partial y}}{\left(0.7 \frac{U}{h}\right)^2} \quad (2.5)$$

Numerous proposed relations between K_y and R_i are summarized in Table 2.4. The relationships all show correct trends, although magnitudes are different. The relations show the decrease of K_y with increasing R_i . The relations proposed by Holzman (1943) and Yamamoto (1959) (both as given by Okubo, 1962) show a limiting value of R_i at which K_y vanishes.

Experiments indicate that there is little vertical mixing when the stability of the ambient water is greater than that corresponding to $R_i = 4$. If the simple relation of Holzman is employed, then the limiting R_i of 4 implies a value for β of 0.25. This gives

$$K_y = K_{y_0} (1 - 0.25 R_i) \quad 0 \leq R_i \leq 4 \quad (2.6)$$

as a simple, physically reasonable estimate of the vertical diffusion coefficient. It must be emphasized that this relation should be viewed with skepticism and revised as soon as adequate data are available.

TABLE 2.4

SUMMARY OF FORMULAS
ON CORRELATION OF VERTICAL DIFFUSION COEFFICIENT K_y
WITH RICHARDSON'S NUMBER R_i (OR DENSITY GRADIENT ϵ)

Note: K_{y_0} : K_y at $R_i = 0$, i. e., the neutral case β : proportionality constant varies from case to case.

INVESTIGATOR	PROPOSED RELATIONSHIP
Rossby and Montgomery (1935)*	$K_y = K_{y_0} (1 + \beta R_i)^{-1}$
Rossby and Montgomery (1935)*	$K_y = K_{y_0} (1 + \beta R_i)^{-2}$
Kent and Pritchard (1959) **	$K_y = K_{y_0} (1 + \beta R_i)^{-2}$ $\beta = .276$ (from James River Data)
Holzman (1943)*	$K_y = K_{y_0} (1 - \beta R_i)$ $R_i \leq \frac{1}{\beta}$
Yamamoto (1959)*	$K_y = K_{y_0} (1 - \beta R_i)^{\frac{1}{2}}$ $R_i \leq \frac{1}{\beta}$
Mamayev (1958)*	$K_y = K_{y_0} \epsilon^{-\beta R_i}$
Munk and Anderson (1948)†	$K_y = K_{y_0} (1 + \beta R_i)^{-3/2}$ $\beta = 3.33$ based upon data by Jacobsen (1913) and Taylor (1931)
Harremoes (1967)	$K_y = 5 \times 10^{-3} \times \epsilon^{-2/3}$ cm ² /sec note: ϵ in m ⁻¹ ; approximate experimental range $5 \times 10^{-9} < \epsilon < 15 \times 10^{-5}$ m ⁻¹
Kolesnikov, et al (1961)††	$K_y = K_{y \text{ min}} + \frac{\beta}{\epsilon}$ in cm ² /sec $K_{y \text{ min}}$ and β are empirically de- termined to be: $K_{y \text{ min}} = 12$, $\beta = 8.3 \times 10^{-5}$ (1958 and 1960 observations) $K_{y \text{ min}} = 2$, $\beta = 10.0 \times 10^{-5}$ (1959 observations)
Koh and Fan (1969)	$K_y = 10^{-4}/\epsilon$ (K_y in cm ² /sec; ϵ in m ⁻¹) $4 \times 10^{-7} \leq \epsilon \leq 10^{-2}$ m ⁻¹

* As given by Okubo (1962)

** As given by Bowden (1967)

† As given by Bowden (1962)

†† The formulas presented in the translated version are apparently erroneous.

A model to predict the fate of dredged material in an estuary should be capable of modeling the short-term dynamic behavior of the types of discharges to be expected and be further capable of following the resultant cloud of material as it is passively diffused. This simulation should be performed while accounting for the ambient conditions of the estuary as they vary in three space dimensions and in time. In addition, the characteristics of the dredged material should be accounted for.

The ambient condition of primary importance is, of course, the velocity distribution. It should be possible to account (if only roughly) for any type of velocity situation to be encountered in an estuary (including reversing flows). Ambient density distributions are of extreme importance in the initial, dynamic stages of discharge and of relatively small importance during passive diffusion. During dynamic computations, the density distribution is a prime determinant of the equilibrium depth of the material cloud. This in turn strongly influences the distance which settling particles can travel during passive diffusion. The ambient density distribution is of lesser importance in passive diffusion (assuming velocity distributions are known) because its only influence is on vertical diffusion. It should be possible to vary the vertical density distribution in time in the case of jet or pipeline discharges that continue for a long period of time.

The model should be able to treat the discharge of any liquid-solid mixture and further be able to keep track of each class of solid particles in the slurry. This means that as different classes of

particles begin falling out of the main cloud or plume at different times and with different fall velocities, they are free to go their separate ways.

The above paragraphs list the physical requirements for a good simulation model. There are also user requirements to be satisfied. From the point of view of the user, the model should be versatile. That is, it should be possible, with extensive preparation, to make a good simulation of an extremely complicated discharge situation; but the same model should be capable of accepting minimal input for those times when the user just wants a "quick look" at some short-term effect.

Added to all of the above requirements is a requirement for clarity. Input data and output results should be clearly labeled. If it is possible for numerical problems to develop, then there should be adequate diagnostics to warn the user and inform him of necessary corrective action. Finally the user's manual should clearly show input requirements and include a discussion of possible trouble that may develop and suitable user response.

In summary, a versatile model that is easy (or at least straightforward) to use even if the code itself is very complicated is needed. This objective is addressed in the following chapters.

3. DEVELOPMENT OF MATHEMATICAL MODELS FOR DYNAMIC COMPUTATIONS

3.1 Introduction

This chapter outlines the mathematical treatment of the behavior of dredged material immediately after it is discharged from a barge or a pipeline. Two modes of discharge have been considered for analysis: instantaneous dumped discharge and jet discharge of arbitrary duration. In either case the material goes through three phases of motion: convective descent, dynamic collapse, and passive diffusion. The developments in this chapter are elaborations on those presented by Koh and Chang (1973) for the first two phases.

3.2 Instantaneous Dumped Discharge

The simplest method of discharge is by instantaneous release of material from a hopper barge. The analysis assumes a single cloud that maintains its identity during convective descent by the formation of a vortex ring structure. The initial cloud is assumed to be a hemisphere simply because this is a convenient figure with which to surround the vortex ring. If the initial cloud is not a hemisphere, it quickly becomes so because of the tendency of a vortex ring to draw fluid in from behind it. After release, the cloud of waste material will descend by virtue of its initial momentum and (negative) buoyancy. As it descends, it will displace the ambient fluid around it, experience drag from the flow field, and entrain some of the ambient fluid. Some of the solid particles contained in the cloud may settle out. In the presence of a stratified ambient fluid, the cloud may decelerate as it approaches the depth of neutral buoyancy, overshoot this point, rise above it, and then continue a decaying oscillation. At this point the vertical motion is much reduced and the

effects of density stratification become dominant. The cloud tends to collapse vertically and spread out horizontally seeking hydrostatic equilibrium with the ambient fluid, since the fluid outside is stratified while the fluid inside is mixed by turbulence. Figure 3.1 shows the phenomena modeled for an instantaneous dump in deep water and Figure 3.2 illustrates the case for shallow water.

3.2.1 Convective Descent

The analysis is based upon the work of Scorer (1957) and Woodward (1959) in establishing the characteristics of the flow field in and around a buoyant thermal. Their work treated clouds composed entirely of fluid. Since the solids concentration in discharged dredged material is usually low, the cloud is expected to behave as a dense liquid, and the buoyant thermal analysis is appropriate. Figure 3.3 shows a schematic diagram for the descending hemispherical cloud.

A mean radius and mean cloud velocity are defined as $a(t)$ and $\vec{U}(t)$ where t is time elapsed since release. Let $\rho(t)$ be the mean density of the element and $\rho_a(y)$ the ambient density. Let $\vec{U}_a(x, y, z, t)$ be the ambient current, which is assumed to be horizontal and variable in three dimensions and in time. The characteristics of the cloud are assumed to remain similar at all stages of the convective descent. The various solid particles inside are assumed to have densities ρ_i , fall velocities v_{fi} , and concentrations (volume ratio) C_{si} . The equations governing the motion are those for conservation of mass, momentum, buoyancy, solid particles, and vorticity.

The time rate of change of mass in the cloud is the rate of ambient fluid mass entrainment minus the rate of solids mass passing out of the cloud:

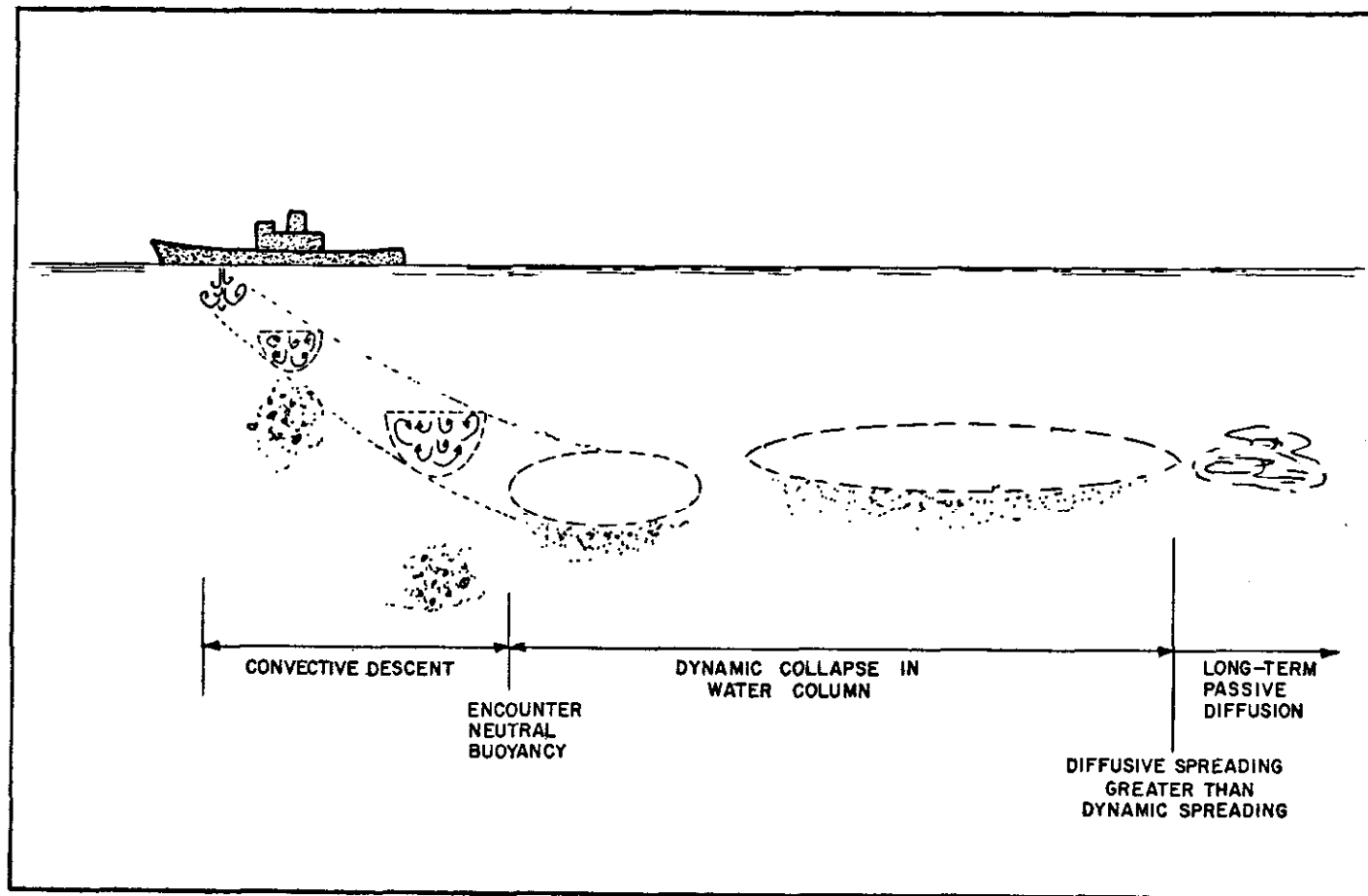


Figure 3.1 Idealized Instantaneous Dump of Dredged Material Described by the Mathematical Model Developed for Descent and Collapse in the Water Column of Section 3.1. Various classes of solid particles are illustrated settling out of the cloud at different times.

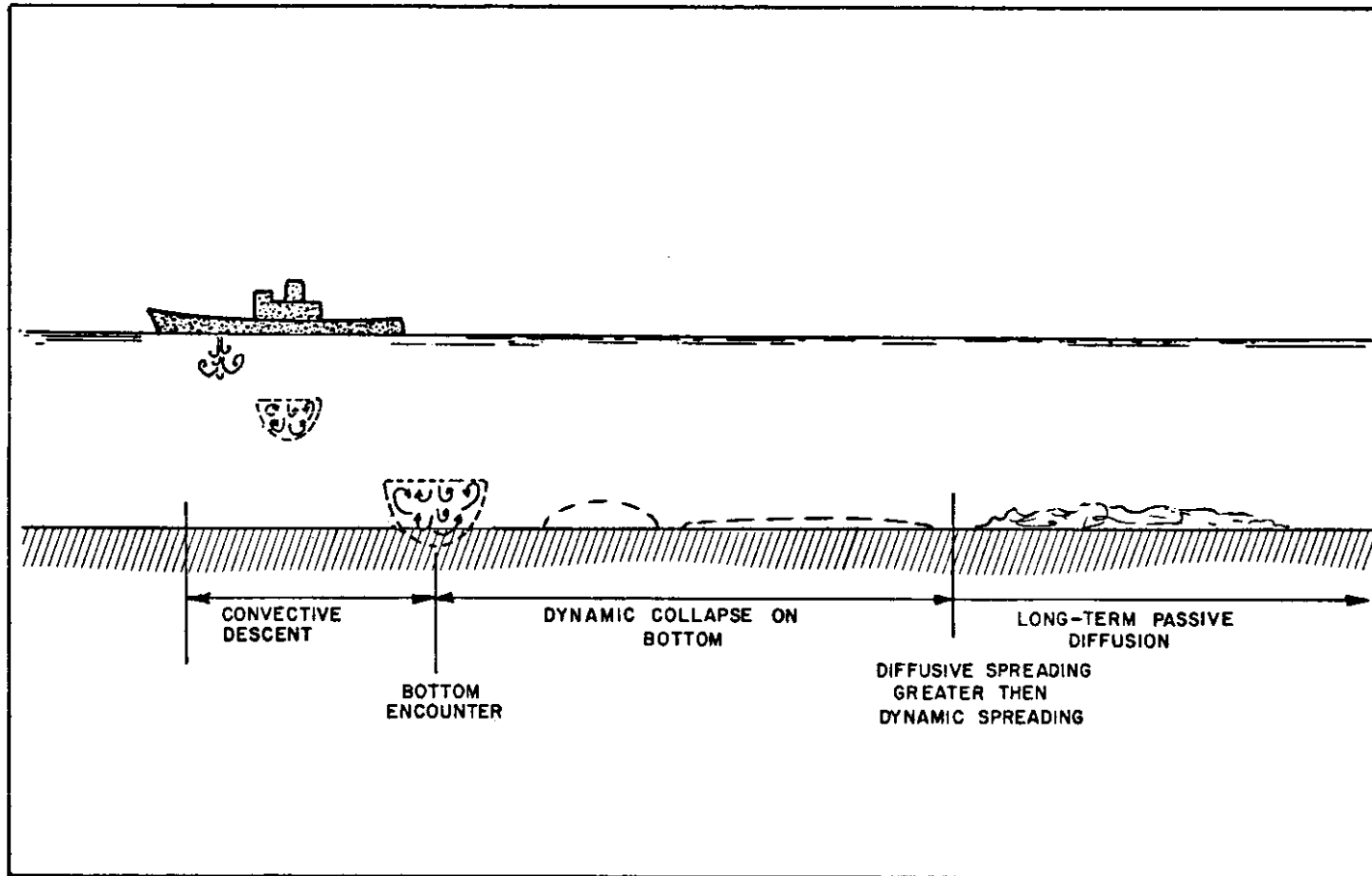


Figure 3.2 Illustration of Idealized Bottom Encounter After Instantaneous Dump of Dredged Material

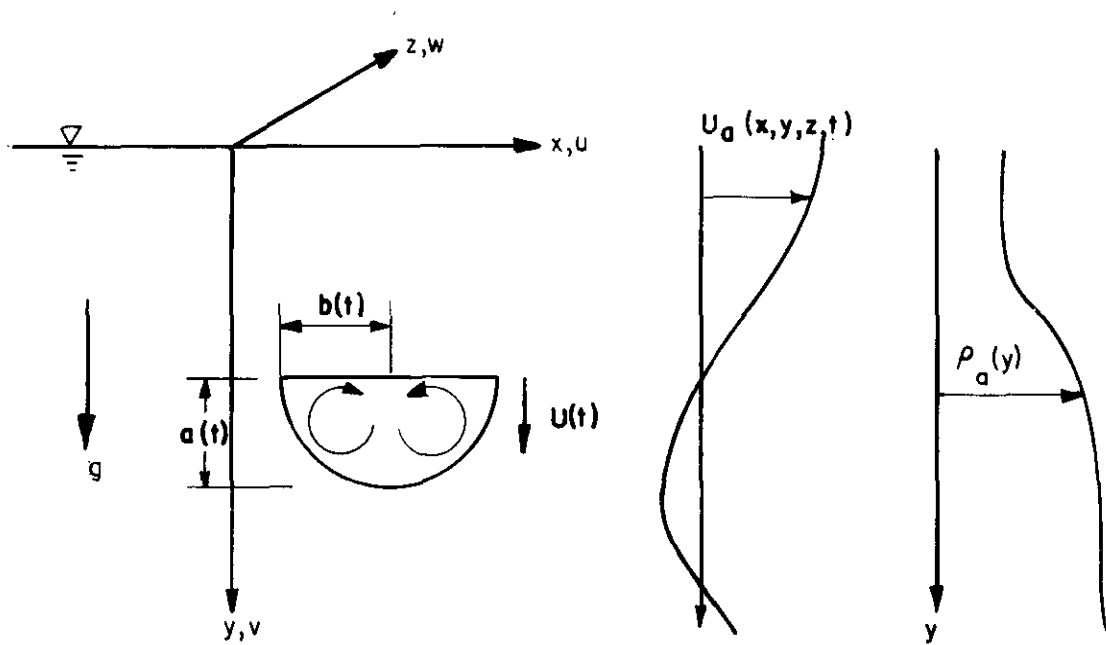


Figure 3.3 Diagram of Descending Hemispherical Cloud

$$\frac{d}{dt} (V_c \rho) = E \rho_a - \sum_i S_i \rho_i \quad (3.1)$$

where the cloud volume is $V_c = \frac{2}{3} \pi a^3$.

The time rate of change of momentum is equal to the buoyancy minus drag plus the rate of ambient fluid momentum entrainment minus the rate of solids momentum passing out of the cloud:

$$\frac{d\vec{M}}{dt} = F\vec{j} - \vec{D} + E\rho_a \vec{U}_a - \sum_i S_i \rho_i \vec{U} \quad (3.2)$$

The time rate of change of relative buoyancy is the rate of ambient fluid relative buoyancy entrainment minus the rate of solids relative buoyancy passing out of the cloud:

$$\frac{dB}{dt} = E(\rho_a(0) - \rho_a) - \sum_i (S_i(\rho_a(0) - \rho_i)) \quad (3.3)$$

The time rate of change of the solid volume of the i^{th} component in the cloud is equal to the rate of the solids volume passing out of the cloud:

$$\frac{dP_i}{dt} = -S_i \quad (3.4)$$

The equation for conservation of vorticity requires a more extended discussion and will be deferred until later. Several auxiliary equations are used for quantities in the above equations. The rate of entrainment in volume is the product of the surface area

of the hemispherical front ($2\pi a^2$), an entrainment coefficient (α), and the magnitude of the velocity difference between the cloud and the ambient fluid:

$$E = 2\pi a^2 \alpha \left| \vec{U} - \vec{U}_a \right| \quad (3.5)$$

The entrainment coefficient will be discussed later in conjunction with the conservation of vorticity equation. The volume rate of solids passing out of the cloud of the i^{th} component is the product of the vertically projected area of the cloud, the magnitude of the fall velocity, the volume fraction of that component in the cloud, and a settling coefficient:

$$S_i = \pi a^2 \left| v_{fi} \right| C_{si} (1 - \beta_i) \quad (3.6)$$

Several additional equations are necessary for the following:

Momentum

$$\vec{M} = C_m \rho \frac{2}{3} \pi a^3 \vec{U} \quad (3.7)$$

Buoyancy force

$$F = \frac{2}{3} \pi a^3 g (\rho - \rho_a) \quad (3.8)$$

Drag force in x-direction

$$D_x = 0.5 \rho_a C_D (0.5 \pi a^2) \left| \vec{U} - \vec{U}_a \right| (u - u_a) \quad (3.9)$$

Drag force in y-direction

$$D_y = 0.5 \rho_a C_D \pi a^2 \left| \vec{U} - \vec{U}_a \right| v \quad (3.10)$$

Drag force in z-direction

$$D_z = 0.5 \rho_a C_D (0.5 \pi a^2) \left| \vec{U} - \vec{U}_a \right| (w - w_a) \quad (3.11)$$

Buoyancy

$$B = \frac{2}{3} \pi a^3 (\rho_a(0) - \rho) \quad (3.12)$$

Solid volume of the i^{th} component in cloud

$$P_i = \frac{2}{3} \pi a^3 C_{si} \quad (3.13)$$

In the above equations, α is an entrainment coefficient; β_i is a settling coefficient; \vec{j} is the unit vector in the vertical direction; C_D is a drag coefficient; C_m is an apparent mass coefficient; and $\rho_a(0)$ is the density at the free surface. The drag coefficient C_D is a function of Reynolds number and therefore depends on a and $|\vec{U} - \vec{U}_a|$. The value of C_D is suggested to be 0.5. The apparent mass coefficient, C_m , is suggested to be between 1.0 and 1.5.

The last governing equation is that for vorticity. The total vorticity is the cloud's identity-preserving mechanism, and it is also important in determining the amount of entrainment. When a cloud of material is ejected into the ambient fluid, some initial vorticity is generated when passing through the entrance boundary. Total vorticity is generated only by shear forces at the fluid boundaries. Once a cloud is in the ambient fluid, there are two possibilities if the bottom is not encountered. In a uniform density ambient fluid, total vorticity is conserved, although cloud growth acts to diffuse the vortex strength. In a stratified fluid, the density gradient acts to decay the total vorticity according to:

$$\frac{dK}{dt} = -A \epsilon \quad (3.14)$$

where K is vorticity; A is a dissipation parameter; and ϵ is the density gradient as defined below:

$$A = \frac{C a^2 g}{\rho_a(0)} \quad (3.15)$$

$$\epsilon = \frac{d\rho_a}{dy} \quad (3.16)$$

C is a vorticity dissipation coefficient which is equal to 3 according to Turner (1960). The vorticity decay mechanism is very likely more complicated than is suggested by Eq. 3.14, and the formulation is subject to change when better knowledge is acquired. Vorticity is of concern here only because it is thought to influence entrainment.

The entrainment coefficient α should in fact be dependent upon the properties of the cloud, the properties of the ambient fluid, and the turbulence structure inside and outside the convecting cloud. In formulating an expression for an entrainment coefficient, it is necessary to account for the structure of the cloud as it changes from a vortex ring to a turbulent thermal. Scorer (1957) and Richards (1961) experimentally determined the entrainment coefficient for turbulent thermals, α_o , to be approximately 0.25. In studying the motion of a vortex ring, Turner (1960) found an entrainment coefficient:

$$\alpha = \frac{B}{2\pi g C_1 K^2} \quad (3.17)$$

by assuming similarity where C_1 was found to be 0.16; B is the buoyancy; and K is the total vorticity. As the cloud descends and its vorticity approaches zero, Turner's assumption of similarity cannot hold. Since α is expected to approach α_0 found in turbulent thermals, Koh and Chang (1973) thought it reasonable to postulate that the dependence of α on B and K might be of the form:

$$\alpha = \alpha_0 \sqrt{\tanh\left(\frac{B}{2\pi g C_1 K^2 \alpha_0}\right)^2} \quad (3.18)$$

Their only justification for Eq. 3.18 was that it tends to the correct limits: to Turner's relation when K is large and to α_0 when K is small. In the absence of any experimental work confirming or rejecting this relation, Eq. 3.18 will be used in this report.

Koh and Chang used dimensional analysis to show that the dimensionless mass rate of settling is a function of the ratio of the descending velocity of the cloud, v ; the fall velocity of the solid particles, v_{fi} ; the concentration of each group of particles, C_{si} ; and total concentration, C :

$$\frac{q}{v_{fi} \rho_i a^2} = \pi C_{si} (1 - \beta_i) \quad (3.19)$$

where β_i is defined to be a settling coefficient which depends upon $\frac{v}{v_{fi}}$, C_{si} , and C . β_i is expected to be between 0 and 1,

representing the two cases of settling freely or no settling. The actual form of β_i remains to be determined by experiment. Koh and Chang's formulation is retained here for the settling coefficient:

$$\beta_i = \begin{cases} 0 & \text{if } \left| \frac{v}{v_{fi}} \right| < 1 \\ \beta_o & \text{if } \left| \frac{v}{v_{fi}} \right| \geq 1 \end{cases} \quad (3.20)$$

where β_o is a constant which is assumed known.

Equations (3.1 through 3.20) constitute a set of equations soluble by any of several numerical schemes, given a set of initial conditions. Discussion of the linkage of this computation with the dynamic collapse and long-term computations will be deferred until Section 5.1 as will the details of specification of the variable velocity field and other details.

3.2.2 Dynamic Collapse in Water Column

As the waste cloud goes through the convective descent phase, it gains mass and momentum by entrainment. The horizontal velocity of the cloud tends to approach that of the ambient fluid. Coincidentally, the waste material concentration is greatly reduced and the vorticity has become insignificant because of dissipation by ambient stratification and turbulence. If the cloud reaches the depth of neutral buoyancy, its momentum will tend to make it overshoot beyond the neutrally buoyant point while the buoyancy force will tend to bring it back to the neutrally buoyant position. The combined action of these forces will make the cloud undergo a decaying vertical oscillation. As the vertical motion of the cloud is being suppressed, the cloud tends to collapse vertically and spread out horizontally, seeking hydrostatic equilibrium within the stratified ambient fluid. As the cloud collapses, its cross section becomes elongated in the

horizontal, and another dimension is needed to describe the cloud shape. If the cross section of the cloud is assumed to be elliptical, its shape may be characterized by its semi-major and semi-minor axes, b and a , respectively (Figure 3.4a).

It is assumed that the cloud always retains the shape of an oblate spheroid. If coordinate axes are chosen to originate from the cloud centroid, the cross-sectional outline of the cloud (Figure 3.4a) may be represented by

$$\frac{y'^2}{a^2} + \frac{r'^2}{b^2} = 1 \quad (3.21)$$

where a and b vary with time. The cloud is assumed to remain symmetrical, which in practice will only be true if there is no relative velocity between the cloud and the ambient fluid and therefore no velocity shear. Following convective descent, the velocity difference between the cloud and the ambient fluid is expected to be small, and its influence on shape can be neglected.

With the exception of vorticity, the conservation equations used for convective descent still hold. Any differences are due to the additional dimension used to describe the cloud. The conservation equations are:

Conservation of mass

$$\frac{d}{dt} (V_c \rho) = E \rho_a - \sum_i S_i \rho_i \quad (3.22)$$

where the cloud volume $V_c = \frac{4}{3} \pi ab^2$.

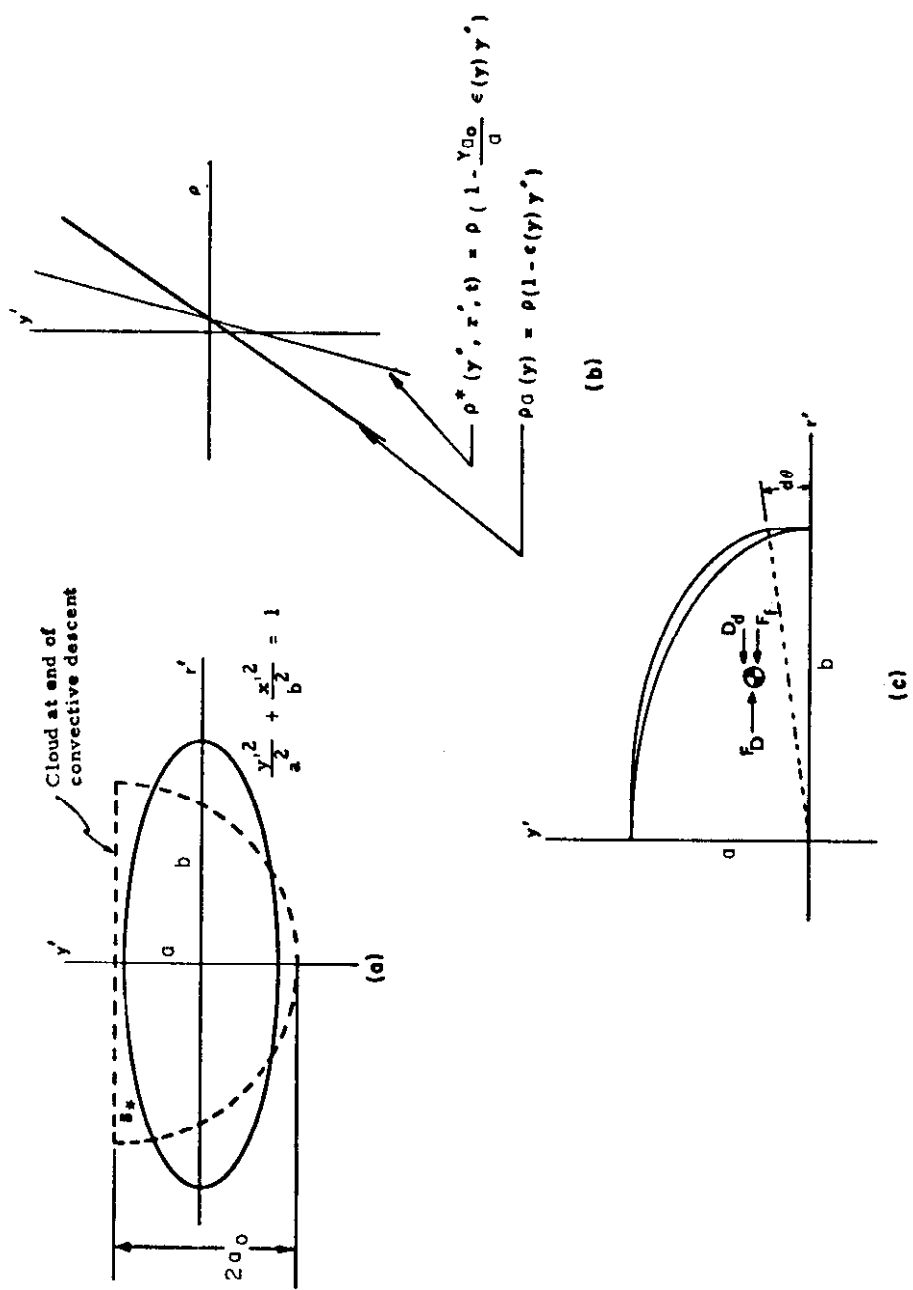


Figure 3.4 Aspects of Cloud Collapse

Conservation of momentum

$$\frac{d\vec{M}}{dt} = \vec{F}j - \vec{D} + E \rho_a \vec{U}_a - \sum_i S_i \rho_i \vec{U} \quad (3.23)$$

Conservation of buoyancy

$$\frac{dB}{dt} = E (\rho_a(0) - \rho_a) - \sum_i S_i (\rho_a(0) - \rho_i) \quad (3.24)$$

Conservation of solid particles

$$\frac{dP_i}{dt} = -S_i \quad (3.25)$$

The major auxiliary equations are those for entrainment of ambient fluid, for the settling of solid particles, and for the collapse of the cloud.

The two contributions to entrainment come from movement of the entire cloud through the ambient fluid and from the additional velocity shear at the cloud boundary due to the cloud collapse. Each contribution is the product of the surface area of the cloud, an entrainment coefficient, and a velocity. The expression for the rate of entrainment of ambient fluid is:

$$E = \left\{ 2\pi b^2 + \pi \frac{a^2 b}{R} \ln \left(\frac{b+R}{b-R} \right) \right\} \left(\alpha \left| \vec{U} - \vec{U}_a \right| + \alpha_c \frac{db}{dt} \right) \quad (3.26)$$

where $R = \sqrt{b^2 - a^2}$; α is the entrainment coefficient for cloud motion; and $\left| \vec{U} - \vec{U}_a \right|$ is the magnitude of the velocity difference.

α_c is introduced into the formulation to account for the entrainment due to collapse, and $\frac{db}{dt}$ is the velocity of the tip of the collapsing cloud. It is assumed that entrainment due to the cloud motion should die out as the cloud settles into the neutral buoyancy position. This may be done by letting the entrainment coefficient be:

$$\alpha = \left(\frac{a}{b}\right)^2 \alpha_0 \quad (3.27)$$

where α_0 is the entrainment coefficient for a turbulent thermal. This relation has not been confirmed by experiment and is offered here merely as an effective and reasonable way to turn off entrainment due to cloud motion.

As in the section on convective descent, the volume rate of solids settling out of the cloud is

$$S_i = \pi b^2 \left| v_{fi} \right| C_{si} (1 - \beta_i) \quad (3.28)$$

where β_i is a settling coefficient defined as before.

The mechanism that drives the collapse of the cloud is density differences between the inside and outside of the cloud. It is assumed that, because of the turbulent mixing, the density gradient inside the cloud is less than that outside. Assume that the cloud is resting at the level of neutral buoyancy and that the ambient density at this level is ρ_0 . Assume further that the different density gradients inside and outside of the cloud are of constant magnitude. Let ϵ be the normalized ambient density gradient:

$$\epsilon = \frac{1}{\rho} \frac{\partial \rho_a}{\partial y} \quad (3.29)$$

The density gradient inside the cloud is assumed to be less than that in the ambient fluid by a factor $\frac{\gamma a_0}{a}$, where γ is a coefficient, and a_0 is half the final radius of the convective descent cloud (Figure 3.4a) and a is the semi-minor axis of the collapsing cloud. Following these assumptions the ambient density in the region of the cloud is

$$\rho_a = \rho_0 (1 - \epsilon y') = \rho_0 (1 - \epsilon (a-y)) \quad (3.30)$$

and the density inside the cloud is

$$\rho = \rho_0 \left(1 - \gamma \frac{a_0}{a} \epsilon y'\right) = \rho_0 \left(1 - \gamma \frac{a_0}{a} \epsilon (a-y)\right) \quad (3.31)$$

where y and y' are as defined in Figure 3.5. These density profiles are illustrated in Figure 3.4b.

The centroid of the collapsing slice of the cloud shown in Figure 3.4c moves with respect to the centroid of the cloud. Consider the slice (of angular dimension $d\theta$) as a free body and integrate the pressures over the surfaces of the slice to obtain the radial force (acting at the slice centroid) driving the collapse of the slice. The pressures are assumed to be hydrostatic. The pressure on the rounded external surface of the slice is simply the pressure in the ambient fluid, $p_a(y)$, and it is integrated over the projected area as shown in Figure 3.5.

$$F_{\text{ext}} = \int_{y=0}^{y=a} p_a(y) r(y) d\theta dy \quad (3.32)$$

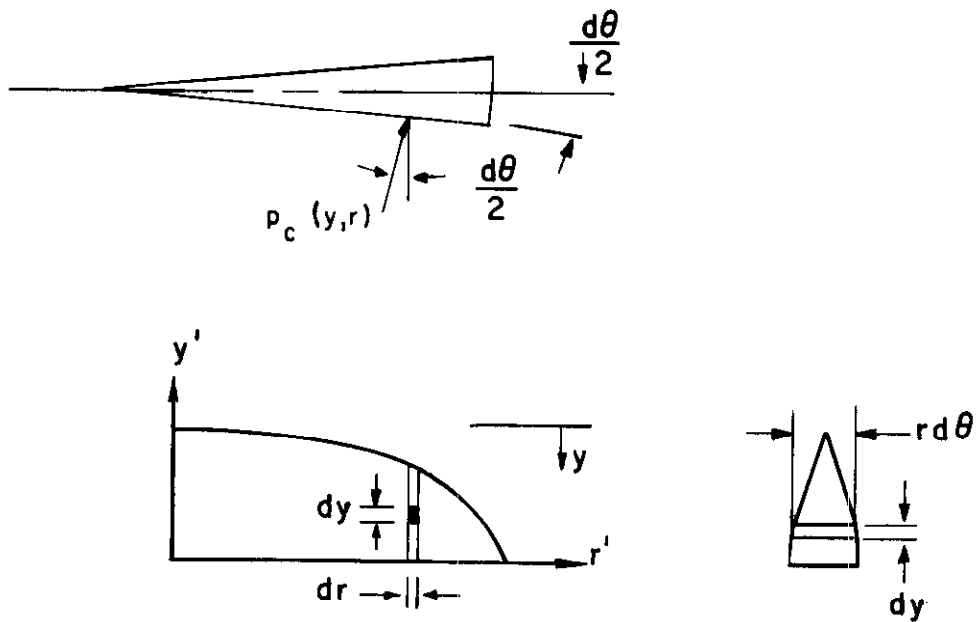


Figure 3.5 Slice of Collapsing Cloud, Showing Integration Elements for Determining the Driving Force of Collapse

The pressure inside the cloud, $p_c(y, r)$, is a function of the vertical and radial position inside the cloud. This pressure is integrated over both side faces of the slice, and $d\theta$ is assumed small to give an expression for the radially outward directed force:

$$F_{\text{int}} = \int_0^b \int_{a(1-R)}^a p_c(y, r) d\theta dr dy \quad (3.33)$$

where $R = \sqrt{1 - \frac{r^2}{b^2}}$.

Once the integrals (3.32) and (3.33) are evaluated and the difference of $F_{\text{int}} - F_{\text{ext}}$ is taken, the radial force driving collapse is obtained:

$$F_D = \frac{\pi \rho_0 (1 - \gamma \frac{a_0}{a}) \epsilon g a^3 b}{16} d\theta \quad (3.34)$$

Since $\epsilon = \frac{1}{\rho_0} \frac{\partial \rho_a}{\partial y}$ the expression may be written for use in the code as

$$F_D = \frac{\pi}{16} (1 - \gamma \frac{a_0}{a}) \left(\frac{\partial \rho_a}{\partial y} \right) g a^3 b d\theta \quad (3.35)$$

In formulating the inertia of the slice and force resisting collapse, it is assumed that the horizontal velocities of the elements inside the slice are related to the radial distance, r , from the centroid of the cloud and that the velocity of horizontal deformation is characterized by the velocity of the centroid of the slice segment. The cloud tip velocity due to collapse (which will be called v_1) is linearly related to the slice centroid horizontal velocity by

$$v_1 = \frac{16}{3\pi} \frac{dc}{dt} \quad (3.36)$$

The forces resisting the collapse of the slice are form drag, D_D , and skin friction drag F_f :

$$D_D = C_{\text{drag}} \rho_a \frac{ab}{4} \left| v_1 \right| v_1 d\theta \quad (3.37)$$

$$F_f = C_{\text{fric}} \rho_a \frac{b^2}{2a} v_1 d\theta \quad (3.38)$$

where C_{drag} is the drag coefficient for a wedge and C_{fric} is the friction coefficient for a flat plate, which is a function of the kinematic viscosity (Hoerner, 1965).

The horizontal inertia of the cloud slice is the time rate of change of the product of its mass and the velocity of the slice centroid:

$$I = \frac{d}{dt} \left(\rho \frac{\pi ab^2}{16} v_1 \right) d\theta \quad (3.39)$$

The dynamic equation is formulated as the summation of the external forces acting on the slice which is equated to the inertia force. $d\theta$ cancels out of all terms.

$$I = F_D - D_D - F_f \quad (3.40)$$

The integral of equation 3.39 over one time step is used to determine the value of v_1 at the end of the time step. The integral of the left side, $\int I dt$, is evaluated using Eq. 3.40 and the value of v_1 at the start of the time step.

The effects of entrainment on mass, momentum, and buoyancy have been considered previously. Entrainment also influences the shape of the cloud cross section, which is assumed to remain symmetric. The rate of volume increase of the cloud due to entrainment is assumed to be accounted for by an increment in the tip velocity with the vertical dimension of the cloud held constant. This increment will be called v_2 . The velocity of the slice tip of the collapsing and entraining cloud is:

$$\frac{db}{dt} = v_1 + v_2 \quad (3.41)$$

Equation (3.22), as it stands, accounts only for the gross amount of mass entrained. It may be rewritten under the assumptions of constant cloud density and constant vertical dimension during each integration step to describe how entrainment adds to the growth of b :

$$v_2 = \frac{E\rho_a - \sum_i S_i \rho_i}{\rho \frac{4}{3} \pi ab} \quad (3.42)$$

Several additional equations are used for:

Momentum

$$\vec{M} = C_M \rho \frac{4}{3} \pi ab^2 \vec{U} \quad (3.43)$$

Buoyancy force

$$F = \frac{4}{3} \pi ab^2 g (\rho - \rho_a) \quad (3.44)$$

Drag force in the x-direction

$$D_x = \frac{1}{2} \rho_a C_{D_3} \pi ab \left| \vec{U} - \vec{U}_a \right| (u - u_a) \quad (3.45)$$

Drag force in the y-direction

$$D_y = \frac{1}{2} \rho_a C_{D_4} \pi b^2 \left| \vec{U} - \vec{U}_a \right| v \quad (3.46)$$

Drag force in the z-direction

$$D_z = \frac{1}{2} \rho_a C_{D_3} \pi ab \left| \vec{U} - \vec{U}_a \right| (w - w_a) \quad (3.47)$$

Buoyancy

$$B = \frac{4}{3} \pi ab^2 (\rho_a(0) - \rho) \quad (3.48)$$

Solid volume of the i^{th} component

$$P_i = \frac{4}{3} \pi ab^2 C_{si} \quad (3.49)$$

In the above equations, C_M is an apparent mass coefficient, C_{D_3} is the drag coefficient for a spheroidal wedge, and C_{D_4} is the drag coefficient for a circular plate. Discussion of suggested numerical values for these and other coefficients will be deferred until Section 5.1.

Equations (3.21) through (3.49) constitute a set of equations soluble by any of several numerical integration schemes, given a set of initial conditions which are obtained from the solution for the convective descent phase described earlier. Discussion of the numerical solution and the details of computation will be deferred until Section 5.1.

3.2.3 Dynamic Collapse on Bottom

If the density stratification is not strong enough to arrest the vertical motion of the cloud, it will eventually hit the bottom. The cloud may then collapse on the bottom or it may rise off the bottom as it collapses. In this section, a variation on the model for collapse in the water column to apply to collapse on the bottom will be made. It is assumed that the shape of the cloud is changed to and maintained as a half ellipsoid as shown in the upper half of Figure 3.4a. The equation for its shape is, as before:

$$\frac{y'^2}{a^2} + \frac{r'^2}{b^2} = 1 \quad (\text{Eq. 3.21})$$

The cloud is assumed to remain symmetrical and velocity differences between the cloud, the bottom, and the ambient fluid are allowed. The bottom is assumed to be horizontal in the region of the cloud. The situation is so close to that for collapse in the water column, that the same equations can be used, modified for the different geometry and to account for the reaction force at the bottom and the friction force at the bed. The governing equations are:

Conservation of mass

$$\frac{d}{dt} (V_c \rho) = E \rho_a - \sum S_i \rho_i \quad (3.50)$$

where the cloud volume $V_c = \frac{2}{3} \pi a b^2$

Conservation of momentum

$$\frac{d\vec{M}}{dt} = F\vec{j} - \vec{D} + E\rho_a \vec{U}_a - \sum_i S_i \rho_i \vec{U} - \vec{F}_f \quad (3.51)$$

Conservation of buoyancy

$$\frac{dB}{dt} = E(\rho_a(0) - \rho_a) - \sum_i S_i (\rho_a(0) - \rho_i) \quad (3.52)$$

Conservation of solid particles

$$\frac{dP_i}{dt} = -S_i \quad (3.53)$$

The major auxiliary equations are those for the entrainment of ambient fluid, for the settling of solid particles, and for the collapse of the cloud. The entrainment function in this case is somewhat different than that for collapse in the water column. If the cloud remains on the bottom, it very quickly comes to rest with respect to the bottom. Since ambient velocity also must become small at the bottom, entrainment due to velocity differences between the cloud and the ambient has been neglected. Entrainment in this case is due only to the collapse of the cloud and is the product of the surface area of the half ellipsoidal cloud exposed to the ambient fluid, an entrainment coefficient, and the tip velocity of the collapsing cloud:

$$E = \left\{ \pi b^2 + 0.5 \pi \frac{a^2 b}{R} \ln \left(\frac{b+R}{b-R} \right) \right\} \alpha_c \frac{db}{dt} \quad (3.54)$$

where $R = \sqrt{b^2 - a^2}$; α_c is the entrainment coefficient for collapse; and $\frac{db}{dt}$ is the tip velocity of the cloud.

As before, the volume rate of solids settling out of the cloud is:

$$S_i = \pi b^2 \left| v_{fi} \right| C_{si} (1 - \beta_i) \quad (3.55)$$

where β_i is the settling coefficient defined in Section 3.2.

The reader is referred to Section 3.2.2 for a discussion of the mechanism of cloud collapse. Aside from the difference in cloud shape, there are no changes and the driving force of collapse of a slice of the cloud is given by:

$$F_D = \frac{\pi}{16} \left(1 - \frac{\gamma a_0}{a} \right) \left(\frac{\partial \rho_a}{\partial y} \right) g a^3 b d\theta \quad (3.56)$$

As in Section 3.2.2, the cloud tip velocity due to collapse, v_1 , is linearly related to the slice centroid horizontal velocity by

$$v_1 = \frac{16}{3\pi} \frac{dc}{dt} \quad (3.57)$$

The forces resisting the collapse of the slice are form drag, D_D ; skin friction drag, F_f ; and bottom friction force F_{bf} :

$$D_D = C_{drag} \rho_a \frac{ab}{4} \left| v_1 \right| v_1 d\theta \quad (3.58)$$

$$F_f = C_{fric} \rho_a \frac{b^2}{2a} \left| v_1 \right| v_1 d\theta \quad (3.59)$$

$$F_{bf} = F_b^{frictn} F_1 d\theta / 2\pi \quad (3.60)$$

where C_{drag} and C_{fric} are defined as before. F_f is the reaction force at the bottom; F_{frictn} is the bottom-cloud interface friction coefficient; and F_1 is a modification factor used in computing the resistance of the friction force to the collapse of an arc of a half ellipsoid.

The horizontal inertia of the cloud slice is the time rate of change of the product of its mass and the velocity of the slice centroid:

$$I = \frac{d}{dt} \left(\rho \frac{\pi a b^2}{16} v_1 \right) d\theta \quad (3.61)$$

The dynamic equation is formulated as the summation of the external forces acting on the slice, which is equated to the inertia force, I ;

$$I = F_D - D_D - F_f - F_{\text{bf}} \quad (3.62)$$

The tip velocity is the sum of contributions due to the collapse of the cloud (v_1) and due to entrainment (v_2);

$$\frac{db}{dt} = v_1 + v_2 \quad (3.63)$$

The value of v_1 at the next time step is obtained by computing the integral $\int I dt$ (using Eq. 3.62 and the current value of v_1) and then solving Eq. 3.61 for the new v_1 . The value of v_2 is obtained by rewriting equation 3.50 under the assumptions of constant cloud density and constant vertical dimension during each integration step:

$$v_2 = \frac{E\rho_a - \sum S_i \rho_i}{\rho \frac{4}{3} \pi a b} \quad (3.64)$$

Several additional equations are used for:

Momentum

$$\vec{M} = C_M \rho \frac{2}{3} \pi ab^2 \vec{U} \quad (3.65)$$

Buoyancy force

$$F = \frac{2}{3} \pi ab^2 g (\rho - \rho_a) \quad (3.66)$$

Drag force in the x-direction

$$D_x = \frac{1}{4} \rho_a C_{D_3} \pi ab \left| \vec{U} - \vec{U}_a \right| (u - u_a) \quad (3.67)$$

Drag force in the y-direction

$$D_y = 0 \quad (3.68)$$

Drag force in the z-direction

$$D_z = \frac{1}{4} \rho_a C_{D_3} \pi ab \left| \vec{U} - \vec{U}_a \right| (w - w_a) \quad (3.69)$$

Resultant horizontal velocity

$$\psi = \sqrt{u^2 + w^2} \quad (3.70)$$

Bottom friction force in the x-direction

$$F_{F_x} = F_b F_{\text{rictn}} u / \psi \quad (3.71)$$

Bottom reaction force in the y-direction

$$F_{F_y} = -F_b = -\frac{2}{3} \pi ab^2 g (\rho - \rho_a) + \frac{d}{dt} [C_M \rho \frac{2}{3} \pi ab^2 v] + \pi b^2 \sum_i \left| v_{f_i} \right| \rho_i C_{si} (1 - \beta_i) v \quad (3.72)$$

Bottom friction force in the z-direction

$$F_{F_z} = F_b F_{\text{frictn}} w / \psi \quad (3.73)$$

Buoyancy

$$B = \frac{2}{3} \pi ab^2 (\rho_a(0) - \rho) \quad (3.74)$$

Solid volume of the i^{th} particle

$$P_i = \frac{2}{3} \pi ab^2 C_{si} \quad (3.75)$$

One additional condition necessary for closure is that the distance of the cloud centroid from the base of the half ellipsoid is 3/8 of its vertical altitude.

In the Koh-Chang model, the vertical velocity of the centroid was computed from the dynamics and integrated to find the change in the vertical position of the centroid. This led to numerical difficulties in many simulations of typical dredging situations. Such difficulties have been avoided in the present model by use of the condition in the previous paragraph.

Equations (3.50) through (3.75) form a set of equations soluble by any of several numerical integration schemes, given a set of initial conditions which may be obtained from the solution for collapse in the water column or from the solution for convective descent. Discussion of the numerical solution and the details of computation will be deferred until Section 5.1.

3.3 Jet Discharge

A large number of dredging vessels discharge dredged material through openings at the bottom of the vessel by gravity or by pumping, while traveling at a certain speed. The typical hopper dredge upon reaching its dumping area will pump water into its hopper to stir up the material before opening its hopper doors one-by-one. Each hopper is mostly empty within a few tens of seconds (although cohesive material can take much longer) and the entire dumping operation is complete within a few minutes. Another mode of discharge is a fixed pipeline in water. In either case the flow phenomenon near the discharge opening is that of a sinking jet in a crosscurrent. The jet entrains ambient fluid and momentum, and it may experience a drag force from the ambient fluid due to pressure differences between the upstream and downstream faces of the jet. As a result, the jet grows in size and bends over in the direction of the ambient current. The dredged material is diluted through entrainment of ambient fluid, and solid particles settle out of the jet as the situation allows. As the jet reaches further downstream, its centerline velocity approaches that of the ambient fluid; the influence of the ambient density gradient becomes dominant; and the jet begins to behave more like a plume. The plume will tend

to spread out horizontally and collapse vertically, seeking a neutrally buoyant position in the ambient fluid. This sequence of events is illustrated in Figure 3.6.

3.3.1 Convective Descent

In what follows, the equations are formulated for a sinking jet in a stratified ambient fluid subject to a variable cross-current of arbitrary magnitude. Figure 3.7 shows a round jet discharging with some flow rate, Q , into a crosscurrent. Assume that the jet cross section remains circular and that velocity, density, and material concentration distributions may be approximated by "top-hat" profiles. Then the jet properties are described by its radius, b ; its velocity, U ; its density, ρ ; the concentrations of the solid components, C_{si} ; and the solid component densities, ρ_i . The solid components have fall velocities v_{fi} . The ambient density and ambient current are designated by $\rho_a(y,t)$ and $\vec{U}_a(x,y,z,t)$.

The jet can flow in any direction from the nozzle, depending upon its initial momentum and the ambient current. In Figure 3.7a, the coordinate axes are fixed on the discharging vessel; s is in the direction of the jet trajectory; θ_1, θ_2 , and θ_3 are its direction angles; δ_1 and δ_3 are the directions the resultant ambient current at position s makes with respect to the x and z axes, respectively; and γ is the angle in a vertical plane between s and the resultant ambient current.

Near the discharge nozzle, the flow is very similar to that in a momentum jet. As the jet slows down and bends over in the direction of the ambient current, the rise and fall of the plume

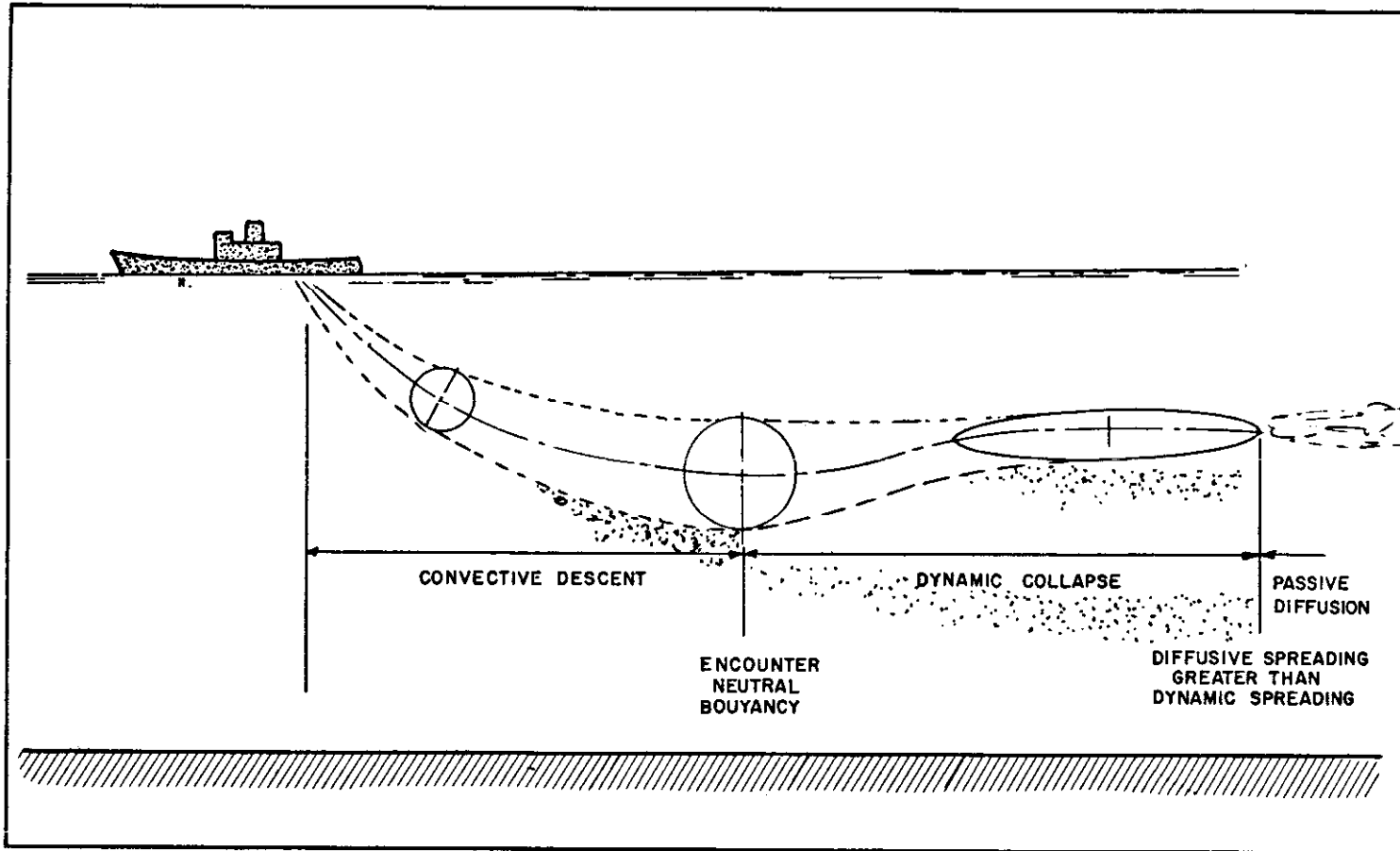
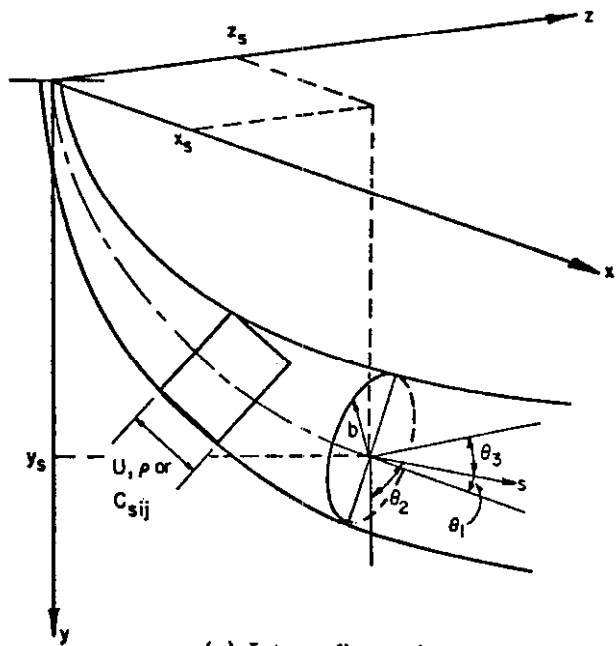
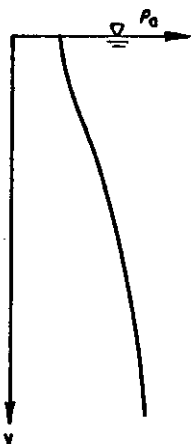


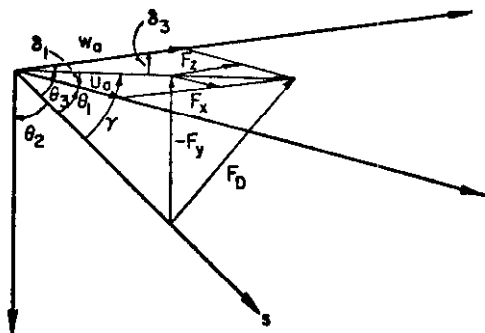
Figure 3.6 Idealized Jet Discharge From Moving Vessel Which is Described by the Mathematical Model Developed in Section 3.2. Cross sections are shown at three stages of the plume. A heavy class of particles is depicted settling out of the plume at an early stage. Lighter particles are shown settling during the collapse phase.



(a) Jet configuration



(b) Ambient density profile



(c) Ambient velocity and drag forces

Figure 3.7 Definition Sketch for Round Jet

is approximated by the behavior of a two-dimensional thermal.

The equations governing the motion are those for conservation of mass, momentum, buoyancy, and solid particles. In momentum jet theory, variations in the above quantities vary only with distance along the jet axis, s , and so rates of change of the above quantities are written as derivatives with respect to s .

The rate of change of mass flux along the jet axis is equal to the rate of ambient fluid mass entrainment per unit jet length minus the rate of solids mass passing out of the jet per unit length.

$$\frac{d}{ds} (\pi b^2 \rho U) = E \rho_a - \sum_i S_i \rho_i \quad (3.76)$$

The presence of a drag term in the momentum equation is necessary to account for the action of the ambient current in bending the jet. A gross drag force is introduced to account for the action of the unbalanced pressure field around the jet caused by the ambient current seen by the jet. This drag force is proportional to the square of the velocity component of the oncoming ambient fluid normal to the jet axis. Referring to Figure 3.7c, the magnitude of the force is:

$$F_D = C_D \rho_a b \left(\left| \vec{U}_a \right| \sin \gamma \right)^2 \quad (3.77)$$

where C_D is the drag coefficient. This drag force may be resolved into components in the x , y , and z directions as:

$$F_{D_x} = \frac{\cos \delta_1 - \cos \gamma \cos \theta_1}{\sin \gamma} F_D \quad (3.78a)$$

$$F_{D_y} = \frac{-\cos \gamma \cos \theta_2}{\sin \gamma} F_D \quad (3.78b)$$

$$F_{D_z} = \frac{-\cos \gamma \cos \theta_3 + \cos \delta_3}{\sin \gamma} F_D \quad (3.78c)$$

The rate of change of momentum flux along the jet axis is equal to buoyancy force per unit length plus the rate of ambient fluid momentum entrainment per unit length minus the rate of solids momentum passing out of the cloud per unit length:

$$\frac{d}{ds} (\pi b^2 \rho \left| \vec{U} \right| \vec{U}) = B \vec{j} + E \rho_a \vec{U}_a - \sum S_i \rho_i \vec{U} - \vec{F}_D \quad (3.79)$$

where \vec{j} is the vertical unit vector.

The rate of change of relative buoyancy flux along the jet axis is equal to the rate of ambient fluid relative buoyancy entrainment per unit length minus the rate of solids relative buoyancy passing out of the jet per unit length:

$$\frac{d}{ds} (\pi b^2 U (\rho_a(0) - \rho)) = E(\rho_a(0) - \rho_a) - \sum S_i (\rho_a(0) - \rho_i) \quad (3.80)$$

The rate of change of the flux of the i^{th} solid component along the jet axis is equal to the rate of solids volume passing out of the cloud per unit length:

$$\frac{dP_i}{ds} = -S_i \quad (3.81)$$

Several auxiliary equations are used for quantities in the above equations. Following Abraham (1970), it is assumed that the entrainment mechanism depends upon the local mean flow and is the sum of contributions due to momentum jet entrainment and due to a two-dimensional thermal type of entrainment. Momentum jet entrainment is proportional to the perimeter of the jet and the velocity difference between the jet and the velocity component of the ambient fluid in the direction of jet travel:

$$E_m = 2\pi b\alpha_1 (|U| - |U_a| \cos \gamma) \quad (3.82)$$

Entrainment experienced by a two-dimensional thermal is proportional to the perimeter of the thermal and the velocity of the thermal. The equation is formulated by visualizing the plume as moving horizontally with the ambient fluid but with a vertical velocity $U_a \sin \gamma$:

$$E_T = 2\pi b\alpha_2 |U_a| \sin \gamma \quad (3.83)$$

In the above equations, α_1 and α_2 are entrainment coefficients. The total entrainment is assumed to be represented by

$$E = E_m + E_T \sin \theta_2 \quad (3.84)$$

where $\sin \theta_2$ is arbitrarily introduced as a convenient way to turn off the thermal type of entrainment when the jet approaches the vertical.

As seen from Koh and Chang (1973), the settling of solid particles from a jet is a most complicated phenomenon. The solid particles in the jet tend to settle out by gravity; however, they are also kept in the main stream by the turbulence of the jet. A settling coefficient, β_1 , is introduced into the formulation just as in Section 3.2.1. Then the rate of the volume flux of the i^{th} solid component out of the jet per unit length is:

$$S_i = 2b \left| v_{fi} \right| C_{si} (1 - \beta_i) \quad (3.85)$$

where v_{fi} is the settling velocity; C_{si} is the solid concentration (volume ratio); and β_i behaves as described in Section 3.2.1.

Several additional equations are necessary for:

Momentum flux

$$\vec{M} = \pi b^2 \rho U \vec{U} \quad (3.86)$$

Buoyancy force per unit length

$$F = \pi b^2 g (\rho - \rho_a) \quad (3.87)$$

Buoyancy flux

$$B = \pi b^2 U (\rho_a(0) - \rho) \quad (3.88)$$

Flux of i^{th} solid

$$P_i = \pi b^2 U C_{si} \quad (3.89)$$

The geometric relationship must also be introduced:

$$\cos^2 \theta_1 + \cos^2 \theta_2 + \cos^2 \theta_3 = 1 \quad (3.90)$$

The locus of the jet centerline may be found by integrating the direction cosines:

$$\frac{dx}{ds} = \cos \theta_1 \quad (3.91a)$$

$$\frac{dy}{ds} = \cos \theta_2 \quad (3.91b)$$

$$\frac{dz}{ds} = \cos \theta_3 \quad (3.91c)$$

Equations (3.76) through (3.90) constitute a set of equations soluble by any of several numerical integration schemes, given a set of initial conditions for $U(0)$, $b(0)$, $\rho(0)$, $C_{si}(0)$, $\theta_1(0)$, $\theta_2(0)$, and $\theta_3(0)$. Discussion of the linkage of this computation with the dynamic collapse and long-term computations will be deferred until Section 5.2 as will discussion of program details.

When the jet plume is far downstream from the nozzle, its velocity approaches that of the ambient fluid and it no longer behaves like a jet. If the jet does not encounter the bottom, it will seek its level of neutral buoyancy. At this point, stratification of the ambient fluid will dominate the motion, and the jet plume will tend to spread out horizontally and collapse vertically, seeking hydrostatic equilibrium. The jet plume is here expected to behave more like a two-dimensional thermal than like a jet.

In what follows, a mathematical formulation is presented to account for the convection and collapse of the dredged material plume. The cross section of the two-dimensional thermal is assumed to have the shape of an ellipse as shown in Figure 3.8a. If a coordinate system $x'y'$ is fixed with origin on the centroid of the thermal, the outline of the thermal is described by:

$$\frac{y'^2}{a^2} + \frac{x'^2}{b^2} = 1 \quad (3.21)$$

where a and b are the semi-minor and semi-major axes, respectively, of the ellipse and both of which vary with time.

A portion of the plume of length L which behaves as a two-dimensional thermal will now be considered. The conservation equations are formulated as the time derivatives of the conserved quantities.

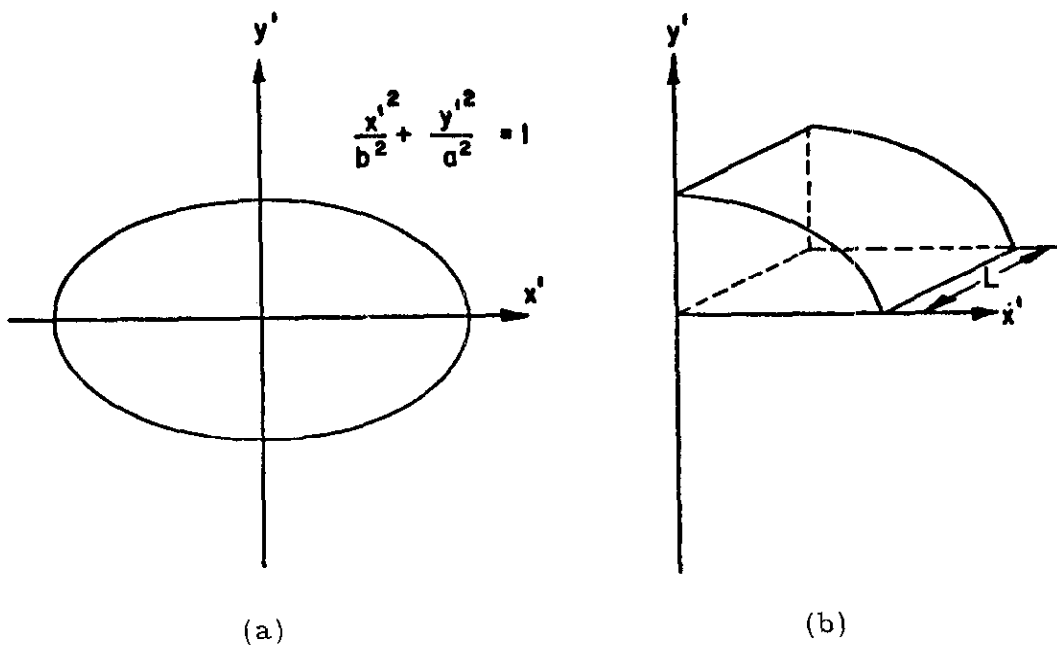


Figure 3.8 Geometry of the Collapsing Jet Plume

The time rate of change of mass in element L equals the rate of ambient fluid mass entrainment minus the rate of solids mass passing out of element L :

$$\frac{d}{dt} (\rho \pi a b L) = E \rho_a - \sum_i S_i \rho_i \quad (3.92)$$

The time rate of change of momentum of the element L equals the buoyancy force (if present) minus the drag force plus the rate of ambient fluid momentum entrainment minus the rate of solids momentum passing out of the cloud:

$$\frac{d\vec{M}}{dt} = B \vec{j} - \vec{D} + E \rho_a \vec{U}_a - \sum_i S_i \rho_i \vec{U}_i \quad (3.93)$$

where \vec{j} is the vertical unit vector.

The time rate of change of relative buoyancy of the element L equals the rate of ambient fluid relative buoyancy entrainment minus the rate of solids relative buoyancy passing out of the element:

$$\frac{dB}{dt} = E (\rho_a(0) - \rho_a) - \sum_i S_i (\rho_a(0) - \rho_i) \quad (3.94)$$

The rate of change of the volume of the i^{th} component in the element L equals the rate of solids volume passing out of the cloud:

$$\frac{dP_i}{dt} = -S_i \quad (3.95)$$

The collapse of the plume proceeds in a manner exactly analogous to that described in Section 3.2.2 for the single cloud. As before, the ambient density distribution seen from the plume centroid is:

$$\rho_a = \rho_0 (1 - \epsilon y') \quad (3.96)$$

and the density inside the plume is:

$$\rho = \rho_0 \left(1 - \frac{\gamma a_0}{a} \epsilon y'\right) \quad (3.97)$$

where ρ_0 is the ambient density at the level of neutral buoyancy; a_0 is the radius of the plume at the end of convective descent; γ is a coefficient; and

$$\epsilon = \frac{1}{\rho_0} \frac{\partial \rho_a}{\partial y} \quad (3.98)$$

By exactly the same method as is presented in Section 3.2.2, the force driving the collapse of the quadrant of the element L illustrated in Figure 3.8b may be found as:

$$F_D = \frac{1}{6} g L \left(1 - \frac{\gamma a_0}{a}\right) \frac{\partial \rho_a}{\partial y} a^3 \quad (3.99)$$

The forces resisting the collapse are form drag:

$$D_D = \frac{1}{2} C_{\text{drag}} \rho_a L a \left|v_2\right| \left|v_2\right| \quad (3.100)$$

and skin friction:

$$F_f = C_{fric} \frac{b}{a} L v_2 \quad (3.101)$$

These forces all act at the centroid of the quadrant of the element L , and their resultant is equated to the inertia of the quadrant to get the dynamic equation:

$$I = F_D - D_D - F_f \quad (3.102)$$

The horizontal inertia of the quadrant is the time rate of change of the product of its mass and the horizontal velocity of its centroid:

$$I = \frac{d}{dt} \left(\frac{ab}{3} L \rho v_1 \right) \quad (3.103)$$

The tip velocity of the quadrant is:

$$\frac{db}{dt} = v_1 + v_3 \quad (3.104)$$

In equations (3.101) and (3.104), v_1 is the quadrant tip velocity due to collapse (obtained by finding the integral $\int I dt$, using the old value of v_1 , and solving the integral of equation 3.103 for the new value of v_1), and v_2 is the combination of the tip velocity due to collapse and that due to the stretching of the element L (obtained by assuming that the minor axis a is kept constant and that no entrainment occurs at that moment):

$$v_2 = v_1 - \frac{b}{L} \frac{dL}{dt} \quad (3.105)$$

Stretching or squeezing of the element L arises because of the following set of conditions. As the buoyant element velocity approaches the ambient velocity, it will be either speeding up or slowing down due to the entrainment of ambient momentum and by drag forces applied to it. Since the supply of material is continuous from the jet, the element should be able to be stretched or squeezed so that the trajectory of one element will be capable of representing the steady picture of a continuous plume. To estimate the stretching of L , it is assumed that:

$$\frac{L}{\sqrt{u^2 + w^2}} = \text{constant} \quad (3.106)$$

v_3 is the contribution to tip velocity due to entrainment. Its magnitude is obtained by solving Eq. 3.92 for v_3 when ρ , a , and L are instantaneously held constant:

$$v_3 = \frac{E \rho_a - \sum S_i \rho_i}{\rho \pi a L} \quad (3.107)$$

Entrainment in the above equations is assumed to be the sum of contributions due to convection of the element through the ambient fluid and to the collapse of the element. Each type of entrainment occurs over the surface area of the element L . The total entrainment is given by:

$$E = 2\pi \frac{\sqrt{a^2 + b^2}}{2} L \left(\alpha_3 \left| \vec{U} - \vec{U}_a \right| + \alpha_4 \frac{db}{dt} \right) \quad (3.108)$$

where α_3 and α_4 are the entrainment coefficients for convection and collapse, respectively.

The rate of settling of the i^{th} solid component out of the cloud is:

$$S_i = 2 b L \left| v_{fi} \right| C_{si} (1 - \beta_i) \quad (3.109)$$

where β_i is a coefficient which behaves as described in Section 3.2.1.

Several additional equations are necessary for:

Momentum of the element

$$\vec{M} = C_M \rho \pi a b L \vec{U} \quad (3.110)$$

Buoyancy force

$$F = \pi a b L (\rho - \rho_a) g \quad (3.111)$$

Drag force in the x-direction

$$\begin{aligned} D_x = & \frac{1}{2} C_{D3} 2 a L \sin \varphi \rho_a \left| \vec{U} - \vec{U}_a \right| (u - u_a) \\ & - 0.5 C_{fric} \rho_a \pi \sqrt{2(a^2 + b^2)} L \left| \vec{U} - \vec{U}_a \right|^2 \cos \theta \end{aligned} \quad (3.112)$$

where φ is the angle between the surface projection of the element centerline with the x-axis; and θ_1 is the angle between the element centerline and the x-axis.

Drag force in the y-direction

$$\begin{aligned}
 D_y &= \frac{1}{2} C_{D_4} 2 b L \rho_a \left| \vec{U} - \vec{U}_a \right| v \\
 &- 0.5 C_{\text{fric}} \rho_a \pi \sqrt{2(a^2 + b^2)} L \left| \vec{U} - \vec{U}_a \right|^2 \cos \theta_2
 \end{aligned}
 \tag{3.113}$$

where θ_2 is the angle between the element center line and the y-axis.

Drag force in the z-direction

$$\begin{aligned}
 D_z &= \frac{1}{2} C_{D_3} 2 a L \cos \varphi \rho_a \left| \vec{U} - \vec{U}_a \right| (w - w_a) \\
 &- 0.5 C_{\text{fric}} \rho_a \pi \sqrt{2(a^2 + b^2)} L \left| \vec{U} - \vec{U}_a \right| \cos \theta_3
 \end{aligned}
 \tag{3.114}$$

where θ_3 is the angle between the element center line and the z-axis.

Buoyancy

$$B = \pi a b L (\rho_a(0) - \rho)
 \tag{3.115}$$

Solid volume of the i^{th} solid component in the element

$$P_i = \pi a b L C_{si}
 \tag{3.116}$$

The trajectory of the two-dimensional buoyant element is furnished by:

$$\frac{dx}{dt} = u \quad (3.117a)$$

$$\frac{dy}{dt} = v \quad (3.117b)$$

$$\frac{dz}{dt} = w \quad (3.117c)$$

In equations 3.112 and 3.114, C_{D_3} is the drag coefficient for a two-dimensional streamlined wedge. In equation 3.113, C_{D_4} is the drag coefficient for a two-dimensional plate. C_{fric} is a skin friction coefficient. Discussion of suggested numerical values for these and other coefficients will be deferred until Section 5.2.

Equations 3.92 through 3.116 constitute a set of equations soluble by any of several numerical integration schemes. The initial conditions are obtained from the information for the end of the convective descent. Note that the numerical integration for collapse in the water column is carried out with respect to an element of the plume length, ds , and not with respect to dt . Since the derivatives in the conservation equations are with respect to time, a special treatment is required. Discussion of this and other details will be deferred until Section 5.2.

3.3.3 Dynamic Collapse on the Bottom

If the density stratification is not strong enough to arrest the vertical motion of the plume or if the discharging vessel is moving too slowly, the plume may hit the bottom in the

short term. A mathematical model will be presented here which is an extension of the model of Section 3.3.2 for application to a plume collapsing on the bottom.

It is assumed that the shape of the plume cross section is changed to, and maintained as, a semi-ellipse as shown in the upper half of Figure 3.8a. This shape is described by

$$\frac{y'^2}{a^2} + \frac{x'^2}{b^2} = 1 \quad (\text{Eq. 3.21})$$

Velocity differences are allowed between the plume element L , the bottom, and the ambient fluid. The bottom is assumed to be horizontal in the region of the plume. The situation is so close to that for collapse in the water column that the same equations, modified for the different geometry and to account for the reaction force at the bottom and the friction force at the bed, can be used. The governing equations are:

Conservation of mass

$$\frac{d}{dt} \left(\frac{1}{2} \rho \pi a b L \right) = E \rho_a - \sum_i S_i \rho_i \quad (3.118)$$

Conservation of momentum

$$\frac{d}{dt} \left(\frac{1}{2} C_M \rho \pi a b L \vec{U} \right) = \vec{F}_j - \vec{D} + E \rho_a \vec{U}_a - \sum_i S_i \rho_i \vec{U}_i - \vec{F}_F \quad (3.119)$$

Conservation of buoyancy

$$\frac{d}{dt} \left(\frac{1}{2} \pi abL (\rho_a(0) - \rho) \right) = E (\rho_a(0) - \rho_a) - \sum S_i (\rho_a(0) - \rho_i) \quad (3.120)$$

Conservation of solid particles

$$\frac{dP_i}{dt} = -S_i \quad (3.121)$$

The equation for the dynamic collapse of a quadrant of the semi-elliptical cylinder is:

$$I = F_D - D_D - F_F - F_{bf} \quad (3.122)$$

where the inertial force is

$$I = \frac{d}{dt} \left(\frac{ab}{3} L \rho v_I \right) \quad (3.123)$$

the driving force of collapse is

$$F_D = \frac{1}{6} g L \left(1 - \gamma \frac{a_0}{a} \right) \left(\frac{\partial \rho}{\partial y} \right) a^3 \quad (3.124)$$

the form drag is

$$D_D = \frac{1}{2} C_{drag} \rho_a L_a \left| v_2 \right| v_2 \quad (3.125)$$

the skin friction is

$$F_f = C_{\text{fric}} \frac{b}{a} L v_2 \quad (3.126)$$

the friction force on the bottom is

$$F_{\text{bf}} = F_b F_{\text{rictn}} F_1 \quad (3.127)$$

These forces all act at the centroid of the quadrant of the element L . The tip velocity of the quadrant is:

$$\frac{db}{dt} = v_1 + v_3 \quad (3.128)$$

The tip velocity due to collapse, v_1 , is obtained by solving the integral of Eq. 3.123 for the new value v_1 . The integral results from the integration of the summation of forces (3.124) through (3.127), evaluated using the old v_1 . v_2 is the combination of the tip velocity due to collapse and that due to the stretching of the element L . v_2 is obtained by assuming that the minor axis, a , is kept constant and that no entrainment occurs at that moment:

$$v_2 = v_1 - \frac{b}{L} \frac{dL}{dt} \quad (3.129)$$

The stretching of the element L is estimated from:

$$\frac{L}{\sqrt{u^2 + w^2}} = \text{constant} \quad (3.130)$$

v_3 is the contribution to tip velocity due to entrainment:

$$v_3 = \frac{E\rho_a - \sum S_i \rho_i}{\rho \pi a L} \quad (3.131)$$

Additional equations are necessary as follows:

Entrainment volume

$$E = \sqrt{\frac{a^2 + b^2}{2}} L \left(\alpha_3 \left| \vec{U} - \vec{U}_a \right| + \alpha_4 \frac{db}{dt} \right) \quad (3.132)$$

Settling rate of the i^{th} solid component

$$S_i = 2 b L \left| v_{fi} \right| C_{si} (1 - \beta_i) \quad (3.133)$$

where β_i is a coefficient which behaves as described in Section 3.2.1

Momentum

$$\vec{M} = \frac{1}{2} C_M \rho \pi a b L \vec{U} \quad (3.134)$$

Buoyancy force

$$F = \frac{1}{2} \pi a b L (\rho - \rho_a) g \quad (3.135)$$

Bottom friction force in the x-direction

$$F_{F_x} = F_b F_{\text{frictn}} (u-u_b) / \psi \quad (3.136)$$

Reaction force at the bottom

$$F_{F_y} = -F_b = -F + \frac{d}{dt} \left(\frac{1}{2} C_M \rho \pi a b L v \right) + \sum S_i \rho_i v \quad (3.137)$$

Bottom friction force in the z-direction

$$F_{F_z} = F_b F_{\text{frictn}} (w-w_b) / \psi \quad (3.138)$$

Resultant velocity difference between the plume element and the bed

$$\psi = \sqrt{(u-u_b)^2 + (w-w_b)^2} \quad (3.139)$$

Drag force in the x-direction

$$D_x = \frac{1}{2} C_{D_3} a L \sin \varphi \rho_a \left| \vec{U} - \vec{U}_a \right| (u-u_a) \\ + \frac{1}{2} C_{\text{fric}} \rho_a \pi \sqrt{2(a^2+b^2)} L \left| \vec{U} - \vec{U}_a \right|^2 \cos \varphi \quad (3.140)$$

Drag force in the y-direction

$$D_y = \frac{1}{2} C_{D_4} 2 b L \rho_a \left| \vec{U} - \vec{U}_a \right| v \quad (3.141)$$

Drag force in the z-direction

$$\begin{aligned}
 D_z &= \frac{1}{2} C_{D_3} a L \sin\varphi \rho_a \left| \vec{U} - \vec{U}_a \right| (w - w_a) \\
 &+ \frac{1}{2} C_{fric} \rho_a \pi \sqrt{2(a^2 + b^2)} L \left| \vec{U} - \vec{U}_a \right|^2 \sin\varphi
 \end{aligned}
 \tag{3.142}$$

Buoyancy

$$B = \frac{1}{2} \pi abL (\rho_a(0) - \rho)
 \tag{3.143}$$

Volume of the i^{th} component in the element

$$P_i = \frac{1}{2} \pi abL C_{si}
 \tag{3.144}$$

Forces that occur in the momentum equation in the y-direction are presented for completeness. However, to avoid numerical problems that sometimes occur and to achieve a certain simplification, the position and vertical velocity of the element centroid are determined by geometry as long as the element contacts the bottom. The vertical velocity is related to the tip velocity due to collapse by:

$$v = \frac{4}{3\pi} \frac{a}{b} v_1
 \tag{3.145}$$

In equations (3.136), (3.138), and (3.139), u_b and w_b are velocities of the bottom with respect to a coordinate fixed on the discharging vessel.

As before, the trajectory of the plume may be determined by

$$\frac{dx}{dt} = u \quad (\text{Eq. 3.117a})$$

$$\frac{dy}{dt} = v \quad (\text{Eq. 3.117b})$$

$$\frac{dz}{dt} = w \quad (\text{Eq. 3.117c})$$

Equations (3.118) through (3.145) constitute a set of equations soluble by any of several numerical integration schemes. The initial conditions are obtained from the information for the end of the convective descent. Note that the numerical integration for collapse on the bottom is carried out with respect to an element of the plume length, ds , and not with respect to dt . Since the derivatives in the conservation equations are with respect to time, a special treatment is required. Discussion of this and other details will be deferred until Section 5.2.

4. DEVELOPMENT OF MODEL FOR PASSIVE
DIFFUSION

The final phase to be incorporated into the model begins when cloud behavior is determined more by ambient currents and turbulence than by any dynamic character of its own. In this phase, then, the cloud is considered passive, its fate being dependent upon features of the ambient fluid. The treatment of this phase in the Koh-Chang ocean dumping model was somewhat simplified by the assumptions of horizontally uniform, steady currents and absence of lateral boundaries. In that case, it was possible to apply a method of moments to solution of the diffusion equation eliminating x and z as independent variables. Significant information regarding the cloud history could be found very economically from the first few moments.

In the present application, nonuniform currents, lateral boundaries, and unsteady flow combine to make adoption of such a method of solution unsatisfactory. The straightforward approach would involve solution of the convection-diffusion equation by finite differences. However, this technique is prohibitively expensive if a three-dimensional treatment is needed for routine use. Instead, this study has adapted and extended a scheme developed by Fisher (1970, 1972), which overcomes these difficulties, is extremely economical and efficient, and--while originally developed for the two-dimensional vertically integrated case--permits the necessary generalization required here. Fischer's approach will first be outlined in order to convey most clearly the fundamental conceptual features of the present model.

Consider an unbounded, steady, uniform mean flow. The concentration of a conservative substance at any point and time

can be found from

$$C(x, z, t) = \frac{1}{4\pi} \iint \frac{C(\xi, \eta, 0)}{t\sqrt{D_x D_z}} \exp\left(\frac{-1}{4t} \left(\frac{(x-ut-\xi)^2}{D_x} + \frac{(z-wt-\eta)^2}{D_z} \right)\right) d\xi d\eta \quad (4.1)$$

where D_x and D_z are horizontal diffusivities; u and w are (constant) vertically averaged velocity components; and the integration extends over the entire plane. This convolution integral states that the concentration at any point at time t is related to the initial (and arbitrary) distribution at an earlier time (taken to be zero) as the summation of contributions from every point in the fluid. This is seen by noting that under the assumptions, $x - ut$ and $z - wt$ are simply the initial coordinates of the fluid now residing at (x, z) ; call these (ξ_0, η_0) . The terms like $(\xi_0 - \xi)^2$ are then simply related to the distances between the source location of the element of interest and all other points. The new concentration at (x, z) , $C(x, z, t)$, is the summation of contributions from points surrounding (ξ_0, η_0) , each having an influence dependent upon separation, diffusivity, and time.

Fischer's approach to the nonuniform, nonsteady (but vertically averaged) case was to approximate the processes implicit in equation 4.1 as follows. Firstly, the terms like $x-ut$ are replaced by

$$\xi_0 = x - \int_0^t u dt \approx x - \sum_{i=1}^N u_i \delta t \quad (4.2)$$

in which δt is a small fraction of the interval t ($\delta t = t/N$) and the u_i are velocity components--assumed given--at each time sub-interval. The particle is simply followed backward in time in small straight-line segment steps.

The double integral in equation 4.1 is approximated by a simple averaging of concentrations found in the vicinity of (ξ_0, η_0) . Adopting a computational grid as shown in Figure 4.1a with space step Δx , consider the point (I, J) at time t . At some earlier time the fluid of (I, J) was located at, say, (M, N) and the earlier concentrations at grid points around (M, N) are known. Consider the expression:

$$C_{\text{NEW}}(I, J) = \frac{1}{5} \left\{ C(M, N) + C(M+1, N) + C(M-1, N) \right. \\ \left. + C(M, N+1) + C(M, N-1) \right\}_{\text{OLD}} \quad (4.3)$$

which is a simple average of the five old concentrations around the source of (I, J) . Such an averaging constitutes an effective diffusion which, as shown by Fischer, is equivalent to a diffusion coefficient of $0.2 (\Delta x)^2 / \Delta t$ where Δx is the mesh spacing and Δt is the total time interval for passage from (M, N) to (I, J) .

Certain boundary conditions are necessary. If the backward convection process carries the marker particle to a boundary of the computational grid located in water, the new concentration at (I, J) is set equal to an arbitrarily chosen background concentration. If the backward convection should carry the marker particle to a land boundary (possible since the integral of velocity is approximated by a discrete summation), the backward marching

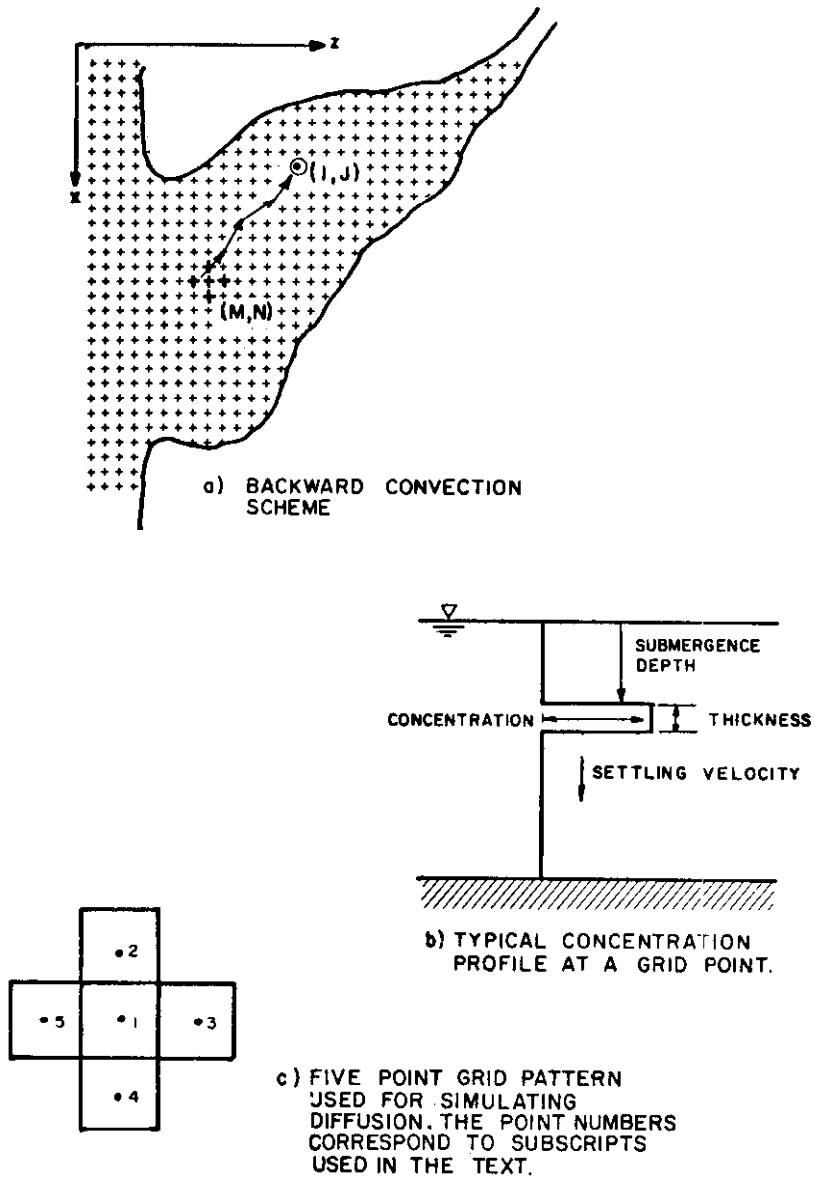


Figure 4.1 Aspects of Passive Diffusion

is stopped and the new concentration at (I, J) is chosen to be the old concentration at the water point nearest the landfall point.

It is seen, then, that one can select the diffusion coefficient by simply selecting appropriate values of Δx and Δt . The simplicity of Equations 4.2 and 4.3 and the fact that Δt can be chosen quite large (up to several hours, in fact) are responsible for the extreme efficiency and economy of the approach.

For purposes of this study, it was necessary to make extensive modifications to the above scheme; chief among which were: additional parameters to describe the locations of various dredged material constituent clouds; improvements in the treatment of horizontal passive diffusion; addition of vertical diffusion; provision for settling of solid particles; provision for recording the cumulative distribution of material settled to the bottom; generalization of the diffusion scheme to allow variations in time and space steps; and, finally, provision for smooth transition from the short-term dynamic computations to the long-term passive diffusion. The term "long-term" here and in what follows is taken to mean a time duration ranging from several to many hours. The various modifications are described below.

Fischer's model treated constituents as well mixed from surface to bottom. Since dredged material particles will tend to segregate themselves according to fall velocity, in effect leading to the formation of layers, it was necessary to add parameters to describe these layers. Each dredged material constituent is allowed to exist at each grid point with a "top-hat" profile, similar to that shown in Figure 4.1 b. Each constituent layer is described by its submergence depth, its thickness, and the concentration of

the constituent within the layer, all of which may vary with time and horizontal position within the estuary. In the absence of other effects to be discussed later, the constituent layer will settle towards the bottom with the settling velocity of the particles it contains.

The expedient of assigning the marker particle location after backward convection to the nearest grid point has caused mass conservation difficulties at land boundaries and pseudo-dispersion in open-water locations. To remedy this, the "nearest gridpoint" scheme was replaced by the following procedure. Once the origination point of the marker particle has been found, it lies in a box defined by the four surrounding grid points. Interim concentrations are found at each corner of the box by a 5-point averaging formula. Then the concentration at the marker particle is found by interpolating among the four points. Actually, the diffusion procedure is somewhat more complicated because of the additional variables introduced into the cloud description. The complications arise mainly from possible differences in the thickness of a constituent layer at adjacent grid points. It is not reasonable to average the layer thicknesses, even if the resultant mass conservation difficulties are ignored. It does seem reasonable to allow the thinner layer to smear out so that its thickness is equal to that at the adjacent point. The concentration of the thinner layer is adjusted accordingly to conserve mass and called the effective concentration. Each five-point average is found by determining the greatest layer thickness, adjusting the thickness and concentration of the other four points, and then averaging the concentrations. The thickness is the adjusted thickness. The submergence depth is determined by the average submergence depth of the points contributing mass.

The convection of the above scheme is exclusively in the horizontal direction. It hardly seems reasonable for a slowly settling dredged material cloud to be convected horizontally to plow into a sloping bottom. Physically one would expect the cloud to drift upward as it passed over the sloping bottom before ultimately settling out. To account for this in rough fashion, the vertical position of the concentration "top-hat" is modified according to the depths at the initial and final positions of clouds and the initial relative depth of the cloud with respect to the bottom.

When the stratification in the ambient fluid is weak or nonexistent, vertical growth of the dredged material clouds, due to turbulent diffusion, may be expected. To account for this a simple vertical diffusion law was introduced as follows. Assuming that the concentration profile is Gaussian in the vertical and that vertical spreading is governed by the simple form:

$$\frac{\partial c}{\partial t} = K_y \frac{\partial^2 c}{\partial y^2} \quad (4.4)$$

where K_y is the representative vertical diffusivity, one finds

$$\frac{d\sigma^2}{dt} = 2K_y, \quad (4.5)$$

which is the rate of growth of thickness of a Gaussian cloud. For the top-hat profile that has been assumed, the distance from the centroid to an upper or lower boundary is taken as $\xi \approx 2\sigma$. Approximating the derivative, putting the expression into terms of ξ , and solving for the growth of one boundary, $\Delta\xi$, in time increment Δt gives:

$$\Delta \xi = 2 \sqrt{2 K_y \Delta t} \quad (4.6)$$

This is the expression used to estimate the vertical growths of the upper and lower boundaries of dredged material clouds.

Tennekes and Lumley (1972) stress that the eddy diffusivity is an artifice which may or may not represent the effects of turbulence faithfully. Nevertheless it is necessary to make some determination of K . For this purpose the formulas developed in Section 2.2.3.2 are used.

The settling of cloud particles is treated very simply. During each step of passive diffusion, clouds of similar solid particles are assumed to fall a distance through the water column, which is the product of the fall velocity of the solid particles and the time elapsed during the step. If the cloud at any grid point encounters the bottom during the settling stage, an appropriate percentage of the solid mass it contains is transferred to a separate array that keeps track of bottom accumulation.

To allow greater latitude in the selection of space steps and time steps in the passive diffusion phase, it was necessary to generalize the diffusion parameter used in the five-point averaging equation. Figure 4.1c shows the five-point grid pattern used in the diffusion process. The cloud thicknesses and the concentrations at the five points have been adjusted as discussed above. The rate of mass exchange between grid points is the product of a diffusion coefficient, a cross-sectional area through which the transfer occurs, and a concentration gradient. The rate of mass transfer between point 1 and an outside point, say point 2, is:

$$\dot{M} = E \cdot (T \cdot \Delta x) \cdot \frac{C_1 - C_2}{\Delta x} \quad (4.7)$$

where E is the diffusion coefficient; T is the cloud thickness; Δx is the grid point spacing; and C_i denotes concentration. The change of concentration in grid point 1 due to interaction with grid point 2 during a time increment Δt is:

$$\Delta C = \frac{E \cdot \Delta t}{(\Delta x)^2} (C_1 - C_2) \quad (4.8)$$

If the original concentration at grid point 1 is C_1 , the new concentration, C'_1 , after a time increment, Δt , is found by summing the concentration changes due to each of the surrounding four points:

$$C'_1 = C_1 - \frac{E \cdot \Delta t}{(\Delta x)^2} (4C_1 - (C_2 + C_3 + C_4 + C_5)) \quad (4.9)$$

It is of interest to compare 4.9 with Fischer's original expression 4.3. Rewriting these equations to be identical in form except for the diffusion parameters and equating these parameters and rearranging, gives:

$$E = \frac{0.2 (\Delta x)^2}{\Delta t} \quad (4.10)$$

The term on the right is Fischer's effective diffusion coefficient when the numerical value of the diffusion parameter is 0.2. This equation shows that Fischer's diffusion coefficient depends entirely

on his choices for space step Δx and time step Δt . The present work seeks to be able to model an estuary using some value for the diffusion coefficient that is deemed appropriate. It is desirable to do this independently of the Δx and Δt that is chosen. For this reason, then, equation 4.9 was derived. With a constant diffusion coefficient, equation 4.9 will reduce the exchange between grid squares as Δt decreases and the equation will increase the exchange as Δx decreases. This behavior is as expected. Numerical stability does require that an upper limit be placed upon the diffusion parameter, $E \cdot \Delta t / (\Delta x)^2$. This upper limit must be 0.2 since any higher value allows transfer of more material from the central square than is originally present.

It remains to determine an appropriate value for the diffusion coefficient, E . The diffusion coefficient is generally taken to be a function of a characteristic length to some power. In the ocean it is fairly well established that the length is that of a diffusing cloud and the power is $4/3$. In estuaries, such a relation has not been well established. The limited experimental data for diffusion in estuaries (Figure 2.4) suggests that a four-thirds law is not an unreasonable way to estimate diffusion coefficients. Because a choice must be made, the following relation is chosen:

$$E = A_\lambda L^{4/3} \quad (4.11)$$

where A_λ is a dissipation parameter and L is a characteristic length. Any power law formulation relies on the assumption that turbulent eddies of all sizes are available to make a diffusing cloud grow. In the present model, any eddy larger than the grid size Δx is treated as part of the mean flow and so it makes no contribution to diffusion. Only eddies up to the size of Δx contribute to diffusion between grid boxes. These arguments lead to the choice of Δx as the characteristic length and give:

$$E = A_{\lambda} (\Delta x)^{4/3} \quad (4.12)$$

There is one last matter to be considered before the above technique for passive diffusion can be implemented. How does one make the transition from the end of short-term dynamic computations to passive diffusion? The results of short-term computation (either jet discharge or instantaneous dump) are interpreted as producing a series of small clouds containing segregated sets of solid particles that are ready to enter passive diffusion at different times. If these clouds are substantially smaller than the grid spacing used for the passive diffusion computation, introducing them directly into the passive diffusion grid would lead to an undue amount of numerical diffusion. To avoid this, each cloud is tracked separately, being convected by ambient currents, diffused horizontally and vertically according to the simple diffusion laws discussed above, and settled according to the fall velocity of its particle type. This process continues for each cloud through each passive diffusion step until the cloud grows to the size of the passive diffusion grid, when it is injected into the grid.

5. DESCRIPTION OF COMPUTER REALIZATIONS OF MODELS

This chapter discusses the structure of each of the two computer codes in detail. The chapter is divided into sections for the instantaneous dump model and the jet discharge model. Each section includes a description of the model, the criteria for transition between computational phases, a block diagram, discussion of the idiosyncracies of individual routines, discussion of diagnostic parameters that are produced, and finally the computational situations that are expected to be troublesome. The notation in this chapter will use the conventions of the FORTRAN language.

5.1 Computer Code for Instantaneous Dump

The dump model is formulated within the framework of longer term passive diffusion. The estuary (or portion of it) of interest is described on a rectangular grid of variable depths spaced at constant intervals in both directions. This constant interval is denoted DX in the code. Passive diffusion computations are carried out on this grid within successive time steps of uniform duration that must be longer than the total time for short-term dynamic phenomena to be completed. The grid is allowed to have arbitrary areas of land (zero depth) within it, and the boundaries may be land or water. The coordinate axes for the estuary are X and Z , and these are oriented as shown in Figure 5.1. Grid points are identified by a coordinate numbering system. A particular grid point is identified by its coordinates (N,M) where N is in the Z -direction and M is in the X -direction. The upper left corner grid point is $(1,1)$, and under this system the origin of coordinates is $(0,0)$. Distances of any grid point from the origin are related to

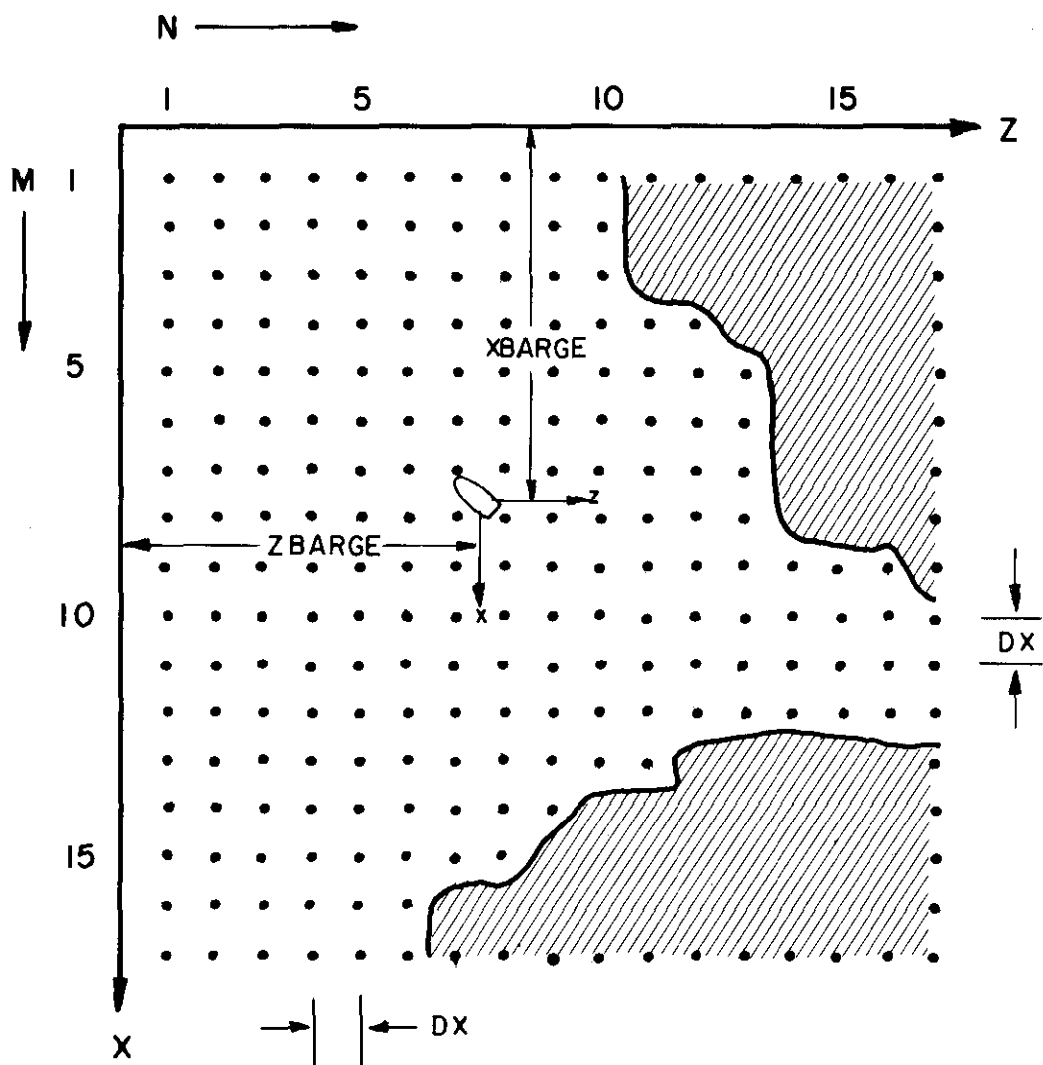
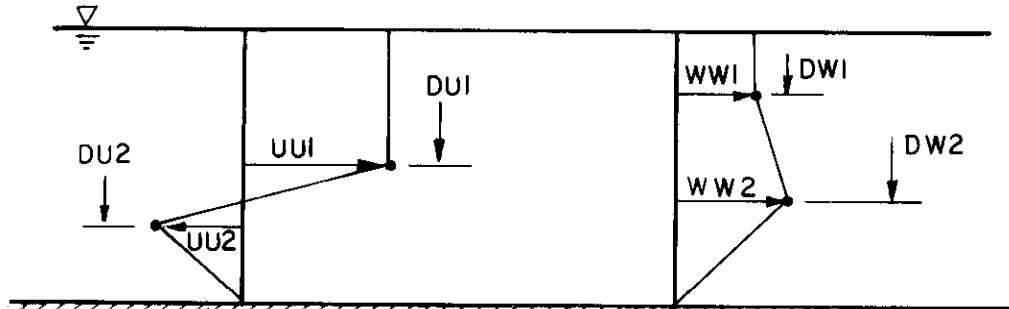


Figure 5.1 Diagram of Long-Term Passive Diffusion Grid in Estuary Showing Coordinate Systems Used

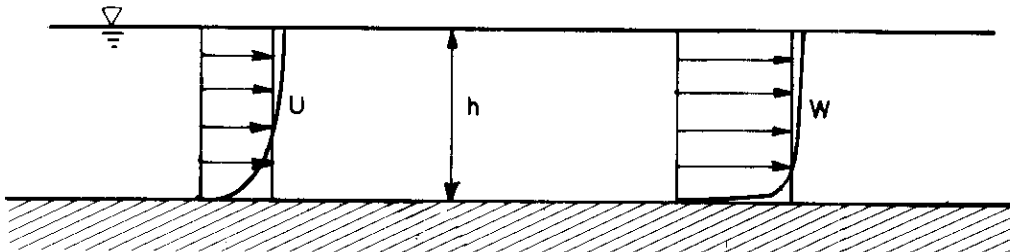
its coordinate numbers by $X_i = M_i * DX$ and $Z_i = N_i * DX$. Located within the estuary is a vessel from which dredged material is to be discharged. Its position is given by distances X BARGE and Z BARGE as shown. To this vessel is attached another set of coordinate axes, x and z in the horizontal and y vertically downward. The x and z axes remain always parallel to the X and Z axes, respectively. In the discussion that follows, a reference to "estuary coordinates" means the X-Z system; while a reference to "vessel coordinates" means the x-z system.

The grid provides a choice of four different ways to specify the ambient velocity field during a particular time step. U velocities are in the X-direction and W velocities are in the Z-direction. These will now be described in order of increasing complexity. The simplest velocity field is specified by the user on one data card. It consists of two orthogonal velocity profiles, typical examples of which are shown in Figure 5.2a and is applicable only to cases where the depth is constant. These velocity profiles are assumed to be the same everywhere in the field of interest and to be invariant with time.

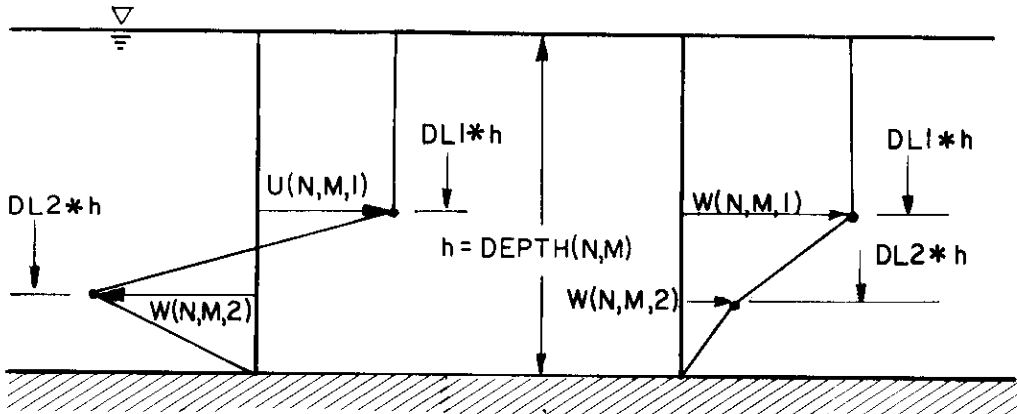
The next level of velocity detail is given by vertically averaged velocities that vary in the horizontal (from one grid point to the next) and in time. The time variation is such that the velocity field is constant within one time step, but varies between steps. This type of velocity information may be applied to a variable depth geometry. The velocity field must satisfy conservation of fluid. If it is assumed that the water surface is a fixed rigid plane, the continuity equation reads:



a) SIMPLE ORTHOGONAL VELOCITY PROFILES FOR CONSTANT DEPTH. APPLIED EVERYWHERE IN FIELD.



b) VERTICALLY AVERAGED VELOCITY PROFILES FOR VARIABLE DEPTHS WITH EQUIVALENT LOGARITHMIC PROFILES SUPERIMPOSED.



c) TWO-LAYER PROFILES FOR VARIABLE DEPTH.

Figure 5.2 Illustration of the Various Velocity Profiles Available for Use in Model

$$\frac{\partial}{\partial x} (h U_h) + \frac{\partial}{\partial z} (h W_h) = 0 \quad (5.1)$$

where h is the water depth and U_h and W_h are depth averaged velocities. Typical velocity profiles of this type are shown in Figure 5.2b. This is the type of velocity information which is produced by the various two-dimensional finite-difference hydrodynamics codes.

The next level of velocity detail accepts vertically integrated velocities as described in the previous paragraph. The velocities are then interpreted as logarithmic profiles, which, when vertically averaged, yield the original averaged velocities. Logarithmic profiles are illustrated superimposed on the vertically averaged velocities of Figure 5.2b.

The most complex form of velocity specification is suited to the sort of velocity distributions expected in highly stratified estuaries. At each point, velocities are given at two different fractions of the total depth. The fractions are constant over the entire depth field during one time step, but they may change from one time step to the next. Typical profiles are shown in Figure 5.2c. If velocity data is given in this form, the velocities must be such that the continuity equation

$$\frac{\partial u}{\partial x} + \frac{\partial w}{\partial z} = 0 \quad (5.2)$$

is satisfied at every depth of every grid point. This requirement will limit the use of this option to those few users who are willing

to make the most extensive and rigorous preparations for a run.

It may be that a user specifies a variable velocity field in one of the above options that does not satisfy continuity everywhere. In such a case, mass will not be conserved where continuity is not satisfied.

The above comments apply to a velocity field specified for one time step. The velocity field varies in time by reading in new velocity fields at successive time steps. The velocity field is read from a tape or other mass-storage device (by subroutine UW) that holds velocity data for one complete tidal day. The tidal day is assumed to be 25 hours and it is divided up into some integer number of time steps. If the velocity field varies in time, then it must be specified at each time step. The tidal cycle is assumed to exactly repeat itself, so that the last set of velocities of the tidal day is followed by the first set. This format allows the user to begin his simulation at any part of the tidal day and continue it for an arbitrary length of time.

Once the velocity field is defined for a time step, subroutine VEL acts to fetch velocity information for any routine that needs it. This routine is called with a position in estuary coordinates; the velocities surrounding the position are interpolated for the needed velocities, and these velocities are returned by VEL.

Information on density profiles within the estuary must also be supplied. For convenience, a single density profile is assumed to define isopycnals, which are constant depth planes extending over the entire grid. The density profile is that measured or otherwise determined at the dump site. Since the

same density profile is used throughout the grid, the profile must be defined down to the deepest depth in the grid, even though the dump site may be much shallower.

The time that the dump occurs is specified as elapsed time since the start of a tidal cycle, measured to the nearest long-term time step. The time is specified in this way so it can be conveniently related to the ambient velocities. The duration of the simulation may be set completely arbitrarily. If the simulation runs over the end of the tidal day, the velocity tape is rewound and simulation continues from the start of the tidal day. The long-term time step is specified independently, but the user must supply a new set of velocities for each new time step.

Once the bathymetry and ambient conditions in the estuary have been defined and the discharging vessel is positioned, a run can be made. Figure 5.3 shows a block diagram of the code. The discharge of dredged material is described by the radius of the initial hemispherical cloud, the depth of the initial cloud centroid, the initial velocity of the cloud, and the initial bulk density of the cloud. The solids (up to 12) within the cloud are described by their solid densities, concentrations, and fall velocities. All of the following short-term calculations describe the cloud position in vessel coordinates.

The convective descent of the cloud is computed using the equations of Section 3.1.1, by subroutine DUMP calling a standard fourth-order Runge-Kutta routine (subroutine RUNGS). This routine is supplied with the necessary derivatives by subroutine DERIVD, and it simultaneously integrates the equations of motion over a small time step, DT. (The time steps referred

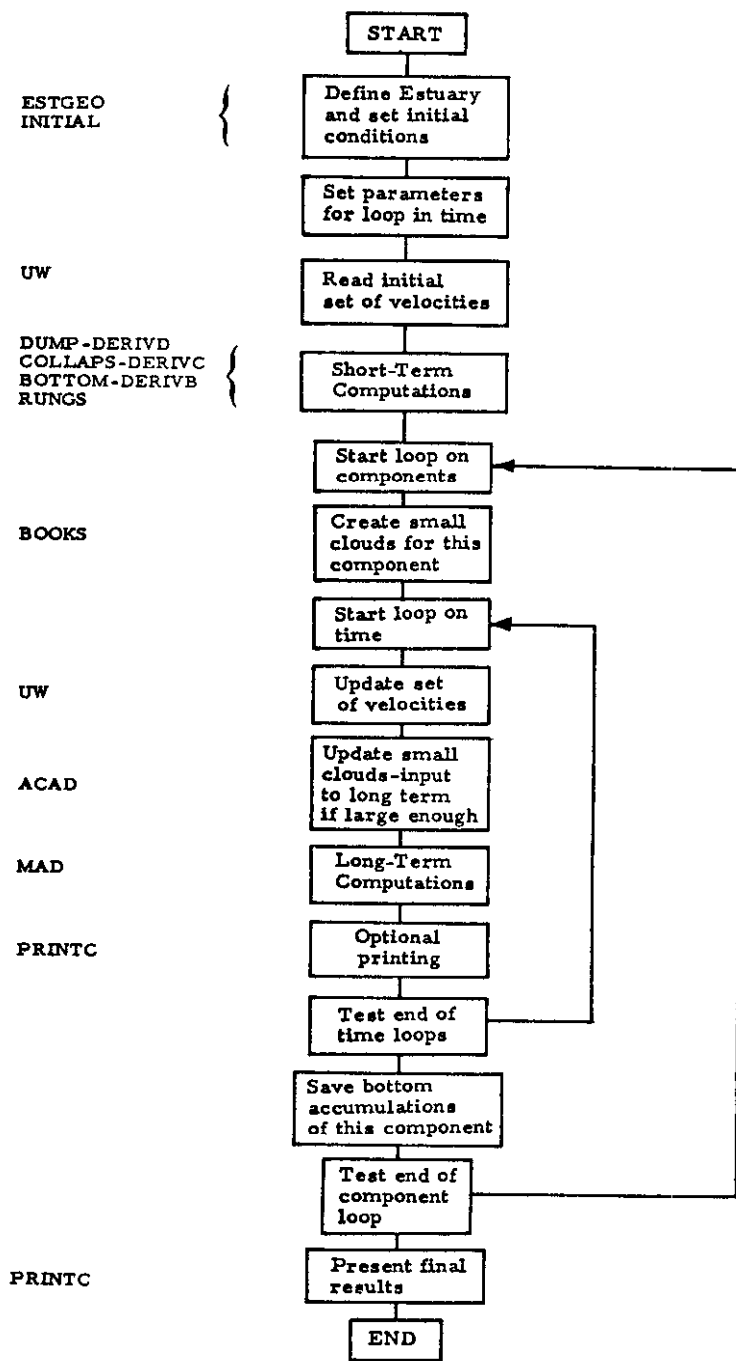


Figure 5.3 Block Diagram of Dump Discharge Model

to in the short-term dynamic computations are not to be confused with the long-term time step DTL used in passive diffusion and over which the fluid velocity varies in time.) Subroutine DUMP is allowed five tries to compute a history of the convective descent. A trial solution is successful when the cloud has taken between 100 and 200 time steps to either reach a level of neutral buoyancy or to hit the bottom.

When the cloud encounters neutral buoyancy, its shape is instantly transformed from a hemisphere to an oblate spheroid and the computation proceeds in subroutine COLAPS (using the equations of Section 3.2.2) again using RUNGS, which is supplied with the necessary derivatives by DERIVC. Initial conditions are obtained from the final step of convective descent. As before, five tries are allowed to complete the solution. A successful solution uses between 100 and 399 time steps to compute the history of cloud collapse from the end of convective descent out to where the spreading of the cloud due to collapse is less than that due to diffusion.

If the descending hemispherical cloud hits the bottom the shape of the cloud is instantly transformed to an upper half oblate spheroid, and the computation proceeds in subroutine BOTTOM solving the equations of Section 3.1.3, using RUNGS with derivatives supplied by DERIVB. The other details are the same as for collapse.

The total elapsed time in the above computations must be less than the long-term passive diffusion time step over which ambient velocities are specified.

In the dynamic calculations summarized above, there are a number of variables which act as computational signposts. These are printed out by DUMP, COLAPS, and BOTTOM, immediately upon completion of any trial solution. They are sometimes useful in diagnosing computational trouble. The computational indicators are NTRIAL, DT, IPLUNG, NUTRL, ISTEP, IBED, and ILEAVE. NTRIAL is the trial solution number. DT is the time step in seconds. IPLUNG indicates the state of the cloud: its initial value is 0; 1 indicates the cloud hit bottom in subroutine DUMP; 2 indicates the cloud hit bottom in subroutine COLAPS; and 4 indicates the cloud has risen off the bottom. NUTRL has an initial value of 0; a value of 1 indicates the cloud has encountered neutral buoyancy; and 3 indicates that the diffusive spreading of the cloud is greater than dynamic spreading. ISTEP is simply the number of time steps in the trial solution. IBED has an initial value of 0; any other value stores the time step when the cloud hit bottom. ILEAVE has an initial value of 999; any other value stores the time step when the cloud rises off the bottom.

Once the short-term dynamic computations are completed, the transition into the long-term grid for passive diffusion must be made. The entire process of passive diffusion is conducted for each component of the cloud by itself. For each solid component in turn and finally for the fluid component, the following sequence occurs. Subroutine BOOKS examines the stored history of the main cloud and creates small clouds as material settles out of the main cloud. The maximum number of small clouds which may be created is set by the input variable NSC. The positions of these clouds are transformed from vessel coordinates to estuary coordinates. This set of small clouds is then convected, diffused, and settled (by subroutine ACAD) over successive long-term time steps until the small clouds grow to the size of the long-term grid. When the small

clouds are large enough, they are injected into the long-term grid, where the convection, diffusion, and settling is handled by sub-routine MAD all the way to the ending time of the simulation. (MAD is the end result of the extensive modifications to the code of Hugo Fischer). Once final results are presented for this component, the code branches back to BOOKS to begin simulation of the next component.

Horizontal diffusion in the transition routines, BOOKS and ACAD, is handled by a formulation based on a four-thirds law, while diffusion in MAD is handled by the averaging scheme of Chapter 4. Vertical diffusion is handled according to the development in Chapter 4. At any point where vertical diffusion is to be computed, the vertical diffusion coefficient is estimated on the basis of the density profile and the local velocity gradient.

There are a number of numerical coefficients used in the program. With two exceptions, these are the same as those used by Koh and Chang (1973). ALAMDA, the dissipation parameter for the four-thirds law, is expected to be somewhat higher in an estuary. This study has chosen to use the value of $0.005 \text{ ft}^{2/3}/\text{sec}$. The maximum value for the vertical diffusion coefficient, AKYO, has been estimated to be $0.05 \text{ ft}^2/\text{sec}$.

The following coefficients are identical in names and default numerical values to those supplied by Koh and Chang for the instantaneous bottom dump configuration. They are presented here for completeness. DINCR1 (default value = 1.0) and DINCR2 (default value = 1.0) are factors used in computing time increments in the descent and collapse phases respectively. These may be modified during program execution. ALPHA0 (default value = 0.235) is the

entrainment coefficient for a turbulent thermal determined experimentally by Koh and Chang. ALPHAC (default value = 0.001) is the coefficient for entrainment due to cloud collapse given by Koh and Chang. BETA (default value = 0.0) is the settling coefficient given by Koh and Chang. The default value is expected to be good for low solids concentrations. GAMA (default value = 0.25) is a coefficient introduced by Koh and Chang to simulate the effect of density gradient differences in causing cloud collapse. The default value is based on an educated guess. CD (default value = 0.5) is the drag coefficient for a sphere in the range of Reynolds numbers expected. CD3 (default value = 0.1) is the drag coefficient for a spheroidal wedge in the range of Reynolds numbers expected. Similarly, CD4 (default value = 1.0) is the drag coefficient for a circular plate normal to the flow. CM (default value = 1.0) is the apparent mass coefficient. The reader is cautioned that the default values for the above drag coefficients were obtained from diagrams presented in Hoerner (1965) for solid shapes in fluid; and as such, they are not strictly applicable to this work. However, in the absence of more relevant data, the listed default values will be used. The default values for the remaining coefficients (CDRAG, CFRIC, FRICTN, F1) were presented by Koh and Chang based on educated guess, and are therefore subject to revision. CDRAG (default value = 1.0) is the drag coefficient for an elliptic cylinder edge on to the flow. CFRIC (default value = 0.01) is a skin friction coefficient. FRICTN (default value = 0.01) is a bottom friction coefficient. F1 (default value = 0.1) is a modification factor for bottom friction used in calculating collapse on the bottom.

The above discussion applies to the "default" coefficients, the coefficients the program will use if the user cannot, or chooses not to, supply his own values.

The program has been designed, as much as possible, to inform the user of any problems that may arise. In short term, about the only times that problems occur are when the program cannot estimate a proper time step in the collapse phase. The user may then examine the history of the time steps and modify the value of DINCR2 accordingly. In the passive diffusion phase, problems are usually associated with the small cloud transition from short-term computations to the long-term grid. All the common troubles will be preceded by a self-explanatory diagnostic message to the user.

There are basically two situations where the user may expect to encounter difficulties. The first is where a very large cloud hits a shallow bottom at high speed. The other arises from a small cloud being convected outside of the long-term grid area due to high ambient velocities.

Users interested in dilution times for the fluid portion of the discharge may specify a conservative chemical tracer in the fluid. The tracer is described by an alphameric name and a concentration in milligrams per liter. The ambient fluid has a user specified background concentration in milligrams/liter. At the end of a run, this information is presented, along with the times required for the initial tracer concentration to be reduced by successive factors of 10. Only the point of maximum tracer concentration is examined in the passive diffusion computation; no effort is made to keep track of tracer concentration at every point in the field.

Appendix A is a user's manual for the instantaneous dump model and it contains further details on the program. A listing of the FORTRAN code is contained in Appendix B.

The model for jet discharge operates within the framework of longer term passive diffusion. The structural difference between this model and the model for an instantaneous dump arises from the continuous nature of the jet discharge. The fact that there is a continuous discharge means that all components of the dredged material must be simulated in parallel rather than in series (to borrow the usage from electronics). In addition to the differences of the short-term dynamics, the routines for transition of material from short term to long term are completely different. The routines for passive diffusion contain only small differences.

The layout of the estuary bathymetry is the same as described in Section 5.1 and illustrated in Figure 5.1, except that the vessel coordinates XBARGE and ZBARGE now describe the initial position of the vessel. During a simulation run, the vessel may move at an arbitrary, constant speed. The vessel coordinate system x-z is maintained parallel with the estuary coordinate system X-Z. Passive diffusion computations are carried out on the grid within successive time steps of uniform, but arbitrary duration, DTL. There is continuous input of material to the long-term grid from the results of short-term dynamic computations. Velocities that vary in time must be specified at intervals of DTL.

The ambient velocity specifications for one time step are done in exactly the same manner as described in Section 5.1 and illustrated in Figure 5.2.

The ambient density profile is allowed to vary in time. As in the dump model, a density profile defines horizontal planes of constant density that extend over the entire estuary. New density profiles may be specified, if desired, over time intervals which are integer multiples of the long-term time step DTL. Each profile is that perceived from the vessel at the start of a particular long-term time step. If simulation continues past the time of the last density profile, the last profile is used for the rest of the run. Because one profile at a time is used throughout the estuary, the profiles must be defined down to the deepest point in the estuary.

The time that the jet discharge starts is specified as elapsed time since the start of a tidal cycle, measured to the nearest long-term time step DTL. The time is specified in this way so it can be conveniently related to the ambient velocity information. The duration of the simulation may be set completely arbitrarily. If the simulation runs over the end of the tidal day, the velocity tape is rewound and simulation continues from the start of the tidal day. The long-term time step, DTL, is specified independently, remembering that a new set of velocities must be specified at each time step. The duration of the jet discharge, TJET, may be specified completely arbitrarily.

Once the bathymetry and ambient conditions in the estuary have been defined and the initial point of discharge has been defined, a run can be made. It is possible to simulate a continuous discharge from a fixed point (i. e. , a pipeline) or from a moving vessel; the choice being made by a change of two parameters in the input. Figure 5.4 shows a block diagram of the code.

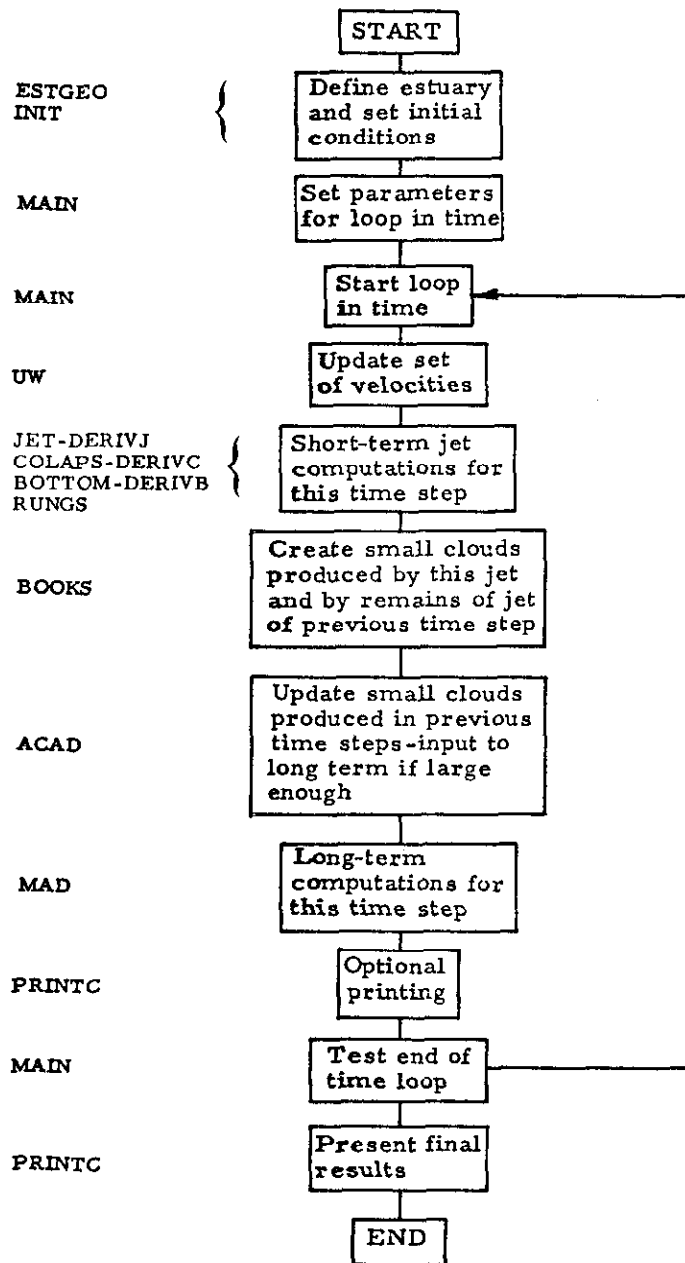


Figure 5.4 Block Diagram of Jet Discharge Model

The discharge of dredged material is described by the volume rate of discharge of the dredged material slurry, the initial radius of the jet, the depth of the discharge nozzle, the vertical angle of the discharge nozzle, and the bulk density of the slurry. The movement of the discharging vessel is described by its position at the start of discharge (XBARGE, ZBARGE), its course SAI (assumed constant and measured anti-clockwise from the positive X-axis), and speed UB. The solids within the jet are described by their solid densities, concentrations, and fall velocities. The surface projection of the initial jet path is opposite to the course, SAI, of the vessel.

As mentioned at the start of this section, the program is organized around the long-term passive diffusion. The main loop in the program is in time-by-time increments, DTL. The first operation in the loop is the updating of the velocity field and the density profile. Within this loop there are calculations in sequence for short-term dynamics, transition of material from short-term plume to long-term grid, and finally the long-term passive diffusion. Each of these will be discussed in more detail.

The convective descent of the jet is computed, using the equations of Section 3.3.1, by subroutine JET calling a standard fourth-order Runge-Kutta routine (subroutine RUNGS). This routine is supplied with the necessary derivatives by subroutine DERIVJ, and it simultaneously integrates the equations of motion over small increments of arc length along the jet axis, DS. Subroutine JET is allowed five tries to compute a history of the convective descent. A trial solution is successful when the cloud has taken between 100 and 190 steps to either reach a level of neutral buoyancy or encounter the bottom.

When the jet encounters neutral buoyancy, its cross-sectional shape is instantly transformed from a circle to an ellipse, and the computation proceeds in subroutine COLAPS (using the equations of 3.3.2) again using RUNGS, which is supplied with the necessary derivatives by DERIVC. Since at this point the jet velocity has become close to that of the ambient, the integration is over time and the path of one element of the plume, which is assumed to behave as a two-dimensional thermal, is followed. Initial conditions are obtained from the final step of convective descent. As before, five tries are allowed to complete the solution. A successful solution uses between 100 and 400 time steps to compute the history of the plume collapse from the end of convective descent out to where the spreading of the cloud due to collapse is less than that due to diffusion.

If the descending jet or collapsing plume encounters the bottom, its cross-sectional shape is instantly transformed to an upper half ellipse and the computation proceeds in subroutine BOTTOM (solving the equations of Section 3.2.3) using RUNGS with derivatives supplied by DERIVB. The other details are the same as for collapse in the water column.

There is no restriction on the long-term time step, DTL, or on the total duration of jet discharge (as they relate to the time required for short-term computations). If the duration of the jet is greater than DTL, new jet-plume histories are computed for as many long-term time steps as are necessary. Ambient velocities and densities may vary between time steps.

In the dynamic calculations summarized above, there are a number of variables that act as computational signposts.

These are printed out by JET, COLAPS, and BOTTOM, immediately upon completion of any trial solution. They are sometimes useful in diagnosing computational trouble. The computational indicators are: NTRIAL, DINCR, IPLUNG, NUTRL, ISTEP, IBED, and ILEAVE. NTRIAL is the trial solution number. DINCR is a factor in setting the integration step. IPLUNG indicates the state of the jet-plume: the initial value is 0; 1 indicates the jet encountered the bottom in subroutine JET; 2 indicates the collapsing plume encountered the bottom in subroutine COLAPS; while 4 indicates the plume encountered the bottom and subsequently rose off of the bottom. NUTRL has an initial value of 0; a value of 1 indicates the jet path has become horizontal; and 3 indicates that the diffusive spreading of the plume is greater than dynamic spreading. ISTEP is the number of time steps in the trial solution. IBED has an initial value of 0; any other value stores the time step when the jet-plume hit bottom. ILEAVE has an initial value of 999; any other value stores the time step when the jet-plume rises off the bottom.

Once the short-term dynamic computations are completed, the transition into the long-term grid for passive diffusion can be made. Passive diffusion is conducted for all components of the plume simultaneously. As diffusion is carried on, there is a continuous movement of material through the transition routines, BOOKS and ACAD, into the long-term grid. For each component, BOOKS breaks up the plume into pieces. A "piece" is a block with thickness equal to the plume thickness, horizontal dimensions equal to the plume width, and containing the amount of material which leaves the end of the plume in a time given by the quotient of the plume width and centerline velocity. All the pieces for each component are stored temporarily in one equivalenced array. The number of pieces produced depends on the duration of the discharge and, to some extent, upon the velocity of the discharging vessel. Since the

temporary storage area for pieces created during one time step, DTL, is limited (to 200 pieces), the combination of a long discharge duration and high vessel speed may create too many pieces during one time step, DTL, for the available storage, leading to a diagnostic message and program termination.

After all pieces are created for one time step, they are updated to the end of the long-term time step, DTL, by appropriate convection, diffusion, and settling. The pieces created here are reassigned to small cloud storage as the last operation of the following call to ACAD. The maximum number of small clouds of one material which may be stored is set by the input variable, NSC.

In the case of a jet of duration greater than one long-term time step, the material just leaving the jet nozzle at the end of a time step must be accounted for. Information for such a case is saved in BOOKS at the end of one time step and this information is used by BOOKS at the beginning of the following time step to create more pieces of the plume.

After BOOKS performs the bookkeeping on the material coming out of the jet-plume, the program calls subroutine ACAD to update any small clouds of material to the end of the time step by convection, diffusion, and settling as appropriate. As its last operation, ACAD accepts input of the pieces of the plume created by BOOKS for storage as small clouds. This frees the equivalenced area of storage for computation of a new jet-plume in the following time step.

When the small clouds, which are convected, diffused, and settled by subroutine ACAD, grow large enough, they are injected into the long-term grid on which subroutine MAD conducts

movement and diffusion. MAD updates all components in sequence to the end of the current time step. This version of MAD differs from that used in the code for dumped discharge only in that it updates all components by one time step at a time instead of updating one component at a time all the way to the end of the simulation.

To summarize, the computations for a typical long-term time step run as follows. A jet-plume is computed accounting for dynamic phenomena. Subroutine BOOKS accounts for the remains of any previous jet-plume before creating plume pieces from the history of the present plume. All pieces are then updated to the end of the present time step. Subroutine ACAD checks the size of each small cloud (as distinct from the temporary pieces created in BOOKS) and, if it is large enough, injects it into the long-term grid. The remaining small clouds are updated to the end of the time step, at which time the temporary pieces created by BOOKS are converted to small clouds. MAD then updates the material in the long-term grid to the end of the time step. This procedure is repeated as many times as necessary, deleting short-term computations when the discharge ceases and deleting small clouds calculations when none are left.

Horizontal diffusion in the transition routines, BOOKS and ACAD, is handled by a formulation based on a four-thirds law, while diffusion in MAD is handled by the averaging scheme of Chapter 4. Vertical diffusion for all three routines is handled according to the development in Chapter 4. At any point where vertical diffusion is to be computed, the vertical diffusion coefficient is estimated on the basis of the density profile and the local velocity gradient.

There are a number of numerical coefficients used in the program. With two exceptions, these are the same as those

used by Koh and Chang (1973). ALAMDA, the dissipation parameter for the four-thirds law, is expected to be somewhat higher in an estuary. This study has chosen to use the value $0.005 \text{ ft}^{2/3}/\text{sec}$. The maximum value for the vertical diffusion coefficient, AKYO, has been estimated to be $0.05 \text{ ft}^2/\text{sec}$.

The following coefficients are identical in names and default numerical values to those supplied by Koh and Chang for the jet discharge configuration. They are presented here for completeness. DINCR1 (default value = 1.0) and DINCR2 (default value = 1.0) are factors used in computing time increments in the descent and collapse phases respectively. These may be modified during program execution. ALPHA1 (default value = 0.0806) is the entrainment coefficient for a momentum jet. ALPHA2 (default value = 0.3536) is the entrainment coefficient for a two-dimensional thermal. The default values for ALPHA1 and ALPHA2 are obtained from Abraham (1970) after correcting for the difference in the similarity distributions used in Abraham's and the present formulations. ALPHA3 (default value = 0.3536) is the entrainment coefficient for a convecting thermal (Abraham, 1970). ALPHA4 (default value = 0.001) is a coefficient suggested by Koh and Chang for entrainment due to collapse. BETA (default value = 0.0) is the settling coefficient given by Koh and Chang. The default value is expected to be good for low solids concentrations. GAMA (default value = 0.25) is a coefficient introduced by Koh and Chang to simulate the effect of density gradient differences in causing cloud collapse. The default value is based on an educated guess. CD (default value = 1.3) is the drag coefficient for a two-dimensional cylinder in cross flow in the range of Reynolds numbers expected. CD3 (default value = 0.2) is the drag coefficient for a two-dimensional wedge. CD4 (default value = 2.0) is the drag coefficient for a two-dimensional plate normal to the flow. The reader is cautioned that the

default values for the above drag coefficients were obtained from diagrams presented in Hoerner (1965) for solid shapes in fluid; and as such they are not strictly applicable to this work. However, in the absence of more relevant data, the listed default values will be used. CM (default value = 1.0) is the apparent mass coefficient. The default values for the remaining coefficients (CDRAG, CFRIC, FRICTN, F1) were presented by Koh and Chang based on educated guess and are therefore subject to revision. CDRAG (default value = 1.0) is the drag coefficient for an elliptic cylinder edge onto the flow. CFRIC (default value = 0.01) is a skin friction coefficient. FRICTN (default value = 0.01) is a bottom friction coefficient. F1 (default value = 0.1) is a modification factor for bottom friction used in calculating collapse on the bottom.

The above discussion applies to the "default" coefficients, the coefficients the program will use if the user cannot, or chooses, not to supply his own values.

The program has been designed, as far as possible, to inform the user of any problems which may arise. In the short term, about the only time that problems occur is when the program cannot estimate a proper time step in the collapse phase. The user may then examine the history of the time steps and modify the coefficient DINCR2 accordingly. In the transition phase, a problem that sometimes occurs is that subroutine BOOKS runs out of temporary storage space for "pieces" created in one time step in the case of a vessel discharging at high speed. The problem is aggravated if the plume does not collapse. The solution is to either slow the vessel down or decrease the duration of the discharge. In the passive diffusion phase, problems are usually associated with the small clouds in transition from short term to long term. In the case of a long

continued discharge and a large grid size, DX, subroutine ACAD may run out of room for small clouds. This is easily fixed by increasing the value of NSC in the input (and in some installations increasing the dimension of A in the main program, DMFJ). Problems also arise when a small cloud is convected outside of the long-term grid area due to high ambient velocities. All of the common troubles will be preceded by a self-explanatory diagnostic message to the user.

The matter of estimating dilution times for a conservative chemical tracer contained in the discharge is more complicated for a jet discharge than for an instantaneous dump discharge. A long continued discharge may significantly alter the background concentration. For this work, dilution times are computed for the first portion of the discharge only. The tracer is described by an alphameric name and a concentration in milligrams per liter. The ambient fluid has a user specified background concentration in milligrams per liter. At the end of a run, this information is presented, along with the times required for the tracer concentration to be reduced by successive factors of 10. Only the point of maximum tracer concentration is examined in the passive diffusion computation; no effort is made to keep track of tracer concentration at every point in the field.

Appendix C is a user's manual for the jet discharge model, DMFJ, and it contains further details on the program. A listing of the FORTRAN code is contained in Appendix D.

As an illustration of the use of the two programs in this report, this section discusses three sample runs: one for an instantaneous dump, one for a jet discharge from a moving vessel, and one for a jet discharge from a fixed pipeline. All three runs were made on the same grid of depths with the same ambient velocities. The depth grid described a plane sloping bottom such that constant depth lines were parallel to the Z-axis. The minimum depth was 30 feet which increased with increasing X to a maximum of 80 feet. The grid size, DX, was 500 feet. There were 30 grid points in the Z-direction and 11 in the X-direction. All boundaries were open.

On this grid was described an ambient velocity distribution that was sinusoidally varying with time. This was the product of a sine function (with a period of one-half a tidal cycle) and a distribution of velocity amplitudes. The velocity amplitudes in the Z-direction vary linearly from a minimum of .5 ft/sec at the boundary described by M=1 (30-foot depth) to a maximum of 2 ft/sec at the boundary described by M=11 (80-foot depth). The velocity amplitudes in the X-direction were zero everywhere. The velocities were to be interpreted as vertically integrated single-layer flow. The velocities were described at intervals of 1,000 seconds for an entire 90,000-second (25 hour) tidal day. The program which was written to do this is listed in Figure 6.1

The first situation modeled was an instantaneous dump in water 55 feet deep. The data prepared according to the user's manual of Appendix A is listed in Figure 6.2. Figure 6.3 shows some of the input data that is printed out for the user's reference.

```

PROGRAM VTAPE(INPUT,OUTPUT,TAPES=INPUT,TAPE6=OUTPUT,TAPE7)
C PROGRAM TO PREPARE VELOCITY TAPE FOR DMF AND DMFJ.
DIMENSION U(35,20),W(35,20),UP(35,20),WP(35,20)
DO 30 M=1,11
DO 22 N=1,30
22 U(N,M)=0.
WRITE(6,26)(U(N,M),N=1,30)
26 FORMAT(*-U-*,20F5.2)
30 CONTINUE
C
WB=.5
DO 40 M=1,11
W1=WB+(M-1)*.15
DO 42 N=1,30
42 W(N,M)=W1
WRITE(6,36)(W(N,M),N=1,30)
36 FORMAT(*-W-*,20F5.2)
40 CONTINUE
DTL=1000.
DAY=90000.
NT=DAY/DTL+.0001
C LOOP ON TIME VALUES
T=-DTL
DO 100 L=1,NT
T=T+DTL
IF(ABS(T) .LT. .01) T=0.
WRITE(7)T
C SET UP VELOCITIES FOR THIS TIME STEP
TVAR=SIN(2.*3.14159*T/45000.)
DO 60 M=1,11
DO 60 N=1,30
UP(N,M)=U(N,M)*TVAR
WP(N,M)=W(N,M)*TVAR
60 CONTINUE
C WRITE VELOCITIES ONTO TAPE
WRITE(7)((UP(N,M),N=1,30),M=1,11)
1 , ((WP(N,M),N=1,30),M=1,11)
100 CONTINUE
WRITE(7) DAY
ENDFILE7
REWIND7
CALL EXIT
END

```

Figure 6.1 Listing of a Simple Program to Prepare Velocity Tape

```

30  11  3  1  20
1   3  1  0
1   1  1  1  0
SAMPLE RUN -- DUMP DISCHARGE -- VARIABLE DEPTH AND CURRENT
500.
30  30  30  30  30  30  30  30  30  30  30  30  30  30  30  30
30  30  30  30  30  30  30  30  30  30  30  30  30  30  30
35  35  35  35  35  35  35  35  35  35  35  35  35  35  35  35
35  35  35  35  35  35  35  35  35  35  35  35  35  35  35
40  40  40  40  40  40  40  40  40  40  40  40  40  40  40  40
40  40  40  40  40  40  40  40  40  40  40  40  40  40  40
45  45  45  45  45  45  45  45  45  45  45  45  45  45  45  45
45  45  45  45  45  45  45  45  45  45  45  45  45  45  45
50  50  50  50  50  50  50  50  50  50  50  50  50  50  50  50
50  50  50  50  50  50  50  50  50  50  50  50  50  50  50
55  55  55  55  55  55  55  55  55  55  55  55  55  55  55  55
55  55  55  55  55  55  55  55  55  55  55  55  55  55  55
60  60  60  60  60  60  60  60  60  60  60  60  60  60  60  60
60  60  60  60  60  60  60  60  60  60  60  60  60  60  60
65  65  65  65  65  65  65  65  65  65  65  65  65  65  65  65
65  65  65  65  65  65  65  65  65  65  65  65  65  65  65
70  70  70  70  70  70  70  70  70  70  70  70  70  70  70  70
70  70  70  70  70  70  70  70  70  70  70  70  70  70  70
75  75  75  75  75  75  75  75  75  75  75  75  75  75  75  75
75  75  75  75  75  75  75  75  75  75  75  75  75  75  75
80  80  80  80  80  80  80  80  80  80  80  80  80  80  80  80
80  80  80  80  80  80  80  80  80  80  80  80  80  80  80
3000.  4000.
4
0.      20.      40.      80.
1.005   1.01     1.018   1.025
1
5000.  20000.  1000.
10.    5.      0.      0.      0.      1.2     0.8
FINE   2.6    0.041667 0.01    0.8
MEDIUM 2.6    0.041667 0.05    0.8
COARSE 2.6    0.041667 0.09    0.8
AMMONIA 10.    0.001

```

Figure 6.2 Listing of Input Data for Instantaneous Dump Case

SAMPLE RUN -- DUMP DISCHARGE -- VARIABLE DEPTH AND CURRENT

NUMBER OF LONG TERM GRID POINTS IN Z-DIRECTION (NMAX) = 30

NUMBER OF LONG TERM GRID POINTS IN X-DIRECTION (MMAX) = 11

GRID SPACING (DX) = 500.00000

BARGE COORDINATES...
 XBARGE (FT) = 3000, ZBARGE (FT) = 4000.

---AMBIENT CONDITIONS---

DEPTH (FT)	0.	20.00	40.00	80.00
AMBIENT DENSITY (GM/CC)	1.005	1.010	1.018	1.025

INTERPOLATED DEPTH AT DUMP COORDINATES, H = 55.00 FT.

SINGLE VELOCITY PLANE USED WITH VELOCITIES CONSTANT IN THE VERTICAL

TIME PARAMETERS FOLLOW...
 TIME OF DUMP = 5000.00 SECONDS AFTER START OF TIDAL CYCLE
 DURATION OF SIMULATION = 20000.00 SECONDS AFTER DUMP
 LONG TERM TIME STEP (DTL) = 1000.00 SECONDS

DISCHARGE PARAMETERS...
 INITIAL RADIUS OF CLOUD, RH = 10.00000
 INITIAL DEPTH OF CLOUD CENTROID, DREL = 5.000
 INITIAL CLOUD VELOCITIES...CV(1) = 0. CW(1) = 0.

BULK PARAMETERS...
 DENSITY, RHO = 1.200000
 AGGREGATE VOIDS RATIO, BVOID = .8000

THERE ARE 3 SOLIDS, PARAMETERS FOLLOW.....

DESCRIPTION	DENSITY(GM/CC)	CONCENTRATION(CUFT/CUFT)	FALL VELOCITY(FT/SEC)	VOIDS RATIO
FINE	2.600	.4167E-01	.1000E-01	.8000
MEDIUM	2.600	.4167E-01	.5000E-01	.8000
COARSE	2.600	.4167E-01	.9000E-01	.8000
FLUID	1.0000	.8750	0.	

USE TETRA TECH SUGGESTED COEFFICIENTS
 DINCR1 1.0000 DINCR2 1.0000
 ALPHA0 .2350 BETA 0.0000 CM 1.0000 CD .5000
 GAMMA .25 CDHAG 1.00 CFRIC .010 CD3 .10 CD4 1.00 ALPHAC .0010
 FRICTN .0100 F1 .1000
 ALAMDA .0050 AKYO .0500

Figure 6.3 Input Documentation of Dump Model

Figures 6.4 through 6.7 show typical printouts of results. It can be seen that all of the solids settle out completely in one long-term time step. The printouts of the fluid distributions are interesting because they show the combined effects of the sloping bottom and the density gradient. The density gradient almost stops the vertical growth of the cloud and consequently the cloud cannot diffuse into the shallower region. The shearing effect of the ambient velocity is also seen clearly in Figure 6.6. Once any material passes out of the grid boundary, it is lost; nevertheless, Figure 6.7 shows the behavior of the fluid which is left in the grid shortly after the velocity field reverses its direction. The printouts of dilution times are (in this case) accurate only to the nearest time step, DTL. This is because once material reaches the long-term diffusion phase, time is resolved only to the nearest long-term time step, DTL.

The second situation modeled was a jet discharge from a moving barge. The initial position of the discharging vessel was at a point where the water depth was 55 feet. The vessel moved straight "offshore" at a speed of 4.2 knots (7.1 ft/sec) while discharging 1600 cubic yards of material in five minutes. The material had the same composition as the material used for the dump simulation. Figure 6.8 shows a portion of the input documentation for the jet discharge model. Results of the dynamic computations are plotted in Figure 6.9. The high rate of dilution of the fluid fraction for this mode of discharge is clearly seen. The printouts of final bottom accumulations shown in Figure 6.10 are of interest because they show a selective dispersal of the solids. The coarse-sized material has all settled out immediately under the path of the discharging vessel. The medium-sized material has settled out mostly under the vessel's path except for some material released

PLOT OF COLLAPSING CLOUD CHARACTERISTICS

INDEPENDENT VARIABLE IS TIME OVER RANGE 0. 87.025

DEPENDENT VARIABLE, ALL NORMALIZED FOR PLOTTING ON UNIT AXIS

SYMBOL	A	B	C	Y
MAX PLOTTED	19.871	200.15	.87500	54.597
MIN PLOTTED	0.	0.	0.	0.
REMARKS	VERT SIZE	HOR SIZE	HOR DIST(CX)	HOR DIST(CZ)

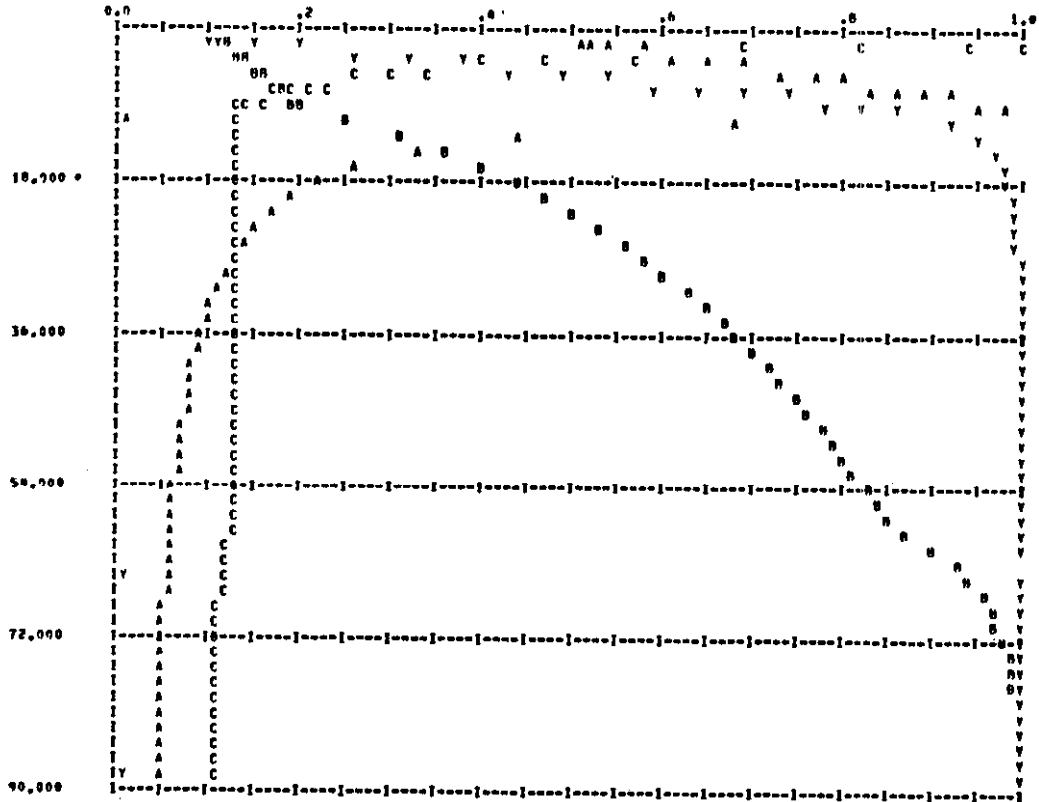


Figure 6.4 Plot of Short-Term Behavior of the Cloud

CONCENTRATIONS OF FLUID (VOLUME RATIO) IN THE CLOUD 10000.00 SECONDS AFTER DUMP
 ..MULTIPLY DISPLAYED VALUES BY .1000E-03 (LEGEND... + = .LT. .01) = .LT. .0001 0 = .LT. .000001)

M No	1	2	3	4	5	6	7	8	9	10	11	12	13	14	15	16	17	18	19	20	21	22	23	24	25	26	27	28	29	30
1	0	0	0	0	0	0	0	0	0	0	0	0	0	0	0	0	0	0	0	0	0	0	0	0	0	0	0	0	0	
2	0	0	0	0	0	0	0	0	0	0	0	0	0	0	0	0	0	0	0	0	0	0	0	0	0	0	0	0	0	
3	0	0	0	0	0	0	0	0	0	0	0	0	0	0	0	0	0	0	0	0	0	0	0	0	0	0	0	0	0	
4	0	0	0	0	0	0	0	0	0	0	0	0	0	0	0	0	0	0	0	0	0	0	0	0	0	0	0	0	0	
5	0	0	0	0	0	0	0	0	0	0	0	0	0	0	0	0	0	0	0	0	0	0	0	0	0	0	0	0	0	
6	0	0	0	0	0	0	0	0	0	0	0	0	0	0	0	0	0	0	0	0	0	0	0	0	0	0	0	0	0	
7	0	0	0	0	0	0	0	0	0	0	0	0	0	0	0	0	0	0	0	0	0	0	0	0	0	0	0	0	0	
8	0	0	0	0	0	0	0	0	0	0	0	0	0	0	0	0	0	0	0	0	0	0	0	0	0	0	0	0	0	
9	0	0	0	0	0	0	0	0	0	0	0	0	0	0	0	0	0	0	0	0	0	0	0	0	0	0	0	0	0	
10	0	0	0	0	0	0	0	0	0	0	0	0	0	0	0	0	0	0	0	0	0	0	0	0	0	0	0	0	0	
11	0	0	0	0	0	0	0	0	0	0	0	0	0	0	0	0	0	0	0	0	0	0	0	0	0	0	0	0	0	

THICKNESS OF FLUID CLOUD (FFFF) 10000.00 SECONDS AFTER DUMP
 ..MULTIPLY DISPLAYED VALUES BY 1.000 (LEGEND... + = .LT. .01) = .LT. .0001 0 = .LT. .000001)

M No	1	2	3	4	5	6	7	8	9	10	11	12	13	14	15	16	17	18	19	20	21	22	23	24	25	26	27	28	29	30
1	0	0	0	0	0	0	0	0	0	0	0	0	0	0	0	0	0	0	0	0	0	0	0	0	0	0	0	0	0	
2	0	0	0	0	0	0	0	0	0	0	0	0	0	0	0	0	0	0	0	0	0	0	0	0	0	0	0	0	0	
3	0	0	0	0	0	0	0	0	0	0	0	0	0	0	0	0	0	0	0	0	0	0	0	0	0	0	0	0	0	
4	0	0	0	0	0	0	0	0	0	0	0	0	0	0	0	0	0	0	0	0	0	0	0	0	0	0	0	0	0	
5	0	0	0	0	0	0	0	0	0	0	0	0	0	0	0	0	0	0	0	0	0	0	0	0	0	0	0	0	0	
6	0	0	0	0	0	0	0	0	0	0	0	0	0	0	0	0	0	0	0	0	0	0	0	0	0	0	0	0	0	
7	0	0	0	0	0	0	0	0	0	0	0	0	0	0	0	0	0	0	0	0	0	0	0	0	0	0	0	0	0	
8	0	0	0	0	0	0	0	0	0	0	0	0	0	0	0	0	0	0	0	0	0	0	0	0	0	0	0	0	0	
9	0	0	0	0	0	0	0	0	0	0	0	0	0	0	0	0	0	0	0	0	0	0	0	0	0	0	0	0	0	
10	0	0	0	0	0	0	0	0	0	0	0	0	0	0	0	0	0	0	0	0	0	0	0	0	0	0	0	0	0	
11	0	0	0	0	0	0	0	0	0	0	0	0	0	0	0	0	0	0	0	0	0	0	0	0	0	0	0	0	0	

POSITION OF TOP OF FLUID CLOUD (FEET BELOW SURFACE) 10000.00 SECONDS AFTER DUMP
 ..MULTIPLY DISPLAYED VALUES BY 1.000 (LEGEND... + = .LT. .01) = .LT. .0001 0 = .LT. .000001)

M No	1	2	3	4	5	6	7	8	9	10	11	12	13	14	15	16	17	18	19	20	21	22	23	24	25	26	27	28	29	30
1	0	0	0	0	0	0	0	0	0	0	0	0	0	0	0	0	0	0	0	0	0	0	0	0	0	0	0	0	0	
2	0	0	0	0	0	0	0	0	0	0	0	0	0	0	0	0	0	0	0	0	0	0	0	0	0	0	0	0	0	
3	0	0	0	0	0	0	0	0	0	0	0	0	0	0	0	0	0	0	0	0	0	0	0	0	0	0	0	0	0	
4	0	0	0	0	0	0	0	0	0	0	0	0	0	0	0	0	0	0	0	0	0	0	0	0	0	0	0	0	0	
5	0	0	0	0	0	0	0	0	0	0	0	0	0	0	0	0	0	0	0	0	0	0	0	0	0	0	0	0	0	
6	0	0	0	0	0	0	0	0	0	0	0	0	0	0	0	0	0	0	0	0	0	0	0	0	0	0	0	0	0	
7	0	0	0	0	0	0	0	0	0	0	0	0	0	0	0	0	0	0	0	0	0	0	0	0	0	0	0	0	0	
8	0	0	0	0	0	0	0	0	0	0	0	0	0	0	0	0	0	0	0	0	0	0	0	0	0	0	0	0	0	
9	0	0	0	0	0	0	0	0	0	0	0	0	0	0	0	0	0	0	0	0	0	0	0	0	0	0	0	0	0	
10	0	0	0	0	0	0	0	0	0	0	0	0	0	0	0	0	0	0	0	0	0	0	0	0	0	0	0	0	0	
11	0	0	0	0	0	0	0	0	0	0	0	0	0	0	0	0	0	0	0	0	0	0	0	0	0	0	0	0	0	

Figure 6.6 Printout Showing Location of the Fluid Cloud.

TIME PARAMETERS FOLLOW...
 TIME OF JET START = 5000.00 SECONDS AFTER START OF TIDAL CYCLE
 DURATION OF SIMULATION = 20000.00 SECONDS AFTER JET START
 DURATION OF JET DISCHARGE = 300.00 SECONDS
 LONG TERM TIME STEP (DTL) = 1000.00 SECONDS

DISCHARGE PARAMETERS...
 VOLUME RATE OF DISCHARGE (CUFT/SEC) = 86.40000
 INITIAL RADIUS OF JET (FT) = 1.458300
 DEPTH OF DISCHARGE NOZZLE (FT) = 10.00
 ANGLE OF DISCHARGE (DEGREES BELOW THE HORIZONTAL) = 86.00
 RANGE POSITION, XARGE (FT) = 3000.
 RANGE POSITION, ZARGE (FT) = 4000.
 COURSE (MEASURED ANTI-CLOCKWISE FROM POSITIVE X-AXIS) = 0, DEGREES
 RANGE VELOCITY (FT/SEC) = 7.100

MILK PARAMETERS...
 DENSITY, RDI = 1.200000
 AGGREGATE VOIDS RATIO, BVOID = .0000

THERE ARE 3 SOLIDS...PARAMETERS FOLLOW...

DESCRIPTION	DENSITY(GM/CC)	CONCENTRATION(CUFT/CUFT)	FALL VELOCITY(FT/SEC)	VOIDS RATIO
FINE	2.600	.4167E-01	.1000E-01	.0000
MEDIUM	2.600	.4167E-01	.5000E-01	.0000
COARSE	2.600	.4167E-01	.9000E-01	.0000
FLUID	1.0000	.0750	0.	.0000

USE TETRA TECH SUGGESTED COEFFICIENTS

DINCR1	1.0000	DINCR2	1.0000	ETA	0.0000	CO	1.3000	CD0	2.0000
ALPHA1	.0006	ALPHA2	.3536	CFRIC	.0100	CD1	.2000	CM	1.0000
GAMA	.2500	CORAG	1.0000	FRICTN	.0100	F1	.1000		
ALPHA3	.3536	ALPHA4	.0010						
LAMDA	.0050	AKYO	.0500						

SINGLE VELOCITY PLANE USED WITH VELOCITIES CONSTANT IN THE VERTICAL

COMPUTE NEW JET-PLUME BEGINNING 0.00 SECONDS AFTER START OF DISCHARGE

AMBIENT VELOCITY DISTRIBUTION CORRESPONDS TO DTL ENDING AT SECOND 5000.00 OF 90000 SECOND (25 HR) TIDAL CYCLE

COORDINATES OF RANGE AT START OF THIS TIME STEP...X0 = 3000.00 , Z0 = 4000.00

INTERPOLATED DEPTH, H = 55.00

---AMBIENT DENSITY PROFILE---

DEPTH (FT)	0.	20.00	40.00	60.00
DENSITY (GM/CC)	1.005	1.010	1.018	1.025

SURFACE VELOCITIES AT RANGE AT START OF THIS COMPUTATION.....UA(FT/SEC) = 0. , WA(FT/SEC) = .0035

Figure 6.8 Portion of the Input Documentation for Jet Discharge Model

PLOT OF JET-PLUME CHARACTERISTICS AS THEY VARY FROM DISCHARGE TO END OF PLUME COLLAPSE.
 PLOT SHOWS CHARACTERISTICS AS SEEN FROM MARKER PARTICLE IN JET-PLUME AS FUNCTION
 OF TIME ELAPSED SINCE RELEASE.

INDEPENDENT VARIABLE IS TIME(SEC) OVER RANGE 0. 134.47

DEPENDENT VARIABLES, ALL NORMALIZED FOR PLOTTING ON UNIT AXIS

SYMBOL	B	D	A	C
MAX PLOTTED	940.00	105.42	15.240	.07500
MIN PLOTTED	0.	0.	0.	0.
REMARKS	ARC DIST	HOR. SIZE	VERT. SIZE,	FLUID CONC

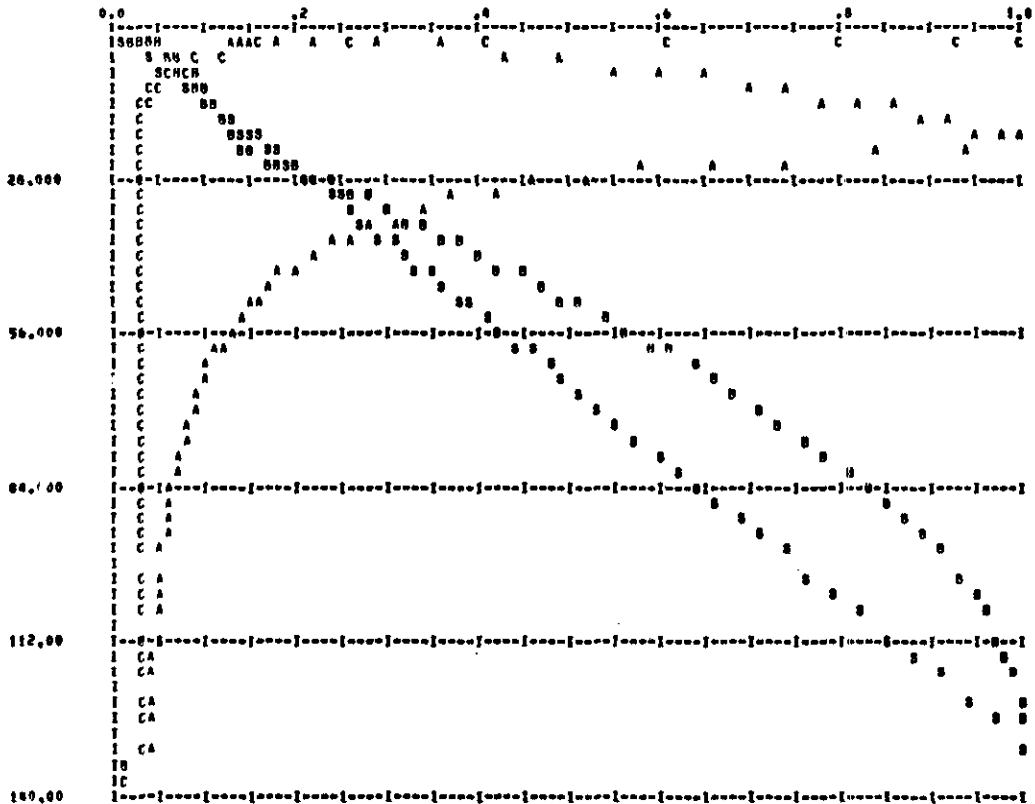


Figure 6.9 Results of Dynamic Computations for Jet Discharge from Moving Barge

BOTTOM ACCUMULATION OF COARSE (CUFT/GRID SQUARE) 5000.00 SECONDS AFTER START OF JET
MULTIPLY DISPLAYED VALUES BY 1.000 (LEGEND... * = .LT. .01 * = .LT. .0001 0 = .LT. .000001)

M No	1	2	3	4	5	6	7	8	9	10	11	12	13	14	15	16	17	18	19	20	21	22	23	24	25	26	27	28	29	30
1	0	0	0	0	0	0	0	0	0	0	0	0	0	0	0	0	0	0	0	0	0	0	0	0	0	0	0	0	0	
2	0	0	0	0	0	0	0	0	0	0	0	0	0	0	0	0	0	0	0	0	0	0	0	0	0	0	0	0	0	
3	0	0	0	0	0	0	0	0	0	0	0	0	0	0	0	0	0	0	0	0	0	0	0	0	0	0	0	0	0	
4	0	0	0	0	0	0	0	0	0	0	0	0	0	0	0	0	0	0	0	0	0	0	0	0	0	0	0	0	0	
5	0	0	0	0	0	0	0	0	0	0	0	0	0	0	0	0	0	0	0	0	0	0	0	0	0	0	0	0	0	
6	0	0	0	0	0	0	0	0	0	105	0	0	0	0	0	0	0	0	0	0	0	0	0	0	0	0	0	0	0	
7	0	0	0	0	0	0	0	0	209	0	0	0	0	0	0	0	0	0	0	0	0	0	0	0	0	0	0	0	0	
8	0	0	0	0	0	0	0	0	314	0	0	0	0	0	0	0	0	0	0	0	0	0	0	0	0	0	0	0	0	
9	0	0	0	0	0	0	0	0	209	0	0	0	0	0	0	0	0	0	0	0	0	0	0	0	0	0	0	0	0	
10	0	0	0	0	0	0	0	0	242	0	0	0	0	0	0	0	0	0	0	0	0	0	0	0	0	0	0	0	0	
11	0	0	0	0	0	0	0	0	0	0	0	0	0	0	0	0	0	0	0	0	0	0	0	0	0	0	0	0	0	

BOTTOM ACCUMULATION OF MEDIUM (CUFT/GRID SQUARE) 5000.00 SECONDS AFTER START OF JET
MULTIPLY DISPLAYED VALUES BY 1.000 (LEGEND... * = .LT. .01 * = .LT. .0001 0 = .LT. .000001)

M No	1	2	3	4	5	6	7	8	9	10	11	12	13	14	15	16	17	18	19	20	21	22	23	24	25	26	27	28	29	30
1	0	0	0	0	0	0	0	0	0	0	0	0	0	0	0	0	0	0	0	0	0	0	0	0	0	0	0	0	0	
2	0	0	0	0	0	0	0	0	0	0	0	0	0	0	0	0	0	0	0	0	0	0	0	0	0	0	0	0	0	
3	0	0	0	0	0	0	0	0	0	0	0	0	0	0	0	0	0	0	0	0	0	0	0	0	0	0	0	0	0	
4	0	0	0	0	0	0	0	0	0	0	0	0	0	0	0	0	0	0	0	0	0	0	0	0	0	0	0	0	0	
5	0	0	0	0	0	0	0	0	0	0	0	0	0	0	0	0	0	0	0	0	0	0	0	0	0	0	0	0	0	
6	0	0	0	0	0	0	0	0	105	0	0	0	0	0	0	0	0	0	0	0	0	0	0	0	0	0	0	0	0	
7	0	0	0	0	0	0	0	0	209	0	0	0	0	0	0	0	0	0	0	0	0	0	0	0	0	0	0	0	0	
8	0	0	0	0	0	0	0	0	314	0	0	0	0	0	0	0	0	0	0	0	0	0	0	0	0	0	0	0	0	
9	0	0	0	0	0	0	0	0	209	0	0	0	0	0	0	0	0	0	0	0	0	0	0	0	0	0	0	0	0	
10	0	0	0	0	0	0	0	0	116	0	0	126	0	0	0	0	0	0	0	0	0	0	0	0	0	0	0	0	0	
11	0	0	0	0	0	0	0	0	0	0	0	0	0	0	0	0	0	0	0	0	0	0	0	0	0	0	0	0	0	

BOTTOM ACCUMULATION OF FINE (CUFT/GRID SQUARE) 5000.00 SECONDS AFTER START OF JET
MULTIPLY DISPLAYED VALUES BY 1.000 (LEGEND... * = .LT. .01 * = .LT. .0001 0 = .LT. .000001)

M No	1	2	3	4	5	6	7	8	9	10	11	12	13	14	15	16	17	18	19	20	21	22	23	24	25	26	27	28	29	30
1	0	0	0	0	0	0	0	0	0	0	0	0	0	0	0	0	0	0	0	0	0	0	0	0	0	0	0	0	0	
2	0	0	0	0	0	0	0	0	0	0	0	0	0	0	0	0	0	0	0	0	0	0	0	0	0	0	0	0	0	
3	0	0	0	0	0	0	0	0	0	0	0	0	0	0	0	0	0	0	0	0	0	0	0	0	0	0	0	0	0	
4	0	0	0	0	0	0	0	0	0	0	0	0	0	0	0	0	0	0	0	0	0	0	0	0	0	0	0	0	0	
5	0	0	0	0	0	0	0	0	0	0	0	0	0	0	0	0	0	0	0	0	0	0	0	0	0	0	0	0	0	
6	0	0	0	0	0	0	0	0	105	0	0	0	0	0	0	0	0	0	0	0	0	0	0	0	0	0	0	0	0	
7	0	0	0	0	0	0	0	0	209	0	0	0	0	0	0	0	0	0	0	0	0	0	0	0	0	0	0	0	0	
8	0	0	0	0	0	0	0	0	0	105	209	0	0	0	0	0	0	0	0	0	0	0	0	0	0	0	0	0	0	
9	0	0	0	0	0	0	0	0	0	0	0	0	0	0	97	0	112	0	0	0	0	0	0	0	0	0	0	0	0	
10	0	0	0	0	0	0	0	0	0	0	0	0	0	0	0	0	242	0	0	0	0	0	0	0	0	0	0	0	0	
11	0	0	0	0	0	0	0	0	0	0	0	0	0	0	0	0	0	0	0	0	0	0	0	0	0	0	0	0	0	

DILUTION TIMES FOR CONSERVATIVE TRACER IN INITIAL FLUID FRACTION FOLLOW,...

TRACER IS AMMONIA INITIAL CONCENTRATION IS .0.00000 GM/L BACKGROUND CONCENTRATION IS .100000E-02 GM/L
DILUTION IS 10 TO 1 WITHIN 4,182 SECONDS AFTER FLUID LEAVES JET NOZZLE
DILUTION IS 100 TO 1 WITHIN 5009,000 SECONDS AFTER FLUID LEAVES JET NOZZLE
DILUTION IS 1000 TO 1 WITHIN 14000,000 SECONDS AFTER FLUID LEAVES JET NOZZLE

DILUTION TIMES ARE FOR POINT OF MAXIMUM CONCENTRATION.

Figure 6.10 Solids Distribution and Dilution Times for Jet Discharge 123

near the end of the discharge. The slowly settling fine-grained material has smeared out so that the bottom accumulation has the shape of an arc. This is because of the increasing depth in the direction down the page, further accentuated by the ambient velocity distribution. The gaps in what are expected to be continuous distributions are caused by the discrete nature of the modeling of convection, diffusion, and settling. The combination of an ambient velocity near the "bottom" of the grid of approximately 2 ft/sec and a time step of 1000 seconds is enough to move material several grid steps downstream between settling phases. Finally, at the bottom of Figure 6.10 are shown the dilution times for this case. The high dilutions of the jet discharge mode can be seen.

The last run simulated a fixed pipeline discharge. All parameters except for an indicator and the vessel speed were identical to those used in the previous case for discharge from a moving vessel. Figure 6.11 shows the final distributions of solids on the bottom. As can be seen, all the material settled out close to the discharge point. Only a small part of the fine material was carried downstream. The time of these distributions is the same as those shown in Figure 6.10 for the moving discharge point.

The two models described in this report are outgrowths of the Koh-Chang model for barged ocean disposal of wastes. One model treats instantaneous dumped discharge of dredged material. The second treats a jet discharge of arbitrary duration from a fixed or moving source. In each model, the appropriate short-term portion of the Koh-Chang model, modified and corrected for bugs found in the course of this work, was coupled to an extensive modification of a model developed by Fischer (1972) for long-term diffusion of chemical wastes in an estuary. This coupling was aided by transition routines developed during this work. The resulting models are capable of tracking up to twelve types of solid fractions and a fluid fraction of a discharge of dredged material through short-term dynamic phenomena and through long-term passive diffusion until the solids eventually settle out of the water column. The models do this for variable depth estuaries with arbitrary land boundaries where ambient velocities may vary in three dimensions and in time. Densities may vary in the vertical dimension and in time.

While the duration of time that may be simulated is arbitrary, the models were developed for the prediction of deposition of solid material on the bottom in the hours after a discharge. For this reason there is no accounting for resuspension. Neither is a treatment of flocculation considered necessary because the high initial mixing leads to completion of any flocculation before solids settle out of the dumped cloud or jet plume. The material that is modeled is considered to be a well-mixed slurry with no cohesive properties.

The models have received limited testing in the course of this work. It was, however, impossible to model all possible situations. Consequently the models need to be exercised to find any bugs that may remain and to suggest improvements that may be made.

It cannot be overemphasized how dependent the models are upon good quality data for ambient velocity. While the models will accept input from a single data card to describe an entire velocity field, those users striving for the most accurate results will need to spend considerable time in determining the ambient velocities. In fact, for highly stratified estuaries of complex geometry, almost the entire effort of a modeling program may be devoted to the determination of velocities.

The remaining important need of the models is for verification. This implies a need for field data on actual discharges of dredged material. The data should include the characteristics of the discharge, the ultimate deposition of the material discharged, and the ambient conditions during and following the discharge. A good verification program will allow the determination of the limits within which the model may be applied with confidence.

LITERATURE CITED

- Abraham, G. , "The Flow of Round Buoyant Jets Issuing Vertically into Ambient Fluid Flowing in a Horizontal Direction," Proc. Fifth International Conference on Water Pollution Research, San Francisco, July, 1970, Paper III-15.
- Alsaffar, A.M. , "Lateral Diffusion in a Tidal Estuary," Journal of Geophysical Research, Vol. 71, No. 24, Dec, 1966, pp. 5837-5841.
- Boyd, M. B. , et al. , "Disposal of Dredge Spoil: Problem Identification and Assessment and Research Program Development," Technical Report H-72-8, Nov. 1972, U. S. Army Engineer Waterways Experiment Station, Vicksburg, Mississippi.
- Bowden, K. F. , "Turbulence," Chapter VI of The Sea, Vol. 1, M. N. Hill, ed. , John Wiley & Sons, New York, 1962.
- Bowden, K. F. , "Circulation and Diffusion," Estuaries, American Association for the Advancement of Science, Publication No. 83, G.H. Lauff, ed. , Washington, D. C. , 1967, pp. 15-36.
- Cameron, W.M. and Pritchard, D. W. , "Estuaries," The Sea, Vol. 2, M. N. Hill, ed. , John Wiley & Sons, New York, 1963, pp. 306-324.

- Clark, B.D. , et al. , "The Barged Disposal of Wastes, A Review of Current Practice and Methods of Evaluation," EPA, Water Quality Office, Northwest Region, Pacific Northwest Water Quality Lab, Corvallis, Oregon, 1971.
- Dyer, K.R. , Estuaries: A Physical Introduction, John Wiley & Sons, New York, 1973.
- Fischer, H.B. , "A Method for Predicting Pollutant Transport in Tidal Waters," Water Resources Center Contribution No. 132, March, 1970, College of Engineering, University of California, Berkeley.
- Fischer, H.B. , "A Numerical Model of Estuarine Pollutant Transport," Proceedings of the 13th Coastal Engineering Conference, American Society of Civil Engineers, New York, 1972, pp. 2265-2274.
- Gunnerson, C.G. , Discussion on "Eddy Diffusion in Homogeneous Turbulence," by G. T. Orlob, Journal of the Hydraulics Division, American Society of Civil Engineers, Vol. 86, No. NY4, April, 1960, pp. 101-109.
- Harremoes, P. , "Diffuser Design for Discharge to a Stratified Water," 1967, The Danish Isotope Center, Copenhagen, Denmark.
- Hetling, et al. , "Estimating Diffusion Characteristics of Tidal Water," NTIS #PB-216 394, May 1965, Federal Water Pollution Control Administration, Charlottesville, Virginia.

- Holley, E. R. , "Unified View of Diffusion and Dispersion," Journal of the Hydraulics Division, American Society of Civil Engineers, Vol. 95, No. HY2, March 1969, pp. 621-631.
- Hoerner, Sighard F. , Fluid Dynamic Drag, Published by the Author, 1965, Brick Town, New Jersey.
- Kent, R. E. and Pritchard, D. W. , "A Test of Mixing Length Theories in a Coastal Plain Estuary," Journal of Marine Research, Vol, 18, 1959, pp. 62-72.
- Johnson B.H. , "Investigation of Mathematical Models for the Physical Fate Prediction of Dredged Material," Technical Report D-74-1, March 1974, U. S. Army Engineer Waterways Experiment Station, Vicksburg, Mississippi.
- Koh, R. C. Y. and Fan L. N. , "Further Studies on the Prediction of the Radioactive Debris Distribution Subsequent to a Deep Underwater Nuclear Explosion," Report No. TC-154, October, 1969, Tetra Tech, Incorporated, Pasadena, California.
- Koh, R. C. Y. and Chang, Y. C. , "Mathematical Model for Barged Ocean Disposal of Water," Environmental Protection Technology Series EPA 660/2-73-029, December 1973, U. S. EPA, Washington, D. C.
- Kolesnikov, A.G. , Ivanova, Z. S. , and Boguslavskaya, S.G. , "The Effect of Stability on the Intensity of Vertical Transfer in the Atlantic Ocean," Okeanologiya, Vol. 1, No. 4, 1961, pp. 592-599, English Translation.

- Okubo, A. , "A Review of Theoretical Models for Turbulent Diffusion in the Sea," J. Ocean. Soc. of Japan, 20th Anniversary Volume, 1962, pp.286-320.
- Orlob, G. T. , "Eddy Diffusion in Homogenous Turbulence," Journal of the Hydraulics Division, ASCE, HY9, September 1959, pp. 75-101.
- Pritchard, D. W. , "The Movement and Mixing of Containments in Tidal Estuaries," Proc. First Conference on Waste Disposal in the Marine Environment (1959), 1960, pp. 512-525.
- Pritchard, D. W. , "Observations of Circulation in Coastal Plain Estuaries," Estuaries, American Association for the Advancement of Science, Publication No. 83, G.H. Lauff, ed. , Washington, D. C. , 1967.
- Richards, J.M. , "Experiments on the Penetration of an Interface by Buoyant Thermal," Journal of Fluid Mechanics, Vol. 11, 1961, p.369.
- Scorer, R. S. , "Experiments on Convection of Isolated Masses of Buoyant Fluid," Journal of Fluid Mechanics, Vol. 2, 1957, p. 583.
- Tennekes, H. and Lumley, J. L. , A First Course in Turbulence, MIT Press, Cambridge, Massachusetts, 1972, pp. 8-14.
- Turner, J. S. , "A Comparison Between Buoyant Vortex Rings and Vortex Pairs," J. Fluid Mechanics, Vol. 7, 1960, pp.419-432.

Woodward, B. , "Motion In and Around Isolated Thermals,"
Quarterly J. Royal Meteorological Society, Vol. 85, 1959,
p. 144.

BIBLIOGRAPHY

- Gameson, A. L. H. (ed), "Mathematical and Hydraulic Modeling of Estuarine Pollution," Water Pollution Research Technical Paper No. 13, 1973, Her Majesty's Stationary Office, London.
- Koh, R. C. Y and Fan, L. N. , "Mathematical Models for the Prediction of Temperature Distributions Resulting from the Discharge of Heated Water into Large Bodies of Water," Water Pollution Control Research Series No. 16130 DWO 10/70, 1970, Water Quality Office, U. S. EPA, 219p.
- Leendertse, J. J. and Gritton, E. C. , A Water Quality Simulation Model for Well-Mixed Estuaries and Coastal Seas: Vol. II, Computational Procedures, R-708-NYC, July, 1971a, The Rand Corp. , Santa Monica, California
- Leendertse, J. J. and Gritton, E. C. , A Water Quality Simulation Model for Well-Mixed Estuaries and Coastal Seas: Vol. III, Jamaica Bay Simulation, R-709-NYC, August, 1971b, The Rand Corp. , Santa Monica, California.
- Postma , H. , "Sediment Transport and Sedimentation in the Estuarine," Estuaries, American Association for the Advancement of Science, Publication No. 83, G. H. Lauff, ed. , Washington, D. C. , 1967, pp. 158-179.
- TRACOR, Inc. , Estuarine Modeling: An Assessment, Water Pollution Control Research Series No. 16070DZV 02/71, 1971, Water Quality Office, U. S. EPA.

APPENDIX A

User's Manual: Model For Instantaneous Dump Program, DMF

This is the user's manual for program DMF, which predicts dredged material fate for an instantaneous dumped discharge in an estuary. The program was developed and tested on a Control Data 6600 Computer. It was written, with minor exceptions, to ANSI standards. The exceptions are noted in the card identifier columns as shown in the listing in Appendix B. There are a total of 15 cards that do not satisfy ANSI standards or that are peculiar to the CDC 6600, and these are flagged in the identifier columns.

DMF was designed to make it simple to do simple things and not too complicated to do complicated things. To this end, the code uses dynamic storage allocation. This is done by placing all of the passive diffusion arrays and one short-term array in a single, variable dimension array (called A) in unlabeled common storage. The first data card of a run deck contains the dimensions of these arrays. The CDC 6600 version computes the core requirements from these dimensions and expands the core area as necessary during execution. On other installations, the instructions that do this (marked "CDC ONLY" in DMF) will have to be removed, and the user will have to recompile routine DMF with the dimension of A set to the following

$$\text{DIMENSION} = .1 + (11 + \text{NS} = \text{NVL}) * \text{NMAX} * \text{MMAX} + 600 * \text{NS} \\ + 6 * \text{NSC}$$

where NMAX, MMAX, NS, NVL, and NSC are as described in the input listed below. The presentation of the input variables includes brief descriptions. For additional details, the user will be referred to notes at the end.

INPUT DESCRIPTION

Card Group No.	No. of Cards	Format
	FORTRAN VARIABLE	DESCRIPTION
1	1 card	16I5
	NMAX	Maximum dimension of long-term passive diffusion array in z-direction (Figure 5.1)
	MMAX	Maximum dimension of long-term passive diffusion array in x-direction (Figure 5.1)
	NS	Number of solid components in discharge (not greater than 12)
	NVL	Number of velocity levels in velocity arrays (must be 1 or 2)
	NSC	Maximum number of small clouds allowed per component for transition from short term to long term (value 20 suggested)
2	1 card	16I5
	KEY1	=1 Use default coefficients suggested by Tetra Tech =2 Use coefficients suggested by user
	KEY2	=1 Computation stops at end of convective descent phase =2 Computation stops at end of dynamic collapse =3 Computation stops at end of long-term diffusion
	KEY3	=1 Long-term diffusion for fluid component =0 No long-term diffusion for fluid component

Card Group No.	No. of Cards	Format
	FORTRAN VARIABLE	DESCRIPTION
	KEY4	=0 No action =1 Substitute user-specified time steps, DT, for descent and collapse. Used in event of repeated runs.
3	1 card	16I5
	IGCN	=0 No graphs of convective descent =1 One line printer graph of convective descent =2 Extra graphs of concentrations for convective phase
	IGCL	=0 No graphs of dynamic collapse =1 One line printer graph
	IPCN	=0 No printed record of convective descent phase =1 Printed output included
	IPCL	=0 No printed record of dynamic collapse phase =1 Printed output included
	IPLT	=0 Print long-term results at default times ($\frac{1}{4}, \frac{2}{4}, \frac{3}{4}, \frac{4}{4}$ of TSTOP) =n Number of values to be read in of times to print long-term results (up to 12)
4	1 card	8A10
	ID	Free-form alphanumeric description of run (up to 80 characters)

Card Group No.	No. of Cards FORTRAN VARIABLE	Format DESCRIPTION
5	1 card DX	8E10.0 Space step (in feet) for long-term grid (See Figure 5.1)
6	Several Cards DEPTH (N,M)	16F5.0 Depths (in feet) read row by row, left to right, top to bottom (See Note 1 and Figure 5.1)
7	1 card XBARGE ZBARGE	8E10.0 X-coordinate of discharging vessel in estuary (See Figure 5.1) Z-coordinate of discharging vessel in estuary (See Figure 5.1)
8	1 card NROA	16I5 Number of points (in depth) where ambient density is specified (up to 10)
9	1 or 2 cards Y(I)	8E10.0 Depths (in feet) where density is specified. (The final value should equal the deepest depth in the estuary.)

Card Group No.	No. of Cards	Format
	FORTTRAN VARIABLE	DESCRIPTION
10	1 or 2 cards ROA(I)	8E10.0 Density (gm/cc) of ambient water
11	1 card IFORM	16I5 This is an indicator of the ambient velocity interpretation. Set to one of the following values (see Note 2 for details of velocity data preparation) <ul style="list-style-type: none"> =1 One-layer flow variable in horizontal and in time. Vertically averaged velocities are read from logical unit 7 (LUN7) at each long-term time step. =2 Same as above except that velocity profiles are assumed to be logarithmic such that the average over the vertical equals the read in value. =3 Two-layer flow variable horizontally, vertically, and in time. These are interpreted as described in Chapter 5 and Figure 5.2c. (See Note 2 for read format) =4 Two-layer flow, constant depth case. Velocity specification is one pair of velocity profiles as shown in Figure 5.2c. These profiles are assumed constant in the horizontal and invariant in time. (See card group 12)

Note: Omit group 12 if IFORM \neq 4

Card Group No.	No. of Cards	Format
	FORTTRAN VARIABLE	DESCRIPTION
12	1 card	8E10.0
	DU1	Depth (feet) to upper U velocity (X-direction)
	DU2	Depth (feet) to lower U velocity
	UU1	Upper U velocity (ft/sec)
	UU2	Lower U velocity (ft/sec)
	DW1	Depth (feet) to upper W velocity (Z-direction)
	DW2	Depth (feet) to lower W velocity
	WW1	Upper W velocity (ft/sec)
	WW2	Lower W velocity (ft/sec)
13	1 card	8E10.0
	TDUMP	Time of dump to nearest DTL seconds after start of tidal cycle (seconds)
	TSTOP	Duration to nearest DTL seconds of simulation after dump (seconds)
	DTL	Long-term time step (seconds) Time varying velocities are speci- fied at this interval
Note: Omit group 14 if KEY4 = 0.		
14	1 card	8E10.0
	DT1U	User-specified time step for con- vective descent phase (used for re- peated runs)
	DT2U	User-specified time step for dy- namic collapse (used for repeated runs)

Card Group No.	No. of Cards	Format
	FORTRAN VARIABLE	DESCRIPTION

Note: If IPLT = 0, omit the following group.

15	1 or 2 cards TPRT(I)	8E10.0 Values of times to print long-term results (integer multiples of DTL in seconds) Number of values equals IPLT.
16	1 card RB DREL CU(1) CV(1) CW(1) ROO BVOID	8E10.0 Radius of initial hemispherical waste cloud (feet) Depth of centroid of initial cloud at release (feet) Initial velocity components in x, y and z directions (See Figure 3.3) Bulk density of initial cloud (gm/cc) Voids ratio of aggregate solids
17	Several cards	A10, 7E10.0

Note: This group has NS cards (Group 1) and each card of this group describes a particle type and has the following variables

PARAM(K)	Alphameric description of solid (10 characters maximum)
ROAS(K)	Solid density (gm/cc, dry weight) of particle

Card Group No.	No. of Cards	Format
	FORTTRAN VARIABLE	DESCRIPTION
	CS(K)	Concentration of these particles in volume ratio
	VFALL(K)	Fall velocity of these particles (ft/sec)
	VOIDS(K)	Voids ratio of these particles
18	1 card	A10, 2E10.0
	TRACER	Alphameric description of conservative chemical tracer in initial fluid fraction
	CINIT	Concentration of tracer in initial fluid (mg/liter)
	CBACK	Background concentration in ambient fluid (mg/liter)

Note: If the fluid fraction is not simulated (KEY3=0), a blank card may be used as group 18.

Note: If KEY1≠2, group 18 completes the required input. If the user desires to use his own values for coefficients, then KEY1=2 and the following card groups must be included.

19	1 card	8E10.0
	DINCR1	Factor used for estimating time step in convective descent
	DINCR2	Factor used for estimating time step in dynamic collapse

Card Group No.	No. of Cards	Format	DESCRIPTION
	FORTTRAN VARIABLE		
20	1 card	8E10.0	
	ALPHA0		Entrainment coefficient for turbulent thermal
	BETA		Settling coefficient
	CM		Apparent mass coefficient
	CD		Drag coefficient for a sphere
21	1 card	8E10.0	
	GAMA		Density gradient factor in the cloud
	CDRAG		Form drag coefficient for the quadrant of a collapsing oblate spheroid
	CFRIC		Skin friction coefficient for the quadrant of a collapsing oblate spheroid
	CD3		Drag coefficient for an ellipsoidal wedge
	CD4		Drag coefficient for a plate
	ALPHAC		Entrainment coefficient for collapse
	FRICTN		Friction coefficient between cloud and estuary bottom
	F1		Modification factor used on computing the resistance of the friction force to the collapse of a quadrant of an oblate spheroid.

Card Group No.	No. of Cards	Format
	FORTRAN VARIABLE	DESCRIPTION
22	1 card	8E10.5
	ALAMDA	Dissipation factor used in computing horizontal diffusion coefficient by four-thirds law
	AKY0	Maximum value of vertical diffusion coefficient

Note 1:

The FORTRAN instructions for reading the depth grid are as follows:

```
DO 10 M=1, MMAX
10 READ (5,15) (DEPTH (N,M), N=1, NMAX)
15 FORMAT (16F5.0)
```

Note 2:

Time-varying velocities that are to be read from tape must be prepared according to the formats discussed here. Since the read statements are unformatted, the velocity tape should be prepared on the same hardware as DMF is to be used on.

Velocity information is supplied in sets, one set per time step. Each set of velocities is preceded by a time label that gives the elapsed time since the start of the tidal cycle in seconds. The first time label on the tape will be 0 seconds; the interval from one time label to the next will be DTL seconds; and the last time label will be (90000-DTL) seconds. Time labels are written WRITE (7) T. Following all data, an end time of 90000 seconds must be written to serve as a rewind mark. This is followed by the end-of-file marker.

Following each time label will be written one set of velocity information according to the value of IFORM. If IFORM is 1 or 2, the time label will be followed by the results of the statement

```
WRITE(7) ((U(N,M,1), N=1, NMAX), M=1, MMAX)
1          , ((W(N,M,1), N=1, NMAX), M=1, MMAX)
```

If IFORM is 3 each time label will be followed by the results of the statements

```
WRITE(7) DL1, DL2
DO 10 L=1, 2
WRITE(7) ((U(N,M,L), N=1, NMAX), M=1, MMAX)
1          , ((W(N,M,L), N=1, NMAX), M=1, MMAX)
10 CONTINUE
```

DL1 and DL2 are the fractions of the total depth at any point where the velocities read in for that point are applied. (See Figure 5.2c)

APPENDIX C

User's Manual: Model for Jet Discharge Programs, DMFJ

This is the user's manual for program DMFJ, which predicts dredged material fate for a jet discharge in an estuary. The program was developed and tested on a Control Data 6600 computer. It was written, with minor exceptions, to ANSI standards. The exceptions are noted in the card identifier columns as shown in the listing in Appendix D. There are a total of 15 cards that do not satisfy ANSI standards or that are peculiar to the CDC 6600, and these are flagged in the identifier columns.

DMFJ was designed to make it simple to do simple things and not too complicated to do complicated things. To this end, the code uses dynamic storage allocation. This is done by placing all of the passive diffusion arrays and one short-term array in a single, variable-dimension array (called A) in unlabeled common storage. The first data card in a run deck contains the dimensions of these arrays. The CDC 6600 version computes core requirements from these dimensions and expands the core area as necessary during execution. On other installations, the instructions that do this (marked "CDC ONLY") will have to be removed, and the user will have to recompile routine DMFJ with the dimension of array A set to the following

$$\text{DIMENSION} = 1 + (7+4 \cdot \text{NS} + 2 \cdot \text{NVL} + 3) \text{NMAX} \cdot \text{MMAX} \\ + 600 \cdot \text{NS} + 6 \cdot \text{NSC} (\text{NS} + 1)$$

where NMAX, MMAX, NS, NVL, and NSC are as described in the input listed below. The presentation of the input variables includes brief descriptions. For additional details, the user will be referred to notes at the end.

INPUT DESCRIPTION

Card Group No.	No. of Cards	Format
	FORTRAN VARIABLE	DESCRIPTION
1	1 card	16I5
	NMAX	Maximum dimension of long-term passive diffusion grid in Z-direction (Figure 5.1)
	MMAX	Maximum dimension of long-term passive diffusion grid in X-direction (Figure 5.1)
	NS	Number of solid components in discharge (not greater than 12)
	NVL	Number of velocity levels in velocity arrays (must be 1 or 2)
	NSC	Maximum number of small clouds allowed per component for transition from short term to long term (value 50 suggested)
2	1 card	16I5
	KEY1	=1 Use default coefficients suggested by Tetra Tech =2 Use coefficients suggested by user
	KEY2	=1 Fixed pipeline discharge =0 Discharge from moving vessel
	KEY3	=1 Long-term diffusion for fluid component =0 No long-term diffusion for fluid component

Card Group No.	No. of Cards	Format
	FORTRAN VARIABLE	DESCRIPTION
3	1 card	16I5
	IGCN	=0 No graphs of convective descent phase =1 Two-line printer graphs of convective descent =2 Extra graphs of concentrations for convective descent
	IGCL	=0 No graphs of dynamic collapse =1 Two-line printer graphs of dynamic collapse.
	IPCN	=0 No printed record of convective descent phase =1 Printed output included
	IPCL	=0 No printed record of dynamic collapse phase =1 Printed output included
	IPLT	=0 Print long-term results at default times ($\frac{1}{4}, \frac{2}{4}, \frac{3}{4}, \frac{4}{4}$ of TSTOP) =n Number of values to be read in of times to print long-term results (up to 12)
4	1 card	8A10
	ID	Free-form alphanumeric description of run (up to 80 characters)

Card Group No.	No. of Cards FORTRAN VARIABLE	Format DESCRIPTION
5	1 card DX	8E10.0 Space step (in feet) for long-term grid (See Figure 5.1)
6	Several cards DEPTH(N, M)	16F5.0 Depth at each grid point in the estuary (in feet) read row by row, left to right, top to bottom (see Note 1 and Figure 5.1)
7	1 card TSJ TSTOP DTL TJET	8E10.0 Time that jet discharge begins (measured in seconds from start of tidal cycle). Barge is at position (XBARGE, ZBARGE) at this time. Duration of simulation (in seconds) --the maximum time elapsed from beginning of jet discharge to which material will be tracked (this is an integer multiple of DTL). Long-term time step (seconds). This is the time increment for passive diffusion. DTL should be set so that it is greater than the maximum time required for the discharged material to go through convective descent and dynamic collapse Duration of jet discharge (seconds)

Card Group No.	No. of Cards	Format
	FORTTRAN VARIABLE	DESCRIPTION
8	1 card	8E10.0
	VDOT	Volume rate of jet discharge of dredged material slurry (cu ft/sec)
	BC(1)	Initial radius of jet (ft)
	DJET	Depth of discharge nozzle (ft)
	ANGLE	Vertical angle of discharge (deg. below horizontal). The azimuth of discharge is assumed to be 180 degrees away from the vessel course SAI in group 9
	ROI	Bulk density of dredged material slurry at discharge nozzle (gm/cm ³)
	BVOID	Aggregate voids ratio
9	1 card	8E10.0
	XBARGE	X-coordinate of discharging vessel in estuary coordinates at time of start of discharge (See Figure 5.1)
	ZBARGE	Z-coordinate of discharging vessel in estuary coordinates at time of start of discharge
	SAI	Straight course maintained by discharging vessel during discharge (measured in degrees anti-clockwise from positive X axis).(See Figure 5.1)
	UB	Constant speed of discharging vessel (measured in ft/sec with respect to surface water). This parameter should be set to 0 for a fixed discharge.

Card Group No.	No. of Cards	Format
	FORTTRAN VARIABLE	DESCRIPTION
11	Several cards	A10,7 10.0

Note: This group has NS cards (Group 1), and each card of this group describes a particle type and has the following variables.

PARAM(K)	Alphanumeric description of solid (10 characters maximum)
ROAS(K)	Solid density (gm/cm ³ , dry weight) of these particles
CS(K)	Concentration of these particles in volume ratio
VFALL(K)	Fall velocity of these particles (ft/sec)
VOIDS(K)	Void ratio of these particles (Used only in estimating final thickness on bottom)

12	1 card	A10, 2E10.0
	TRACER	Alphanumeric description of conservative chemical tracer in initial fluid fraction
	CINIT	Concentration of tracer in initial fluid (mg/l)
	CBACK	Background concentration in ambient fluid (mg/l)

Note: Omit groups 13-16 if KEY1 = 1

13	1 card	8E10.0
	DINCR1	Trial value used in obtaining distance step DS for the integration in the jet convection phase. DS = DINCR x (initial jet radius)

Card Group No.	No. of Cards	Format	DESCRIPTION
	FORTTRAN VARIABLE		
	DINCR2		Trial value used in obtaining initial distance step DS for the integration in the dynamic collapse phase. DS=DINCR2 x (jet radius at end convective descent)
14	1 card	8E10.0	
	ALPHA1		Entrainment coefficient for momentum jet
	ALPHA2		Entrainment coefficient for two-dimensional thermal
	BETA		Settling coefficient for solid particles
	CD		Drag coefficient for a cylinder
15	1 card	8E10.0	
	GAMA		Density gradient factor in collapsing plume. Density gradient inside plume at start of collapse is assumed to be GAMA times local ambient density gradient
	CDRAG		Form drag coefficient for the quadrant of a collapsing elliptical cylinder
	CFRIC		Skin drag coefficient for the quadrant of a collapsing elliptical cylinder
	CD3		Drag coefficient for an elliptical wedge
	CD4		Drag coefficient for a two-dimensional plate

Card Group No.	No. of Cards	Format
	FORTTRAN VARIABLE	DESCRIPTION
	FRICTN	Friction coefficient between cloud and ocean bottom
	F1	Modification factor used in computing the resistance of the friction force to the quadrant of an elliptical cylinder
	CM	Apparent mass coefficient
16	1 card	8E10.0
	ALAMDA	Dissipation factor used in computing horizontal diffusion coefficient by four-thirds law
	AKYO	Maximum value of vertical diffusion coefficient.
17	1 card	215, E10.0
	NPROF	Number of successive long-term time steps for which density profiles are to be read. Each profile is that perceived from the discharging vessel at the start of a particular time step. If the vessel continues to discharge after the last DTL for which a profile is given, the most recent profile will be used. NPROF=1 implies a constant profile over time (Maximum value 50)
	NROA	Number of points in each profile This is the same for all profiles Range is from 2 through 8.
	DTROA	Time interval (seconds) between density profiles. (Must be integer multiple of DTL).

Card Group No.	No. of Cards	Format
	FORTTRAN	DESCRIPTION
	VARIABLE	

18	2*NPROF Cards	8E10.0
----	---------------	--------

Note: This group is read in pairs of cards. Each pair of cards contains the depths (first card) and densities (second card) for one density profile. The profiles may be at up to 8 points, the last of which should be at the deepest depth of the estuary. Each pair of cards is defined as follows.

YROA(I, N)	(First card of pair) Depths (ft) where density specified.
ROAP(I, N)	(Second card of pair) Densities (gm/cm ³) (I=Point number N=profile number)

19	1 card	16I5
	IFORM	<p>This is an indicator of the ambient velocity interpretation. Set to one of the following values (See Note 2 for details of velocity data preparation)</p> <p>=1 One-layer flow, variable in the horizontal and in time. Vertically averaged velocities are read from logical unit 7 (TAPE7) at each long term time step</p> <p>=2 Same as above except that velocity profiles are assumed to be logarithmic such that the average over the vertical equals the read in value</p> <p>=3 Two-layer flow, variable horizontally, vertically, and in time. These are interpreted as described in Chapter 5 and Figure 5.2c. (See Note 2 for read format)</p>

Card Group No.	No. of Cards	Format
	FORTTRAN VARIABLE	DESCRIPTION

=4 Two-layer flow, constant depth case. Velocity specification is one pair of velocity profiles as shown in Figure 5.2c. These profiles are assumed constant in the horizontal and invariant in time. (See card group 19)

Note: Omit group 19 if IFORM \neq 4

20.	1 card	8E10.0
	DU1	Depth (feet) to upper U velocity (X-direction)
	DU2	Depth (feet) to lower U velocity
	UU1	Upper U-velocity (ft/sec)
	UU2	Lower U-velocity (ft/sec)
	DW1	Depth (feet) to upper W-velocity (Z-direction)
	DW2	Depth (feet) to lower W-velocity
	WW1	Upper W velocity (ft/sec)
	WW2	Lower W velocity (ft/sec)

Note: If IPLT = 0, Omit the following group.

21	1 or 2 cards	8E10.0
	TPRT(I)	Values of times to print long-term results (integer multiples of DTL in seconds) Number of values equals IPLT.

--- END OF INPUT ---

Note 1:

The FORTRAN instructions for reading the depth grid are as follows.

```
      DO 10 M=1, MMAX
10    READ(5,15)(DEPTH(N,M), N=1, NMAX)
15    FORMAT (16F5.0)
```

Note 2:

Time varying velocities that are to be read from tape must be prepared according to the formats discussed here. Since the read statements are unformatted, the velocity tape should be prepared on the same hardware as program DMFJ is to be run on.

Velocity information is supplied in sets, one set per time step. Each set of velocities is preceded by a time label that gives the elapsed time since the start of the tidal cycle in seconds. The first time label on the tape will be 0 seconds; the interval from one time label to the next will be DTL seconds; last time label that has velocity data behind it will be (90000-DTL) seconds. After the last set of data is written a time of 90000 seconds. This last time label acts as a tape-rewind marker. Time labels are written by the statement WRITE(7)T.

Following each time label (except the last) will be written one set of velocity information according to the value of IFORM. If IFORM is 1 or 2, the time label will be followed by the results of the statement

```

      WRITE (7) (( U(N,M,1), N=1, NMAX), M=1, MMAX)
1          ,(W(N,M,1), N=1, NMAX), M=1, MMAX)

```

If IFORM is 3, each time label will be followed by the results of the statements

```

      WRITE (7) DL1, DL2
      DO 10L=1,2
      WRITE (7) (( U(N,M,L), N=1, NMAX), M=1, MMAX)
1          ,(W(N,M,L), N=1, NMAX), M=1, MMAX)
10 CONTINUE

```

DL1 and DL2 are the fractions of the total depth at any point where the velocities read in for that point are applied. (See Figure 5.2c)

APPENDIX E

NOTATION

Symbols of secondary importance which appear only briefly in the text are omitted from the following list.

A	Vorticity dissipation parameter
A_λ	Dissipation parameter for turbulent diffusion
B	Relative buoyancy
C_{drag}	Drag coefficient
C_D	Drag coefficient
C_{D_3}	Drag coefficient
C_{D_4}	Drag coefficient
C_{fric}	Friction coefficient
C_m	Apparent mass coefficient
C_{si}	Concentration of solid particles
D	Drag force
D_D	Form drag of collapsing element
E	Entrainment function
E_m	Momentum jet entrainment
E_T	Entrainment by a two-dimensional thermal
F	Buoyancy force
F_{bf}	Bed friction force
F_D	Driving force of collapse

F_f	Skin friction drag of collapsing element
F_l, F_{rictn}	Friction coefficients
K	Total vorticity
K_y	Vertical diffusion coefficient
L	Length of jet-plume element
P_i	Volume of i^{th} solid in element
I	Inertial force
R_i	Richardson number
S_i	Volume rate of i^{th} solid passing out of element
\vec{U}	Velocity vector
\vec{U}_a	Ambient velocity vector
V_c	Volume of element
a	Radius of hemispherical cloud, or Semi-minor axis of collapsing element
a_o	Radius of element at end of convective descent
b	Semi-major axis of collapsing element
g	Acceleration of gravity
\vec{j}	Unit vector in vertical direction
q	Mass rate of settling
r'	Horizontal axis of coordinates fixed on element
s	Distance along jet axis
t	Time
u	Velocity in x-direction
u_a	Ambient velocity in x-direction

v	Element velocity in vertical direction
v_{fi}	Fall velocity of solid particles i
v_1	Tip velocity due to collapse
v_2	Tip velocity due to entrainment
w	Element velocity in z-direction
w_a	Ambient velocity in z-direction
y	Vertical coordinate
y'	Vertical axis of coordinates fixed on element
α	Entrainment coefficient
α_c	Coefficient for entrainment due to collapse
α_1, α_2	Entrainment coefficients
α_3, α_4	Entrainment coefficients for collapsing plume
β_i	Settling coefficient
δ_1, δ_3	Angles ambient current at s makes with x and z axes respectively
ϵ	Density gradient
γ	Coefficient for density gradient difference inside and outside of collapsing element
ρ	Density
ρ_a	Ambient density
ρ_c	Element density
ρ_i	Density of solid particles i
$\theta_1, \theta_2, \theta_3$	Direction angles

In accordance with ER 70-2-3, paragraph 6c(1)(b), dated 15 February 1973, a facsimile catalog card in Library of Congress format is reproduced below.

Tetra Tech, Inc.

Development of models for prediction of short-term fate of dredged material discharged in the estuarine environment, by Maynard G. Brandsma and David J. Divoky. Vicksburg, U. S. Army Engineer Waterways Experiment Station, 1976.

1 v. (various pagings) illus. 27 cm. (U. S. Waterways Experiment Station. Contract report D-76-5)

Prepared for Environmental Effects Laboratory, U. S. Army Engineer Waterways Experiment Station, Vicksburg, Mississippi, under Contract No. DACW39-74-C-0075, Work Unit 1B02.

Includes bibliography.

1. Dredged material disposal. 2. Estuarine environment.
3. Mathematical models. I. Brandsma, Maynard G.
II. Divoky, David J., joint author. (Series: U. S. Waterways Experiment Station, Vicksburg, Miss. Contract report D-76-5)

TA7.W34c no.D-76-5